Universidade Federal do Rio de Janeiro

Programa de Pós-Graduação em Tecnologia

de Processos Químicos e Bioquímicos

WAX PRECIPITATION TEMPERATURE REVISITED

Felipe Leis Paiva

Master's thesis presented to the Programa de Pós-graduação em Tecnologia de Processos Químicos e Bioquímicos, from the Escola de Química of the Universidade Federal do Rio de Janeiro, as partial fulfillment of the requirements for the degree of Mestre em Tecnologia de Processos Químicos e Bioquímicos.

Advisors: Prof. Verônica Maria de Araújo Calado, D.Sc.

Flávio Henrique Marchesini de Oliveira, D.Sc.

Rio de Janeiro

March, 2016

WAX PRECIPITATION TEMPERATURE REVISITED

Felipe Leis Paiva

MASTER'S THESIS SUBMITTED TO THE FACULTY BODY OF THE PROGRAMA DE PÓS-GRADUAÇÃO EM TECNOLOGIA DE PROCESSOS QUÍMICOS E BIOQUÍMICOS (TPQB) FROM THE ESCOLA DE QUÍMICA OF THE UNIVERSIDADE FEDERAL DO RIO DE JANEIRO AS PARTIAL FULFILLMENT OF THE REQUIREMENTS FOR THE DEGREE OF MESTRE EM CIÊNCIAS EM TECNOLOGIA DE PROCESSOS QUÍMICOS E BIOQUÍMICOS.

Approved by:

_____
Prof. Verônica Maria de Araújo Calado, D.Sc. – TPQB/UFRJ

_____
Flávio Henrique Marchesini de Oliveira, D.Sc. – Halliburton

_____
Prof. Márcio Nele de Souza, D.Sc. – TPQB/UFRJ

_____
Prof. Roney Leon Thompson, D.Sc. – UFF

_____
Márcia Cristina Khalil de Oliveira, D.Sc. – PETROBRAS

RIO DE JANEIRO, RJ – BRAZIL
MARCH, 2016

Acknowledgements

Wow, where do I begin?

I would like to, first, thank my family, and specially my parents Sandra and Heluisio, for always providing me with the best education possible. I also wish to start by thanking my beloved girlfriend Juliana for her unconditional support in every aspect of my life.

There are no words to express my gratitude toward my advisors Verônica Calado and Flávio Marchesini, although I will do my best to try to deliver it. Prof. Verônica, thank you for, from the very beginning, sparing no effort in making sure that I wrote my Master's thesis on a subject that I deeply enjoyed working with. Your tireless commitment to a high-quality level of research and work ethics are truly admirable, and have been an inspiration for me in the past year to grow as a scientist and as a person. Flávio, in turn, gave me a fascinating present: the specific theme of the present work. I am forever indebted to him for this; for taking time out of his corporate duties to explain to me topics that I had not fully understood; for all the incentive in learning LaTeX; for general career advise; for writing academic recommendation letters; and, overall, for contributing so significantly to my professional growth.

I had never imagined I would be able to work with such an amazing group of people such as that of the Thermal Analysis and Rheology Laboratory (LABTeR). I would like to thank my right arm in the laboratory, André, for his alacrity and for all the help conducting experiments and handling data. While I thank everyone from LABTeR in general, special thanks must go out to Felipe, Alfredo, Rosana, and Aienicla, for all the helpful technical (and philosophical) discussions; patience; help with experiments; and overall incentive.

I would also like to express my most sincere gratitude to Prof. Marcio Nele for granting me ample access to the equipment that I needed, namely the Rheometer and Microscope; and Carla Barbato, for training me on these equipment; for her patience; and also for some very helpful technical suggestions.

I am also grateful to Prof. Elizabete Lucas – for making the chromatographic, microcalorimetric, and FTIR analyses possible; Michele Frota – for all her help with these experiments; and to Prof. Elisabeth Monteiro for valuable technical

discussions.

"A scientist in his laboratory is not a mere technician: he is also a child confronting natural phenomena that impress him as though they were fairy tales."
Marie Curie

TEMPERATURA DE PRECIPITAÇÃO DE PARAFINAS REVISITADA

Felipe Leis Paiva

Março/2016

Advisors: Prof. Verônica Maria de Araújo Calado, D.Sc.

Flávio Henrique Marchesini de Oliveira, D.Sc.

Programa: Tecnologia de Processos Químicos e Bioquímicos

No presente trabalho, a aplicabilidade de vários métodos de medição do início da cristalização de parafinas em dois petróleos parafínicos brasileiros é analisada. Isso se faz necessário tendo em vista os potenciais problemas de obstrução de dutos associados com escoamento de óleo em ambientes frios, que favorecem a cristalização de parafinas. Além disso, técnicas que são padrões amplamente utilizados com esse propósito possuem limitações inerentemente próprias. Após uma extensa caracterização das amostras de petróleo, Reometria, Microscopia e Calorimetria são empregadas para que, respectivamente, as temperaturas de gelificação, de aparecimento e de precipitação de parafinas sejam investigadas, além de como elas são afetadas por parâmetros como temperatura inicial de resfriamento e o tamanho de *gap* do reômetro. Correlações também são feitas entre a dimensão dos cristais de parafinas, de acordo com diferentes temperaturas de início de resfriamento, e composição geral dos óleos. Os resultados sugerem que a questão de dissolver completamente os cristais de parafina ou não, para que condições reais de escoamento sejam corretamente reproduzidas, é um assunto complexo, pois as propriedades reológicas são significativamente afetadas pela escolha da temperatura inicial. Há também indícios de que um diferente e específico tipo de técnica calorimétrica (StepScan), assim como a microcalorimetria, são promissores no que diz respeito à sua sensibilidade em detectar a temperatura de precipitação de parafinas. Contudo, a Microscopia de Luz Polarizada é a única técnica capaz de detectar o real aparecimento dos primeiros cristais.

Abstract of Master's thesis presented to TPQB/UFRJ as a partial fulfillment of the requirements for the degree of Master of Science (M.Sc.)

WAX PRECIPITATION TEMPERATURE REVISITED

Felipe Leis Paiva

March/2016

Advisors: Prof. Verônica Maria de Araújo Calado, D.Sc.
           Flávio Henrique Marchesini de Oliveira, D.Sc.

Graduate Program: Technology of Chemical and Biochemical Processes

In this work, we assess the suitability of several methods for detecting the start of wax crystallization in two Brazilian waxy crude oil samples. This is necessary in view of the potential gelation problems associated with oil flow in cold environments, which favors wax crystallization. Additionally, existing standard techniques that are widely used to this purpose have their own inherent limitations. After a comprehensive characterization of the oil samples, Rheometry, Microscopy, and Calorimetry are employed to investigate, respectively, the wax gelation, appearance, and precipitation temperatures, and how these are affected by parameters such as the initial cooling temperature and rheometer gap size. Furthermore, correlations are made between wax crystal dimensions; different initial temperatures; and overall oil composition. Results suggest that the question of whether or not to completely dissolve wax crystals in order to better reproduce operational conditions is a rather complex matter, given that their flow properties are significantly affected by the choice of the initial cooling temperature. We also present indications that a novel, specific type of calorimetric technique (StepScan), as well as microcalorimetry, show promise in being more sensitive for detection of the wax precipitation temperature. However, Cross-Polar Microscopy is the only one that is able to detect the appearance of the first wax crystals.

Contents

List of Figures

List of Tables

Chapter 1

Introduction

In this introductory chapter, the problematic subject of waxy crude oils is set in context (Sections 1.1 and 1.2) and important measurement parameters for investigating their complex rheological behavior and crystallization process are defined (Section 1.3). Additionally, objectives are delineated and an overview of the entire work is presented (Sections 1.4 and 1.5).

1.1   Flow Assurance

Flow assurance can be defined as the reliable, manageable, and profitable flow of fluids from the reservoir to the sales point and has been discussed in the literature many times [1]. The term was coined by Brazilian oil company Petrobras in the early 1990s and comprehends the science and engineering solutions for hydrates, paraffins or waxes, asphaltenes, scale, fluid transport and corrosion [1, 2]. Hence, naturally, the characteristics of production fluids play a fundamental role in every aspect of this highly multidisciplinary field [1].

Depending mainly on flow conditions and on crude oil origin, flow assurance issues arise from pipelines and equipment becoming eventually obstructed or damaged during an oilfield operation and this generates very significant financial losses to oil companies worldwide. Therefore, flow assurance represents an increasing challenge to the oil and gas industry, especially as the latter progresses offshore into deeper water [1].

When oil companies are faced with flow assurance concerns, there are basically two approaches to solving them: remediation, when deposits have already formed, and inhibition. Remediation methods may include pipeline heating, pigging or the use of dispersants, so as to, respectively, reheat/melt the production fluid; mechanically remove; and dissolve the deposits. On the other hand, inhibition strategies are based on the use of chemicals designed to prevent deposit formation.

1.2 Paraffin Deposition and Waxy Oil Gelation

The present work addresses the Flow Assurance problem of paraffin deposition or waxy oil gelation, which has been catching the industry's attention as early as the 1920s [3–7]. Petroleum waxes are mostly composed of approximately C_{20} - C_{40} n-alkanes that are generally called macrocrystalline or paraffin waxes. However, the oil wax fraction termed microcrystalline or amorphous wax may also be present, in the form of high-molecular weight isoalkanes and cyclic alkanes [8–11]. After hydrates, oil wax is the second most common cause for obstructed flowlines in the oil production industry [12].

Both wax/paraffin deposition and crude oil gelation phenomena result from wax crystallization. However, they differ in the way that they take place: wax deposition occurs commonly in steady-state scenarios and is characterized by accumulation along pipe walls; waxy oil gelation is more common during production shutdowns, when there is the formation a solid, dense wax column [13]. Accordingly, this is partly why the study of waxy crude oil rheology is so important: the gelation of waxy crude oils gives rise to a yield stress. Therefore, in flow restart operations following an eventual production shutdown, if the waxy oil has gelled, a pressure gradient larger than the usual operating pressure has to be applied in order to surpass the yield stress of the gel at the pipeline wall [14]. Other important aspects of the rheological characterization of waxy crude oils, aside from the existence of a yield stress, such as rheometer gap size, geometry and wall slip, will be discussed further in the next sections of the present work.

1.3 Wax Appearance, Precipitation, and Gelation Temperatures

There are a number of variables that determine the wax crystallization rate and the amount of wax that deposits for example the flow rate and the pipe's internal surface properties [2, 13]. But, ultimately, when it comes to ensuring that pipelines or equipment will not become plugged from wax crystallization, perhaps the main parameter to be controlled is temperature. The reason for this is the existence of a critical, crude oil-dependent temperature, called Wax Appearance Temperature (WAT).

There are also other important, temperature-related parameters called the Cloud Point (CP) and the Pour Point (PP) and, in the literature, the former is sometimes referred to interchangeably with the WAT [15–21]. Standard procedures for measuring them are in accordance with the American Society for Testing and Materials (ASTM) and they also give an estimate of a crude oil's wax deposition issues. How-

ever, they either possess intrinsic limitations of their own [15, 16, 18, 21–23] or fail to detect the very early, actual start of wax crystallization [9, 15, 18, 22, 24].

Over the last decades, many researchers have dedicated themselves to either comparing methods for determination of the WAT with respect to their precision or to obtaining a deeper understanding of wax crystallization phenomena [8, 9, 15, 16, 18, 22, 25–35]. However, it is worth noting that, when it comes to investigating wax crystallization using rheometric techniques, the transformation that is detected does not pertain to the onset of wax crystallization and does not correspond to the WAT or the appearance of the first wax crystals, even at low cooling rates. It is believed that there needs to be a sufficient amount of crystallized wax in crude oil and model oil samples for viscometric/rheometric effects to be distinguished [9, 27].

A sharp increase in viscosity, for instance, may be detected by Rheometry and derives from the formation of a gel network of wax crystals [12]. This is an indication of oil gelation, for which the measured parameter is accordingly the gelation temperature (T_{gel}). During cooling of a waxy crude oil, for example in a pipeline, while its flow properties are relatively simple above this temperature, in the sense that it behaves as a Newtonian fluid, they eventually change to a very complex non-Newtonian behavior upon cooling below it. At best, the T_{gel} obtained by Rheometry correlates with the pour point method, instead of the WAT, because the latter also resembles a flow-related measure, much like Rheometry, aimed at determining oil gelation specifically under static cooldown conditions [36].

Furthermore, when waxy crude oils experience a drop in temperature and gel, their complex rheological behavior is determined not only by displaying a yield stress and time, temperature and shear rate dependencies, but also by the variables of the entire cooling process that the oil had been submitted to, namely its thermal and shear rate histories [8].

Moreover, the heat release that arises from wax crystallization can also be detected by Differential Scanning Calorimetry (DSC). However, there is evidence that this technique is not effective in detecting the very start of wax crystallization, especially for samples with low wax content [30, 37]. In fact, there is evidence that exothermic crystallization peaks shift to lower temperatures with a decreasing wax content, indicating that there must be a sufficient amount of precipitated paraffins in order for thermal effects to be detected by DSC [30]. Therefore, we herein refer to the start of wax crystallization measured by Calorimetry as the Wax Precipitation Temperature (WPT).

1.4   Research Objectives

The main objectives of this work are:

i. To compare different measurement techniques for the WPT/T_{gel} – Microscopy (WAT), DSC, and Rheometry – as to their accuracy in determining the true start of wax crystallization for two Brazilian waxy crude oil samples (A1 and A2);

ii. To evaluate the choice of a initial temperature for the cooling process that is representative of the operational scenario, instead of a higher, "memory-erasing" one;

iii. To investigate the effect of rheometer gap size on the measurement of T_{gel};

iv. To investigate the effect of thermal history on wax crystal dimensions.

1.5   Thesis Overview

The present work is divided in five chapters. This first Chapter deals with the motivation behind the subject of waxy crude oils and introduces some basic concepts for understanding investigations that pertain to detecting the start of wax crystallization.

Chapter 2 enables a deeper understanding of available methods for measuring the phenomenon of wax crystallization, and also of experimental factors governing the complex behavior of waxy crude oils. The theoretical basis behind several crude oil characterization techniques, as well as a detailed discussion of the most commonly used WAT/WPT/T_{gel} determination techniques, is also laid out.

In Chapter 3, a comprehensive description of the experimental procedures used in the present work, as well as a broad overview of the methodology used, is given. Justification for their use is also provided.

Results from this Master's thesis can be found in Chapter 4, where correlations between results are also made to some extent. The sensitivity of the techniques employed, and the influences of the initial cooling temperature and rheometer gap size are also evaluated.

In Chapter 5, as a conclusion, interconnections and relationships between individual results, both from crude oil characterization and crystallization onset determination, are presented. Furthermore, the importance of taking into consideration the realistic temperature gradients of wax crystallization processes in ultra deep, submarine pipelines is emphasized.

Chapter 2

Literature Review

In this Chapter, a review of available techniques that are suited for detection of the start of wax crystallization is provided, as well as an evaluation of their intrinsic limitations (Sections 2.1 and 2.5). In addition, further, essential, and more complete information on waxy crude oils is given (Section 2.2 and 2.3), along with a brief explanation of specific characterization methods employed in this work (Section 2.4).

2.1 Pour Point and Cloud Point

The terms Pour Point (PP) and Cloud Point (CP) both relate to wax crystallization events. However, a couple of differences apply even if the WAT and CP are sometimes referred to interchangeably in the literature [15–21]. While the CP is described as the temperature at which the oil becomes "cloudy", indicating that wax crystallization has already started, the PP serves as an estimate of the oil's T_{gel}, that is, the temperature below which the oil will no longer flow due to its gelation. In a way, the measurement of CP corresponds to an attempt at measuring the WAT and investigating the onset of the wax crystallization phenomenon, whilst the PP relates to crude oil gelation problems, that is, when solid, crystallized wax is present and changes the oil's rheological properties.

In their work, Venkatesan, Singh, and Fogler [36] differentiated the PP from the CP very clearly. They also concluded that PP tests would only be representative of quiescent gelation scenarios and do not apply to flowing conditions, when a shear stress is applied to the crude oil sample. Hence, according to them, the PP temperature is a special case of the T_{gel}, the latter being a broader term. Furthermore, it is also worth mentioning that Marchesini *et al.* [27] did not verify a change in gap-independent T_{gel} values whether a shear rate of $2\,\text{s}^{-1}$, $20\,\text{s}^{-1}$ or $200\,\text{s}^{-1}$ had been used. This may indicate that gap-independent measurements of T_{gel} do not depend on the applied shear rate after all.

The PP and CP parameters originate from determination methods that have always been broadly accepted as the ASTM standard procedures for evaluating the likelihood of a crude oil to exhibit wax-related, flow assurance problems. They correspond respectively to ASTM D97 and ASTM D2500 - or IP219, from the Institute of Petroleum (IP). As they are both obtained from visual observation of the sample, these standard procedures do not detect the very first wax crystal, but rather the physical effects that are unveiled by a sufficient amount of solid wax that had setlled in the sample. Furthermore, cloud point determinations by ASTM D2500, for example, are limited to liquids that are transparent in very thin layers of thickness, excluding black oils from measurement suitability [9, 21, 22, 38].

2.2 Thermal and Shear Histories

One of the most significant contributions to the study of waxy crude oils, especially with respect to their rheology, was that of Wardhaugh and Boger [8, 39]. It was previously known that the yield stress; the oil's flow behavior in the non-Newtonian region at a low temperature; and the size and shape of wax crystals were all somehow dependent on the thermal and shear histories imparted to the sample being tested, that is, mainly the cooling rate and the shear rate applied during the cooling process [40, 41]. However, in their work, Wardhaugh and Boger [8, 39] explained that for the true rheological properties of waxy crude oils to be measured, and then for the results from different instruments to be meaningfully compared, the so-called "memory" of the oil sample has to be erased. This is achieved by heating the sample to a temperature above the WAT to dissolve wax crystals [8, 39].

Nevertheless, erasing of the thermal and shear histories does not ensure repeatability of the subsequent cooling experiments: the sample must be allowed to stand for some time beforehand so as to reach not only thermal equilibrium, but also an equilibrium of shear forces. According to Wardhaugh and Boger [8], only then are flow curves of the sample time-independent and account for comparisons made between different instruments, such as rheometers with different geometries. Tiwary and Mehrotra [33], for example, investigated the behavior of several model "waxy" mixtures by viscosity measurements at different testing temperatures. The sample in their concentric-cylinder rotational viscometer had to be allowed to isothermally stand at each testing temperature for 30 minutes so that the viscosity readings would decrease and eventually reach an equilibrium value. Marchesini *et al.* [27] also elected an isothermal holding time (t_i) of 30 minutes right before cooldown started for their samples based on the work of Wardhaugh and Boger [8].

The influence of the thermal and shear histories on the properties of waxy crude oils is often studied in the form of cooling rate and shear rate/shear stress. Generally,

when the sample is not sheared during cooling, which corresponds to the study of static, shutdown conditions in the oil field, it possesses a very high resistance to flow and solid-like characteristics, because no gel-network degradable forces are acting on it [39].

On the other hand, in order to reproduce steady-state, wax deposition scenarios, a shear rate or stress may be practiced upon a waxy crude oil sample and it is not hard to imagine that the higher the shear rate, the weaker is the gel or crystal network that forms.

However, this may be true only to a certain extent. Venkatesan *et al.* [42] observed that, when a low shear (gelation) stress was utilized at a fixed cooling rate, it was able to induce entanglements between individual wax crystals, instead of breaking them up. According to the authors, only higher gelation stresses were able to break down the crystal network and compromise the final state of the gel. Therefore, they identified a value of gelation stress (shear history) corresponding to a maximum in yield stress, which arose from a balance between constructive (shear-induced) and destructive forces within the sample, as far as the cooling process is concerned. This maximum is a function of the cooling rate because the latter establishes how long the experiment will last, that is, how long the sample will be submitted to shear. This work of Venkatesan *et al.* [42] is a good example of how the effects of thermal history (cooling rate) and shear history (shear/gelation stress) interact to determine the final state of the waxy crude oil gel.

It is also worth mentioning that, whether under shear or quiescent cooling conditions, lower cooling rates have been reported to be associated with lower wax crystallization rates; formation of larger, more aggregated wax crystals; and higher viscosity/yield stress [4, 9, 34, 43–45]. Lower cooling rates also allow the whole sample to be in thermal equilibrium and supercooling effects are avoided this way, making WAT measurements more accurate [16, 21]. As to higher cooling rates, they usually yield a large number of nucleation sites and smaller crystals because, given that the wax crystallization rate is higher, the crude oil becomes supersaturated and wax crystals do not have the time to diffuse to existing nuclei [34]. However, in contrast to these findings, Guo *et al.* [46] came to the conclusion that the gel yield stress of mixtures of decane and long-chain paraffins - C28, C32 and C36 - generally increased with increasing cooling rate, the exception being the C28 mixture, for which the yield stress decreased at higher cooling rates. This raises the question of whether the influence of cooling rate on the yield stress of model waxy oils might depend on the composition of these mixtures to some extent. For example, in model waxy oil mixtures of long chain n-alkanes, there are indications that, when carbon numbers vary by more than 4, separate crystal phases are formed [47].

2.3 Initial Temperature and Loss of Light Ends

The need to heat the waxy crude oil sample first, in order to erase its thermal and shear histories, engenders another subject that is investigated by many researchers: what exactly that final heating temperature should be, that is, the initial temperature (T_i) from which the cooling process will start. This has generated much discussion because results have shown that T_i does have an effect on the final viscosity of the cooling process, on T_{gel} and/or on the yield stress [27, 48].

In fact, it appears that there is a critical temperature range for T_i that yields maximum values for these properties. This is attributed to the presence of other crude oil components, such as resins and asphaltenes, which are able to actively participate in the wax crystallization, mainly in the crystal-growth process [34]. These polar petroleum fractions may not be entirely dissolved in the waxy crude oil when its temperature is lower than the critical T_i value and therefore, in this case, do not interfere with its final viscosity, T_{gel} or yield stress. However, the memory-erasing pretreatment of a waxy crude oil might involve heating to temperatures above which there is a large enough amount of asphaltenes and resins dissolved and free in the sample to alter the crystallization mechanism [27]. This is why asphaltenes and resins are the components of crude oil often termed as natural Pour-Point Depressants (natural PPDs). When the waxy crude oil is pretreated at a temperature above the critical T_i, they are able to reduce the pour point of waxy crude oils and it goes without saying that the lower the pour point of a waxy crude, the easier it will flow in cooler environments [24, 49]. Other effects deriving from the action of these natural PPDs include lowering the yield stress and final viscosity observed at the end of the cooling process [9, 24, 27, 41, 48, 50, 51]. Furthermore, not only lower Pour-Point values have been observed: Differential Scanning Calorimetry (DSC) analysis of waxy oil samples has also shown a decrease in crystallization onset values with increasing asphaltene content [30, 51].

Another question that is raised by the prior thermal treatment is due to the possibility of losing lighter components that were originally dissolved in the oil. Light ends tend to stabilize wax under supercritical, reservoir conditions, delaying the start of wax crystallization [2, 21]. Researchers have tried to evaluate the influence of this effect on both stock-tank (dead) and live oil [18, 23, 28, 52]. Because the loss of lighter ends augments the crystallization temperature of waxy crude oils, WAT measurements in dead oil samples tend to be more conservative than in live oil samples.

Naturally, the choice of the initial cooldown temperature (T_i) determines the extent of light end solubilization in the sample. Zhu, Walker, and Liang [21] analyzed the impact of this effect on wax crystallization by viscometry for three of their

samples. They evaluated samples with initial test temperatures of 50 °C ("non-erased thermal history") and 60 °C ("erased thermal history") and identified wax crystallization at higher temperatures when they had preheated the samples to the higher temperature, or in the authors' words, when the histories had been erased. According to them, this result may be due either to the loss of lighter ends from preheating at a higher temperature, which would indeed raise the WAT; or to sampling from a supposedly inhomogeneous sample container [21]. Marchesini *et al.* [27] and Andrade *et al.* [50] also verified similar trends when varying the initial test temperature T_i. However, in their case, a stable composition had been previously established for their experiments and evaporation of lighter ends had also been minimized. Hence, Marchesini *et al.* [27] attributed the increase in T_{gel} with increasing T_i to the partial dissolution and subsequent recrystallization of low-molecular-weight wax. According to them, this contributed to the development of a weaker network, while high-molecular-weight paraffins remained suspended in the oil.

The loss of light ends becomes a more serious problem especially for a series of experiments made on a single sample that needed to be reheated over and over again, which is the case of the McKee crude oil in the work of Wardhaugh and Boger [53]. Marchesini *et al.* [27] evaded this issue by using a different sample for each of the experiment runs and by pretreating the oil in an open bottle at a temperature that is representative of the industrial process and higher than the testing temperature. This and the use of a solvent trap, respectively, ensured previous evaporation of lighter ends and a stable composition during the experiments. The pretreated waxy crude oil was exposed to the process temperature only once and served then as a source of sampling for a large number of experiments.

2.4 Crude oil characterization

Explained next are the methods that were used for shedding light on the chemical composition of the waxy crude oils studied (Sections 2.4.1, 2.4.2, 2.4.3, 2.4.4, and 2.4.5). A brief description of the theoretical principles governing each technique is presented, along with how they are appropriately situated within the larger context of waxy crude oils.

2.4.1 Gas Chromatography

Gas Chromatography (GC) encompasses a separation method in which, as the name implies, an inert carrier gas is the mobile phase, that is forced through a chromatographic column containing the stationary phase (solid or liquid). This method functions under the principle that different components of a complex mixture are

retained in the column to varying extents, depending on their affinity with the stationary phase. Therefore, distinct retention times are obtained for these substances [54, 55].

Chromatographic columns are normally coil-shaped so as to be placed in an oven, the temperature of which will depend on the kind of sample: if the latter has a broad boiling point, it is preferable that a temperature ramp be applied for an improved chromatogram [54].

In a chromatogram, identification of species is done by extant peaks at characteristic retention times, and comparison of peak height or area with that of standard substances yields quantitative data about the analyte. For this purpose, GC equipment are often coupled with Mass Spectrometer (MS) or with Flame Ionization Detectors (FID) [54].

In the field of waxy crude oils, GC finds application in the determination and quantification of n-paraffin and carbon number distributions [56]. More specifically, High-temperature GC coupled with MS (HTGC/MS) is able to provide these two distributions, which correspond, respectively, to the proportions of n-alkanes and total hydrocarbon components with a given carbon number [9, 33, 51, 57–59]. This is important because, for example, there is evidence that the average carbon number of petroleum wax plays a fundamentally important role in determining wax crystal size of PPD-modified waxy oils under shear. In other words, the average carbon number of waxes is very important in determining the oil's rheological behavior [56].

2.4.2 Fourier Transform Infrared Spectroscopy

Infrared (IR) radiation in the wavelength region of $400\,\mathrm{cm^{-1}}$ to $4000\,\mathrm{cm^{-1}}$, between the visible and microwave regions of the eletromagnetic spectrum, can be absorbed by specific groups in an organic molecule, which in turn vibrate in stretching and bending ways. This yields a spectrum of absorption bands at radiation wavenumbers corresponding to certain functional groups, which is helpful in identifying and investigating the chemical structure of the sample. In Fourier Transform Infrared Spectrometry (FTIR), results are obtained much faster, and in general with a higher signal-to-noise ratio than older, dispersive IR spectrometeres [54, 60].

In petroleum science, FTIR has been useful, for instance, in the identification of carbonyl groups that absorb in the $1710\,\mathrm{cm^{-1}}$ wavenumber region of the IR spectrum, and that may be an indication of the total acid number of a given crude oil [61, 62]. Moreover, using FTIR analyses, Seth and Towler [63] were able to ascertain the spontaneous loss of light ends of a given waxy crude oil that was left open to the atmosphere. Even so, FTIR is normally used together with other characterization

techniques to yield satisfactory and more complete information on the chemical nature of a given sample, especially if the analyte is a complex mixture of compounds, such as petroleum or its fractions [54–56, 60, 64–66].

2.4.3   Elemental Analysis

Elemental Analysis is an analytical method that provides the weight percentage of elements commonly found in organic compounds, such as carbon, hydrogen, sulfur, nitrogen, and oxygen. Elemental Analysis that provides the relative amount of carbon, hydrogen, nitrogen, and sulfur is termed shortly CHNS and involves the high-temperature (900 °C to 1000 °C) combustion of these elements in a dynamic or static oxygen-rich environment, often with a catalyst. The gaseous mixture deriving from the combustion process is swept with an inert gas into a heated chamber containing copper, which is responsible for converting oxides of nitrogen into nitrogen gas, as well as for reducing the remaining oxygen that comes from the prior combustion step. The course and mechanism of this measurement technique may vary depending on the elements of interest, but, for CHNS, ultimately only nitrogen, carbon dioxide, water and sulphur dioxide are left. These gases are subsequently detected either by GC separation, followed by thermal conductivity detection, or by several infra-red and thermal conductivity cells for detection of individual compounds. Furthermore, calibration for each element of interest is necessary for their quantification [54, 67].

2.4.4   Nuclear Magnetic Resonance

Nuclear magnetic resonance spectrometry (NMR) is based on the measurement of absorbed electromagnetic radiation in the radiofrequency range of approximately 4 MHz to 900 MHz. Atomic nuclei are involved in the absorption process and, in order for the nucleus to acquire sufficient energy for absorption, it is necessary to submit the analyte to an intense magnetic field. Subsequently, relaxation times, that is, the rate at which each nuclear spin aligns with the applied field, are measured. The spin-lattice or longitudinal relaxation time (T_1) is a measure of the average lifetime of the nuclei in the high-energy state, while the spin-spin or transverse relaxation time (T_2) describes the rate at which nuclear spin coherence is lost and the nucleus relaxes to the lower energy state [54, 68].

The rotation of the spins as they re-align with the applied magnetic field generates a voltage which in turn brings about small magnetic fields that usually oppose the applied field. Consequently, the nuclei are exposed to an effective field that is usually smaller than the external field and certain nuclei (containing an odd number of protons and neutrons), in different chemical/electronic environments, give rise to

a dispersion of signals. Therefore, the values of T_1 and T_2 – which relate to the response of, for example, ^{1}H and ^{13}C nuclei to the applied magnetic field – hold information about the interactions of nuclear spins with their physical and chemical environment.

The voltage generated by circulation of electrons in the molecule is stored as the raw data of the NMR analysis. In high field, high resolution NMR, the Fourier transformation of this signal yields a spectrum with peaks corresponding to hydrogen or carbon nuclei in different environments. The areas under the peaks are quantitavely related to the amount of ^{1}H and ^{13}C present as that chemical type [54, 68]. For example, the chemical shift region of 6.0 ppm to 9.0 ppm on the ^{1}H-NMR spectrum is assigned to aromatic hydrogens, although the exact limits of the chemical shift regions may vary slightly among researchers.

There a few inherent problems with carbon-13 NMR (^{13}C-NMR) technology that may be overcome by certain operational procedures. For instance, the Nuclear Overhauser Effect (NOE) causes peaks corresponding to carbons attached to different protons to be enhanced to varying extents. This renders the data obtained from the ^{13}C spectrum non-quantitative among the different types of carbon atoms. Another problem associated with ^{13}C-NMR are the longer T_1 values from paramagnetic interactions. However, both these issues can be corrected respectively by inverse gated decoupling during the acquisiton of the free induction decay, and by adding a paramagnetic relaxation agent to the solution, which is able to reduce the ^{13}C long relaxation time T_1 [55, 68, 69].

2.4.5 Estimation of Average Structural Parameters

Many researchers have used proton NMR (^{1}H-NMR) and ^{13}C-NMR in combination with Elemental Analysis in order to estimate average structural parameters (ASP) of compounds present in petroleum or coal-derived products, while some of them also relied on molecular weight measurements for such calculations [69–79]. They have characterized their samples using these techniques in order to obtain information on the relative proportion of straight-chain alkanes and their average chain length, for example, although many other ASP may also be estimated [69, 73–75, 80, 81]. Table 2.1 illustrates typical chemical shift regions for specific types of ^{13}C and ^{1}H nuclei, as well as a few examples of ASP that can be calculated. These have been commonly used in the literature [69, 73, 74].

The combined use of ^{1}H-NMR and ^{13}C-NMR is advantageous because, while ^{13}C-NMR provides data on the backbone of molecules, ^{1}H-NMR provides information about the periphery [54, 69]. Furthermore, although ^{13}C-NMR is less sensitive than ^{1}H-NMR because of the low natural abundance of ^{13}C nuclei, it generates less

Table 2.1: Chemical shift assignment of the different regions in ^{13}C and ^{1}H spectra and examples of ASP.

	Symbol	Chemical shift (ppm)	Assignment
	C_{sat}	0-70	Aliphatic carbons
	C_{ar}	110-160	Aromatic carbons
	C_{ar-alk}	137.5-160	Alkyl substituted aromatic carbons
^{13}C	C_α	14.1	Paraffinic α-carbons
	C_{Me-b}	19.7	Carbons in branched methyl group
	C_β	22.9	Naphthenic/paraffinic β-carbons
	C_n	29.7	Paraffinic/Further removed carbons (n-carbons)
	C_γ	32.2	Paraffinic γ-carbons
	H_α	2.0-4.5	α-CH, α-CH$_2$ and α-CH$_3$ (aromatic rings)
	$H_{\beta 1}$	1.0-1.6	β-CH$_2$ (aromatic rings); naphthenic/paraffinic CH
	$H_{\beta 2}$	1.6-2.0	n-CH$_2$ (aromatic rings); naphthenic/paraffinic CH$_2$
	H_β	1.0-2.0	$H_{\beta 1}$ + $H_{\beta 2}$
^{1}H	H_γ	0.0-1.0	n-CH$_3$ (aromatic rings); terminal/isolated CH$_3$
	H_{sat}	0.0-4.5	Aliphatic hydrogens (H_α + H_β + H_γ)
	H_{mar}	6.0-7.3	Hydrogen in monoaromatic ring systems
	H_{dar}	7.3-9.0	Hydrogen in diaromatic ring systems or greater
	H_{ar}	6.0-9.0	Aromatic hydrogens (H_{dar} + H_{mar})
	C_{ar-H}	-	Aromatic protonated carbons: $H_{ar}/(C/H)$
	f_a	-	Aromaticity factor: $C_{ar}/(C_{sat} + C_{ar})$
ASP	SCA	-	Straight-chain alkanes: $C_n + C_\alpha + C_\beta + C_\gamma$
	ACL	-	Average chain length: $2 \cdot (C_n + C_\alpha + C_\beta + C_\gamma)/C_\alpha$
	$H_{\alpha-alk}$	-	H_α in alkyl-substituted aromatic rings: $C_{ar-alk} \cdot \frac{C}{H} \cdot 2$

References: adapted from [68, 69, 73, 74, 80].

peak overlapping than ^{1}H-NMR because of its greater chemical shift scale [55, 69]. This is especially important for estimating ASP because it allows the computation of individual contributions of certain hydrogen and carbon types that would be otherwise unobtainable from the integration of peaks from the ^{1}H-NMR spectrum alone [69–71, 73, 74].

When calculating ASP, the carbon to hydrogen ratio (C/H) is a very important variable and it can be assessed by Elemental Analysis; by ^{13}C-NMR; or by both ^{1}H-NMR and ^{13}C-NMR [54, 70, 71]. In fact, Gillet *et al.* [70, 71] verified the accuracy of ^{1}H-NMR and ^{13}C-NMR analyses by comparing these with Elemental Analysis results. Between both methods, they obtained very similiar C/H values for a synthetic base oil and for various heavy ends from an Arabian light crude oil [70, 71].

2.4.6   Thermogravimetric Analysis

Thermogravimetric Analysis (TGA) is a Thermal Analysis method that monitors the change in sample mass with respect to temperature or time. Unlike DSC, where fast

scan rates allow for increased sensitivity, TGA benefits from lower cooling/heating rates because they favor the completion of processes involving mass loss [82].

TGA curves are often studied with the help of derivative TGA (DTG) thermograms, obtained from the TGA curve itself. The reason for this is the efficiency of DTG in better distinguishing and separating overlapping events [82].

Among examples of studies where TGA finds application are mainly those of decomposition kinetics and polymer thermal and oxidative stability [82]. In the present work, this characterization method was useful for estimating how relevant the loss of light ends is for the waxy crude oil samples within the temperature range under investigation.

2.5   Techniques for measuring WPT/T_{gel}

A number of techniques have been employed in the literature with the aim of quantifying the WPT/T_{gel} of waxy crude oil and model oil samples as alternatives for the ASTM standard cloud and pour point determination methods. This wide variety of methods includes Near-Infrared Scattering (NIR); Photoelectric signal; X-Ray Diffraction (XRD); Laser based solids detection system (SDS); ultrasonic experiments; FTIR; NMR. However, the three most widely used methods for this purpose are Rheometry, Cross Polar Microscopy (CPM), and DSC [19, 23, 28, 30, 35, 83–85]. Each of them is naturally based on different physical and/or chemical principles and has its own peculiarities that make for a lack of precision among detection methods as far as the measurement of this property is concerned.

A brief theoretical basis and bibliographic review are given in Sections 2.5.1, 2.5.2, and 2.5.3 for each technique used in the present work, all of which pertaining to efforts in detecting wax crystallization in petroleum.

2.5.1   Rheometry

Identification of waxy oil gelation by rheometric techniques can be undertaken by stationary experiments, which are based on a sharp increase in viscosity at T_{gel}; or by dynamic (oscillatory) experiments, which are based on the viscoelastic behavior of the oil gel.

Newtonian fluids are ones that present an unvariable viscosity value at a fixed pair of temperature and pressure with respect to time or when the shear rate is varied. For these fluids we can write Equation (2.1):

$$\sigma = \mu \cdot \dot{\gamma} \qquad\qquad (2.1)$$

where σ is the shear stress; μ is the dynamic viscosity; and $\dot{\gamma}$ is the shear rate.

On the other hand, non-Newtonian fluids exhibit shear rate-dependent values for viscosity and a far more complex behavior. The Ostwald-de-Waele or power-law model for non-Newtonian fluids, for example, is given by

$$\sigma = K \cdot \dot{\gamma}^n \tag{2.2}$$

or

$$\sigma = K \cdot \dot{\gamma}^{n-1} \cdot \dot{\gamma} = \eta \cdot \dot{\gamma} \tag{2.3}$$

where K is the consistency index; n is the power-law index; and η is the apparent viscosity, which is a function of the shear rate according to Equation (2.4):

$$\eta = K \cdot \dot{\gamma}^{n-1} \tag{2.4}$$

It is also not difficult to see that Equation (2.1) for Newtonian fluids is a special case of the power-law model when n equals 1 [86, 87].

During cooling of a waxy crude oil sample, as long as the oil still behaves as a Newtonian liquid, the Arrhenius temperature-dependence equation applies (Equation 2.5):

$$\eta = A \cdot \exp \frac{E_a}{RT} \tag{2.5}$$

or

$$\log \eta = A + \frac{E_a}{RT} \tag{2.6}$$

where A is a constant largely dependent on the entropy of activation of flow; E_a is the activation energy; R is the universal gas constant; and T is the temperature [9]. The linearized version of the Arrhenius equation is a plot of $\log \eta$ versus $\frac{1}{T}$, cf. Equation (2.6), and the wax crystallization phenomenon can be observed as the point that first deviates from the straight line. The deviation indicates that the Arrhenius equation is no longer valid and, thus, may be associated with the transition to non-Newtonian behavior. This was the methodology employed by many authors to study waxy oil gelation [9, 12, 21, 25–27, 35, 43, 84, 88].

The investigation of wax crystallization by means of rheometry by oscillatory experiments is based on the viscoelastic behavior of the gel that is formed, a behavior that is intermediate between the elastic solid and viscous liquid behaviors. The contribution of the solid-like and liquid-like behaviors to the overall state of the oil gel relate to the in-phase and out-of-phase response of the resultant motion of the fluid and these are studied by measurements of the elastic - or storage - and viscous - or loss - moduli, respectively. When a waxy crude undergoes cooling, both moduli increase and, eventually, the storage modulus value surpasses the loss modulus value. The increase of both moduli is an indication that waxy crude oil gelation has taken

place and the gelation point is identified as the point where they start increasing.

Wall Slip

The phenomenon of wall slip is often also referred to as wall depletion effects, or simply wall effects. Although they indeed possess very similar meanings, it would be advantageous to first gain insight into wall depletion in order to understand how wall slip presents a problem for Rheometry.

The contact between a smooth, solid surface or wall, and a simple suspension is characterized by a concentration gradient. The concentration of particles right adjacent to the wall is essentially zero, differing from the random spatial concentration of particles in the bulk liquid. It takes about five particle diameters for the concentration of the disperse phase to, in an oscillatory manner, reach an average concentration value. Consequently, the concentration at and near the wall is not representative of that from the bulk fluid, which means the liquid's properties that are being measured at the solid-liquid boundary, for example viscosity on rheometers, will also be different [87, 89].

Wall depletion may result from steric, hydrodynamic, viscoelastic, gravitational, and chemical forces present in suspensions, in spite of the restoring osmotic force arising from the concentration gradient. It is mainly common in concentrated solutions of high-molecular weight polymers; suspensions of large or flocculated particles; and emulsions of large droplet size. As the thickness of the depleted layer is a function of particle or floc size, it is also a function of the shear rate: this low-viscosity, low-concentration, lubricating layer of typical thickness between $0.1\,\mu m$ and $10\,\mu m$ is commonly relevant at low shear rates, when floc sizes are larger [87, 89].

The lubricating or slip layer that stems from wall depletion, as well as its consequences, compose what is called wall slip. Unexpected lower Newtonian plateaus and a decrease in apparent viscosity with decreasing geometry size (tube radius, rheometer gap size), for example, are two ways wall slip may present itself [87, 89].

Although broadly termed in the literature as "slip", the phenomenon described in this section is not characterized by the surface actually losing physical contact with the fluid and "slipping". Instead, it simply relates to the existence of a microscopic liquid layer adjacent to a wall that is poor in the disperse phase and interferes with measurements. An occurrence that more closely resembles actual slip is called adhesive failure in the literature [27, 58].

In the context of rheology, wall slip is evidently an unwanted phenomenon that one might want to try to eliminate or, at least, minimize, as the goal is to measure the fluid's bulk properties. This is achieved, for example, by sandblasting/profiling the contact surface or by the use of rheometric geometries such as cross-hatched parallel plates [87, 90]. These types of surfaces are able to break the depleted layer

16

if their rugosity is higher than the microstructure components. When this is the case, assumptions must be made that no flow occurs between the protrusions and that shear occurs in the space between imaginary surfaces, each one consisting of the protrusion tips of each plate [4, 27].

Rheometer Gap Size

There are several reasons why investigating the influence of rheometer gap size plays an important role in the study of waxy crude oils. The way wall slip manifests itself; thermal control and homogeneity within the sample; and reliable gap-independent results are three illustrations of how choosing the appropriate rheometer gap matters.

The existence of a depleted layer, or the effect of wall slip, interplays with the geometry size - tube radius, rheometer gap size, etc - affecting viscosity measurement values and their veracity. One can instinctively come to the conclusion that, for larger gaps, the depleted layer becomes increasingly unimportant because its thickness, relative to the whole gap, becomes negligible. On the other hand, the smaller the gap, the more important wall slip effects tend to be. Consequently, a decrease in geometry size yields lower viscosity that does not reflect the bulk properties because of the stronger relevance of the depleted layer's low-concentration, continuous phase-rich characteristics [87].

Thermal inhomogeneity is also an aspect that generates some concern in rheometry of waxy crude oils. Thermal homogeneity is desired to ensure the same thermal history within the whole sample. It may be specially a problem when excessively wide gaps are used, given that a Peltier plate undertakes temperature control on one end of the sample only and that a larger sample volume is required for wider gaps [27].

As far as ensuring shear homogeneity is concerned, the cone and plate geometry is the one more prone to impose the same shear rate (or in other words shear history) throughout the sample and has been used by many authors in the study of waxy crude oils [8, 12, 39, 42–44, 53, 86, 91, 92].

However, there is evidence that the cone and plate geometry is inadequate for this purpose because of the small gaps near the cone tip that invalidate the assumptions made in continuum mechanics theory [4, 27]. The reason behind this is the fact that wax crystal aggregates as large as $74\,\mu m$ and $132\,\mu m$ have been observed by Japper-Jaafar *et al.* [4] and Webber [93], respectively. This size dimension surpasses typically available truncation heights for the cone and plate geometry [4, 27]. Therefore, in the rheological analysis of waxy crude oils, the type of geometry used must provide a minimum gap size for which the continuum hypothesis will be ensured and wall slip effects become negligible.

In order to shed light on this matter, Barnes [94] explained how the minimum

gap required for analyzing suspensions of large particles or flocs is a function of the effective phase volume and that a gap-to-particle-size ratio greater than 10 is required for phase volumes above 25%. On the other hand, more recently, Japper-Jaafar *et al.* [4] found that there are some disagreements between minimum-gap determination techniques, including the previously mentioned reasoning of Barnes [94], and that these disagreements probably arise from interlocking and interactions between wax crystals. Japper-Jaafar *et al.* [4] explained from their results that, because wax crystallization and subsequent oil gelation are complex processes, at least for their crude oils, gap-independency analysis should not be based on wax crystal or aggregate size alone. However more work on investigating this relationship still has to be done in the literature.

Besides rendering gaps that are not wide enough for measuring rheological properties of waxy crude oils, the cone and plate geometry has also been associated with too high values of T_{gel} and viscosity, as pointed out by Marchesini *et al.* [27]. According to the authors, also supported by the results from Roenningsen *et al.* [9], it appears that decreasing geometry sizes also tend to promote earlier wax crystallization.

2.5.2 Differential Scanning Calorimetry

DSC is the most often used thermal analysis method, mainly because of its speed, simplicity and availability. It is based on recording the difference in heat flow between a sample and a reference. There are two general, different ways a DSC instrument may operate: power-compensated DSC or heat flux DSC [54].

In the first type, both sample and reference temperatures are kept equal to each other while they are increased or decreased according to the applied temperature ramp. The temperature signal from the sensors is compared to the programmer's signal and the difference is fed into an amplifier, which in turn sends power so as to correct the temperature imbalance arising from thermal transformations in the material. Power-compensated DSC enables the use of very rapid heating/cooling rates with separate furnaces for the sample and the reference [54, 82].

In heat flux DSC, the difference in temperature is measured while the sample temperature is changed at a constant rate through a single heating/cooling unit. Because the primary signal that is measured is temperature, which is then converted into heat flow information, this type of DSC is considered to have grown out of Differential Thermal Analysis (DTA) [54, 82].

The event of interest to the present work that can be detected by means of DSC is an exothermic crystallization peak that pertains to wax crystallization. On the whole, when waxy crude oils or their distillates are characterized by means of

DSC, some commonly obtained thermograms present very broad and/or modest crystallization peaks that may span over $100\,^{\circ}$C in view of the natural complexity of these fluids [25, 26, 32, 95–97]. Nevertheless, these peaks turn out somewhat better defined when model waxy oil samples are utilized [33, 46, 47, 98, 99].

When using scanning rates such as $10\,^{\circ}$C min^{-1}, supercooling effects may occur, and this yields lower temperature values for the crystallization peak. On the other hand, very low cooling rates ($0.1\,^{\circ}$C min^{-1} and lower), in spite of better resembling field conditions and yielding more accurate WPT values, compromise sensitivity because the DSC signal is the time derivative of the enthalpy change [9]. Table 2.2 provides an overview of experimental conditions used for DSC analyses of crude oils.

Table 2.2: Determination of the start of wax crystallization in crude oils by DSC.

Published Work	Cooling Rate ($^{\circ}$C min^{-1})	T_i ($^{\circ}$C)	t_i (min)	Pretreatment
Alcazar-Vara and Buenrostro-Gonzalez [24]	5	85	1	-
Chen, Zhang and Li [100]	5	80	1	2 h at 80 $^{\circ}$C
Elsharkawy, Al-Sahhaf and Fahim [25]	10	70	-	1 h at 80 $^{\circ}$C
Hansen et al. [96]	10	70	-	70 $^{\circ}$C/80 $^{\circ}$C
Claudy et al. [97]	2	Variable	-	1 h at 70 $^{\circ}$C
Kök et al. [101]	2	80	-	15 min at 55 $^{\circ}$C
Kök, Letoffe and Claudy [102]	2	80	-	1 h at 80 $^{\circ}$C
Letoffe et al. [103]	2	80	-	1 h at 80 $^{\circ}$C
Kök et al. [26]	2	80 or 60	-	1 h at 80 $^{\circ}$C
Visintin et al. [45]	10; 5; 2 and 1	60	-	1 h at 50 $^{\circ}$C
Meray et al. [28]	10	90	60	1 day at 50 $^{\circ}$C
Coto et al. [49]	3	80 $^{\circ}$C	-	-

In fact, there is evidence that the wax content might also play a role in DSC sensitivity [30, 37]. Recently, Zhao et al. [30] verified a reduced amplitude of normalized heat flow ($J\,g^{-1}\,K^{-1}$) and lower WPT values with a decreasing weight fraction of wax for their model oil samples.

Additionally, Jiang, Hutchinson, and Imrie [37] concluded that conventional DSC is not sensitive enough to clearly identify the onset of wax crystallization in samples with low wax content, especially at low cooling rates. Instead, according to them, conventional DSC would only be applicable to samples with relatively high wax content. They used a type of MTDSC comercially termed Alternating Differential Scanning Calorimetry (ADSC) and compared results with those from conventional DSC analysis. The former was able to better distinguish wax crystallization in samples with low wax content by the step-like change in the phase angle between the cooling rate and heat flow.

Furthermore, Noel [32] observed that paraffin type or wax composition determines how broad the temperature range for wax crystallization will be. From that work, through the analysis of lube oils by DSC, it became clear that different oil grades and also lube oils originating from distinct crude oils render narrower or broader crystallization peaks according to the composition of the wax phase. For example, a lube oil having a greater proportion of linear alkanes would show an earlier onset of crystallization upon cooling, i.e. located at a higher temperature, than would other oils containing mostly branched paraffins.

Good correlations have been achieved between WPT values determined by DSC and ASTM cloud points, although there is a lack of agreement between correlations from different authors because of the different cooling rates used [97]. In contrast with the results of Noel [32], who reported DSC values $5\,^\circ\text{C}$ higher than ASTM cloud points, Claudy *et al.* [31] and Heino [104] found lower values for DSC experiments. Nevertheless, when pour point experiments are brought into play, Claudy *et al.* [31] and Noel [32] agree that a weight percentage of crystallized paraffins of 1% would be enough to cage the hydrocarbon matrix. This was the amount of precipitated paraffins for which Claudy *et al.* [31] attained the best correlation between PP and DSC experiments.

Modulated Temperature DSC

It appears that there is only one work in the literature that deals with the analysis of wax crystallization in waxy crude oils by MTDSC, which is that of Jiang, Hutchinson, and Imrie [37]. Results from these analyses, however, are not very promising [22, 57]. In this work, we present a different MTDSC technique, comercially termed StepScan, that, as far as we know, has never been used before in the field of waxy crude oils. Details of this specific MTDSC technique, as well as how it differs from the work of Jiang, Hutchinson, and Imrie [37], are given in the next chapter of the present work. Thus, the suitability of StepScan for detecting the WPT has been assesed.

In Modulated Temperature DSC (MTDSC), a function is superimposed on the overall temperature program to produce various heating and cooling cycles as the overall temperature ramp is applied. For a sinusoidal modulation, as an illustration, the temperature at any given time can be obtained by:

$$T = T' - \beta \cdot t + A_T \cdot \sin\left(\omega t\right) \qquad (2.7)$$

where T' is the initial temperature; β, the underlying cooling rate; and A_T and ω are the amplitude and the angular frequency of the temperature modulation, respectively [37]. The advantage of this type of DSC is that the raw signal, or the total

heat flow $\frac{dH}{dt}$, may be subsequently deconvoluted into two parts: one pertaining to transformations controlled by kinetic processes and another associated with changes in heat capacity:

$$\frac{dH}{dt} = C_p\frac{dT}{dt} + f(T,t) \tag{2.8}$$

where H is the enthalpy in $\mathrm{J\,mol^{-1}}$; C_p is the specific heat capacity – heat capacity per mole – in $\mathrm{J\,K^{-1}\,mol^{-1}}$; and $f(T,t)$ is the kinetic response of the sample in $\mathrm{J\,mol^{-1}}$ [54]. Thereby, MTDSC is able to separate overlapping events according to the reversibility of the heat flow signal. The reversing heat flow signal is associated with the heat capacity component, whereas the nonreversing part relates to kinetic processes. Glass transitions, for example, which are associated with a change in heat capacity, appear in the reversing part of the whole thermogram because they are fast enough to be reversing on the time scale of the modulation. Nonetheless, a MTDSC reversing process is not equivalent to a thermodynamically reversible process. Vaporization, for example, is a reversible phase transition that appears in the nonreversing portion of the thermogram because the loss of mass results in a nonreversing event [82].

Glass transition is a transformation that materials containing an amorphous phase undergo and that marks the passage from a glass to a rubbery state upon heating. Beyond this temperature, the long-range translational motion of polymer chain segments, for example, is active; below it, this type of motion is frozen and only the vibrational motion is active. This transition is characterized by a change in viscosity, volume and heat capacity, the latter being identified in a DSC heating thermogram by a relatively sudden increase in the heat flow baseline [54]. This increase in heat capacity takes place not at a definite temperature, but rather in a temperature range [82]. A series of authors detected the glass transition temperature (T_g) of their waxy crude oil and distillate samples using DSC and obtained T_g values as low as approximately $-120\,^\circ\mathrm{C}$ [25, 32, 96, 97, 103].

Differential Scanning Microcalorimetry

There is also some published work in which Microcalorimeters are used to assess wax crystallization [105–107]. These equipment have higher resolution and have been associated with better calorimetric sensitivity than conventional DSC equipment on account of the possibility of utilizing a greater sample mass [82, 105]. This greater sensitivity is associated with the appearance of two exothermic, wax-related crystallization peaks at different temperatures [107]. Microcalorimetric instruments also provide lower scanning rates without compromising sensitivity, which would be useful in simulating operational, waxy crude oil cooling conditions [82, 105].

It is also worth mentioning the work of Gimzewski and Audley [105], who inves-

tigated the onset of paraffin crystallization in diesel with several cooling rates by both DSC and Differential Scanning Microcalorimetry (μDSC). Their results suggest that equilibrium cooling conditions have not been reached, even at $0.01\,°C\,min^{-1}$. They also came to the conclusion that the WPT by DSC with a cooling rate of $1\,°C\,min^{-1}$ agrees fairly well with that obtained by μDSC with a lower cooling rate of $0.01\,°C\,min^{-1}$.

2.5.3 Microscopy

When waxy crude oils are placed between crossed polarizers and illuminated by monochromatic light under an optical microscope, the anisotropic characteristics of paraffin crystals, which give rise to birefringence within the sample, allow for observation of crystal morphology, fractal dimension, and microstructure [12].

In a more detailed manner, the working principle of CPM can be described as follows:

i. After the passage of monochromatic light through the first polarizer, unidirectional light is let through the polarizing filter [12, 108, 109];

ii. The anisotropic characteristics of wax crystals account for rotation of the plane of polarized light [57, 108];

iii. Once the direction of this plane has been altered, the other polarizing filter, often termed "Analyzer", whose light-filtering properties are perpendicular to the first one in terms of direction, allows some light to pass [108, 109];

iv. Finally, observation of paraffin crystallization in dark crude oils becomes possible.

Additionally, CPM may work under two different optical pathways: reflected or transmitted light, although, ultimately, the aforementioned operational basis is the same [109].

Even though there is a small degree of subjectivity that arises from the operator's perception, CPM has consistently been reported to be the most sensitive of detection techniques for the start of wax crystallization [9, 16, 18, 57]. In fact, in a very recent review, Fogler, Zheng and Huang [57] gathered published data on commonly used measurement techniques, and analyzed pairs of comparison between CPM and DSC; and CPM and viscometry. They discerned a greater number of cases in which CPM presented higher temperature values for the start of wax crystallization than the other two methods. In other words, according to them, there were 35 examples of WAT$> T_{gel}$, against 8 for WAT$< T_{gel}$; and also 35 examples of WAT$>$WPT, against 16 in which WAT$<$WPT. A few examples of previous works on WAT determination

by CPM, as well as the experimental conditions used in them, are given in Table 2.3.

One of the shortcomings of CPM is that the light intensity observed by the operator depends to some extent on wax crystal orientation [108, 110]. If a paraffin crystal has its long, optical axis oriented parallel to the direction of the plane of light that comes from the first polarizer, it will be in a "position of extinction", which virtually means it will be invisible to the operator [108]. As Paso *et al.* [110] explained, maximum brightness of wax crystals observed by CPM will occur for crystals oriented in a way that this long axis forms a 45° angle with either axes of the polarizers [108]. Therefore, according to Paso *et al.* [110], measurements of exact crystal dimensions by CPM may become compromised and upper-bound output parameters, such as maximum crystal length, may be more accurate for estimation.

Table 2.3: Determination of WAT in crude oils by CPM.

Published Work	Cooling Rate ($°C \, min^{-1}$)	T_i (°C)	t_i (min)	Pretreatment
Visintin *et al.* [45]	1; 0.05	50	-	1 h at 50 °C
Cazaux, Barre and Brucy [35]	-	60	10	50 h at 80 °C
Brown, Niesen and Erickson [52]	0.2	65	60	-
Karan, Ratulowski and German [34]	1	60/80	-	60 °C/80 °C
Hammami and Raines [23]	1	60	-	30 min at 60 °C
Erickson, Niesen and Brown [18]	0.6	-	-	Preheating
Paso, Kallevik and Sjöblom [83]	0.5	20-30°C above WAT	-	-
Coto *et al.* [49]	3	50	-	1 h at 50 °C

While the aforementioned "extinction" effect may be true, in previous works, many authors have obtained valuable information on the microstructure and dimension of waxy components in their aggregated/crystallized form by analyzing paraffin crystal fractal dimension, maximum length or size distribution [4, 11, 49, 56, 109–114]. Furthermore, model oil samples are expected to generate sharper images by CPM owing to their lower chemical complexity in comparison with crude oils, which might aid the study of wax crystal morphology [99].

For instance, the fractal dimension parameter provides an estimation of the non-linear, irregular, and complex morphological characteristics of wax crystals and their aggregates [112]. Yi and Zhang [56, 111], as well as Gao, Zhang, and Ma [112], studied the effect of PPD on wax crystal size and fractal dimension by Microscopy. They verified that addition of PPD under static cooling conditions resulted in an increase

of wax crystal fractal dimension and size, suggesting a more intricate, complex microstructure when the PPD was present. Moreover, Yi and Zhang [56] also evaluated the effect of shear on their PPD-modified samples, and observed that shear could break wax crystal aggregates to varying extents depending on oil composition, resulting in a decrease of their fractal dimension and size.

Chapter 3

Methodology

This chapter begins by giving the reader an overview of the methodology used in this work (Figure 3.1), as well as by predefining the general test conditions that the oils were submitted to in characterization experiments. Furthermore, general test conditions for WAT, WPT and T_{gel} experiments are also defined and properly justified (Table 3.1). Additionally, a third oil sample (A3) is presented, which was kindly provided by Marchesini [115]. This previously pretreated waxy crude oil also underwent TGA characterization in order for the potential source of error of loss of light ends to be evaluated (Section 3.1.5).

Figure 3.1: Summary of the methodology employed in the present work.
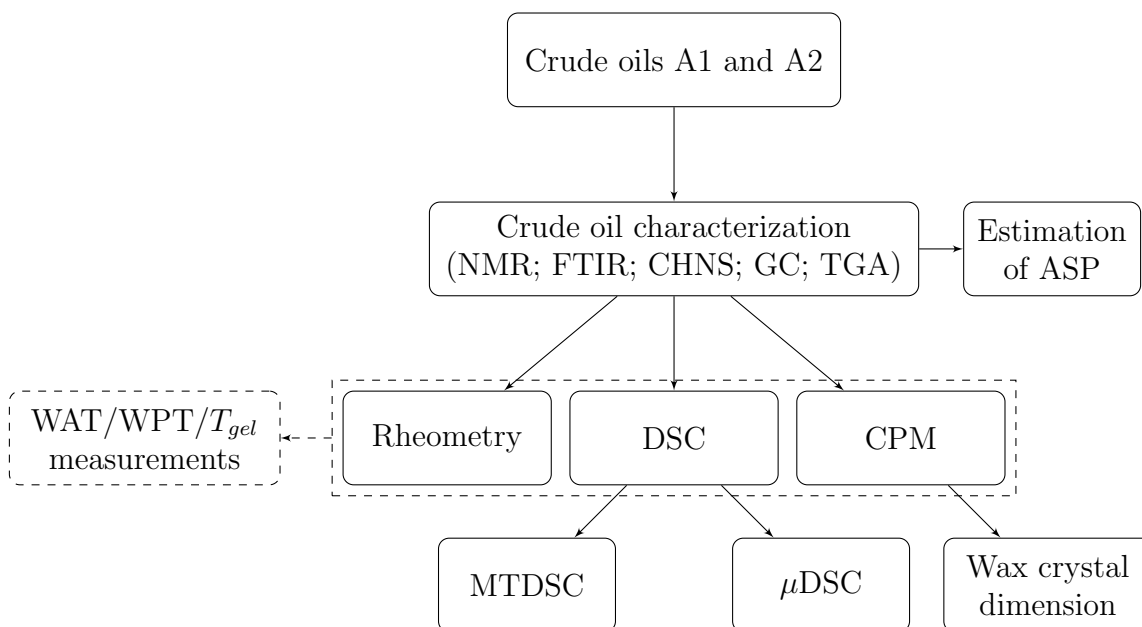
Reference: elaborated by the author.

3.1 Crude oil characterization

In addition to the techniques described in this Section, American Petroleum Institute (API) gravity analyses were made for both samples according to ASTM D4052. These analyses were provided by the Centro Nacional de Pesquisas Leopoldo Américo Miguez de Mello from PETROBRAS.

3.1.1 GC

Waxy crude oils were analyzed by GC/FID in a Shimadzu GC-QP2010 Ultra system coupled to an RTX-1MS column. The temperature program was: $100\,°C$ for $5\,min$; $10\,°C/\,min$ to $300\,°C$ and hold for $15\,min$; followed by $10\,°C/\,min$ to $310\,°C$ and hold for $30\,min$. The injector and detector temperatures were set at $290\,°C$ and $320\,°C$, respectively. Moreover, xylene was used as a solvent, and the injection volume was $1\,µL$, while helium was employed as a carrier gas. Additionally, the linearity standard used was ASTM D5442 C_{12} - C_{60}. GC characterization was executed in the Laboratório de Macromoléculas e Colóides na Indústria de Petróleo (LMCP), at the Instituto de Macromoléculas from UFRJ.

3.1.2 FTIR

Spectra of crude oil samples were recorded on a PerkinElmer Frontier FTIR/FIR spectrophotometer with a resolution of $4\,cm^{-1}$, as a result of 20 accumulated scans. Before being placed in the instrument, oil samples were painted on a KBr plate. These analyses were carried out in the Laboratório de Apoio Instrumental, at the Instituto de Macromoléculas from UFRJ.

3.1.3 CHNS

Elemental analysis was performed on a Thermo Scientific Flash 2000 CHNS Organic Elemental Analyzer, onto which the samples were loaded without any kind of previous treatment, and results correspond to the average of three individual determinations. CHNS analysis was carried out at the Centro Nacional de Pesquisas Leopoldo Américo Miguez de Mello from PETROBRAS.

3.1.4 NMR and Estimation of ASP

The ^{1}H-NMR spectrum was obtained on a Varian Inova-300 spectrometer at $500\,MHz$, operating at $303.2\,K$. 128 scans were accumulated, with a line broadening of $0.3\,Hz$ and acquisition time of $3.27\,s$. ^{13}C-NMR analysis was carried out on a Bruker Advanced NMR equipment at $75\,MHz$ with 5000 repetitions; in the

inverted gated decoupling mode; at 300.1 K; with an acquisition time of 0.86 s; and line broadening of 5 Hz.

Both ^{1}H-NMR and ^{13}C-NMR analyses, along with ASP calculations, were provided by the Centro Nacional de Pesquisas Leopoldo Américo Miguez de Mello from PETROBRAS. ASP calculation and chemical shift regions and assignments, in turn, were based on the works of Hasan, Ali, and Bukhari [69, 73]. The C/H ratio obtained from ^{13}C-NMR, which can be calculated using Equation (3.1), served as input information for ASP estimation in the present work.

$$\frac{C}{H} = \frac{C_{\text{sat}} + C_{\text{ar}}}{2 \cdot C_{\text{sat}} + C_{\text{ar}}} \tag{3.1}$$

3.1.5 TGA

TGA results are useful for evaluating the potential experimental error deriving from the loss of lighter components at higher temperatures. This was estimated for our crude oil samples by comparison with the pretreated waxy crude oil sample used in the work of, and kindly provided by Marchesini [115]. For practical reasons, this sample is herein referred to as A3.

Waxy crude oils A1, A2, and A3 were analyzed on a Pyris 1 TGA equipment from Perkin Elmer under flowing (30 mL/ min) oxygen atmosphere. This analysis was run only once with a sample mass of around 4 mg to 9 mg and the goal was to reproduce as close as possible the cooling and heating conditions used in the T_{gel} rheological experiments (Section 3.2). Therefore, the cooling program on the instrument obeyed the following procedure:

i. heating the sample from ambient temperature to T_i at 20 °C/ min;

ii. isothermally keeping the sample at T_i for a period of time t_i;

iii. cooling to ambient temperature (uncontrolled);

iv. repeating the heating process from ambient temperature to T_i, this time at a heating rate of 1 °C/ min.

Because of our TGA device's limitations, this method differs to some extent from the one employed for rheological experiments in the sense that cooling from T_i to ambient temperature cannot be controlled and occurs naturally. Additionally, cooling to 4 °C is also unfeasible.

However, the high-temperature extremes represent a zone where the loss of light ends is more likely to take place and this zone can be correctly reproduced by the aforementioned TGA method. Thus, we are in a position to estimate this potential source of error by comparing results for oils A1 and A2 with those for the pretreated

oil sample A3, given that, for the latter, this source of error had been previously minimized [115].

3.2 WPT/T_{gel} experiments

In the present work, when it comes to distinguishing the start of wax crystallization using different measurement techniques, a few general rules apply. In other words, for CPM, rheological, and conventional DSC experiments, the two Brazilian waxy crude oil samples were:

i. shaken vigorously in their respective bottles before sampling from them in order to promote homogenization;

ii. loaded on the respective analytical instruments at ambient temperature and taken to the corresponding initial temperature T_i at approximately $20\,°C/\min$;

iii. submitted to two different thermal history conditions, which are presented in Table 3.1;

iv. cooled at $1\,°C/\min$ to a final cooling temperature (T_0) of $4\,°C$, a typical minimum seabed temperature in deepwater, offshore oil production [4, 116].

v. tested for each experimental condition at least three times. Wall slip, MTDSC, and μDSC tests were run only once.

Table 3.1: Conditions used in experiments for WAT/WPT/T_{gel} determination.

Thermal treatment	T_i (°C)	t_i (min)	Measurement technique
"Erased history"	80	15	Rheometry
			DSC
			CPM
			MTDSC
			μDSC
"Non-erased history"	50	30	Rheometry
			DSC
			CPM[1]

Tests for different thermal history conditions were conducted in order to study the process of wax crystallization with distinct initial temperatures: one that is more representative of the operational thermal conditions that both crude oils are exposed to ($T_i = 50\,°C$), and another ($T_i = 80\,°C$) that is necessary for complete wax dissolution, and for reproducible rheological measurements to be obtained [8]. The

---

[1]Thermal history condition only applicable to wax crystal dimension analysis.

choice of additionally utilizing a lower initial temperature of $50\,°C$ is also justified by the fact that higher, more conservative values of flow-related measures have been obtained in this temperature range in the past [27, 34, 48, 50] and this is naturally desirable for commercial interests of preventing Flow Assurance problems.

A longer isothermal holding time, t_i, was elected for $T_i = 50\,°C$ to allow for increased dissolution of wax crystals. Furthermore, it is also important to mention that, because wax crystals were still present after both samples were kept at $50\,°C$ for 30 min, only CPM experiments with $T_i = 80\,°C$ were taken into account for WAT determination (Table 3.1). Therefore, CPM results for $T_i = 50\,°C$ were only used in the analysis of wax crystal dimension and not for WAT determination.

Also according to the aforementioned reasoning, MTDSC and μDSC tests with $T_i = 50\,°C$ and $t_i = 30$ min were not carried out. The goal was to ascertain how sensitive these techniques are with respect to detecting the very start of wax crystallization in crude oils A1 and A2. Hence, employing the "non-erased history" conditions for these tests would not suit our purposes. Furthermore, specific test conditions for these calorimetric techniques will be described separately in Sections 3.2.2.

3.2.1   Rheometry

Rheological experiments were conducted with the aim of investigating how oil gelation correlates with the start of wax crystallization by identifying T_{gel}. Moreover, the effects of thermal history and various gap sizes on T_{gel}; final viscosity (η_{h0}) of the cooling process; and the overall non-Newtonian behavior of waxy crude oils below T_{gel} during the cooling process have also been analyzed.

The tests described in the present section were based on the method used by Marchesini [115] called thermal-cycle test. According to this method, a constant temperature ramp and shear rate are applied to the waxy crude oil sample during cooling from T_i to T_0. When T_0 is reached, the sample undergoes heating at the same rate back up to the initial temperature T_i. Viscosity values are then plotted as a function of temperature [115]. Figure 3.2 illustrates this entire procedure and highlights the important rheological parameters that can be derived thereof.

In Figure 3.2, ξ denotes the difference in viscosity between the two Arrhenius portions of the thermal-cycle test, the cooling and heating portions, which do not coincide [115]. This factor relates to irreversible changes in chemical composition during the test and these seem to be common for chemically complex fluids such as waxy crude oils [115]. For instance, mineral oils studied by Webber [93] did not display a value of ξ ubiquitously greater than zero the way the waxy crude oil tested by Marchesini [115] did.

Figure 3.2: Thermal-cycle test employed by Marchesini, where T_c is the crystallization temperature, equivalent to T_{gel}.
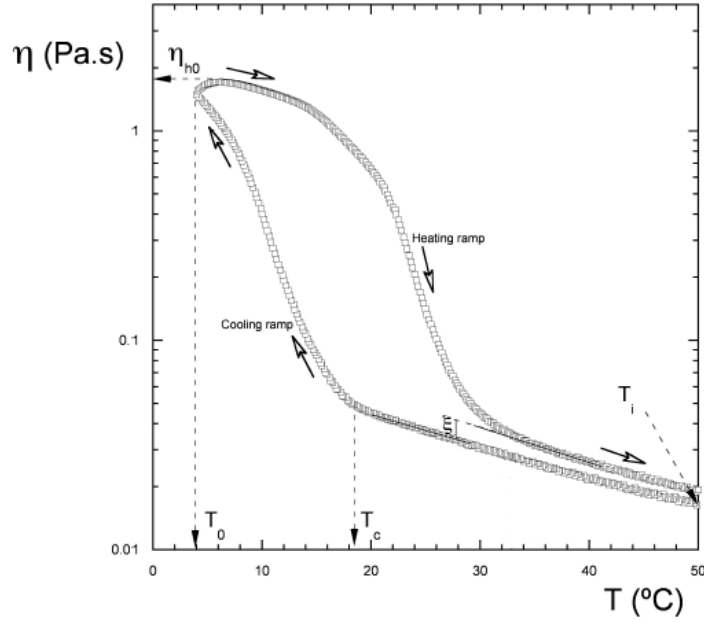
Reference: Adapted from [115].

The waxy crude oil samples were submitted to a shear rate of $20\,\mathrm{s}^{-1}$ on a Discovery HR-3 Rheometer from TA Instruments fitted with $60\,\mathrm{mm}$ smooth parallel plates (SPP). Temperature control was achieved with a Peltier device and T_{gel} values were measured using onset-point determination on the TRIOS software from TA Instruments.

Various gap sizes were used for each crude oil in order to ascertain their gap-dependent behavior with SPP, as displayed in Table 3.2. Rheological tests with a gap size of $3.0\,\mathrm{mm}$ were experimentally impracticable with a initial temperature as high as $T_i = 80\,°\mathrm{C}$ because, due to low viscosity values at this temperature, the oil would flow out of the geometry during the equilibration time period of $15\,\mathrm{min}$.

Table 3.2: Rheometric gap sizes used for T_{gel} determination with SPP.

Waxy crude oil	Gap sizes (mm)	
	$T_i = 50\,°\mathrm{C}$	$T_i = 80\,°\mathrm{C}$
	1.5	1.5
A1	2.0	2.0
	2.5	2.5
	-	1.5
A2	2.0	2.0
	2.5	2.5
	3.0	$-^2$

---

[2]Impracticable experimental conditions.

30

In order to evaluate whether each gap was large enough for obtaining gap-independent results, Fisher's Least Significant Difference (LSD) test was made using the software Statistica from StatSoft. Based on a 95% confidence interval, pairs of comparisons between any two gaps that yielded statistically different values either for T_{gel} or η_{h0} were rendered not sufficiently large for obtaining gap-independent results.

Additionally, crude oil A1 was also tested for wall slip with 60 mm cross-hatched parallel plates (XPP); gap sizes of 1.5 mm and 2.5 mm; $T_i = 50\,°C$; and $t_i = 30\,min$.

3.2.2 DSC

Conventional DSC experiments were carried out on a Pyris Diamond DSC instrument from PerkinElmer and baseline runs were completed for every test with empty sample and reference furnaces. Then, around 7 mg to 9 mg of crude oils A1 and A2 were weighed and sealed in 10 µL aluminum pans. The subsequent procedure follows the one described in the beginning of Section 3.2, while the sample furnace was continuously purged with dry nitrogen (20 mL/ min). Finally, all DSC data and calculations, such as determination of WPT, were processed using the Pyris software.

MTDSC

The Brazilian waxy crude oil samples from the present work were also analyzed by means of MTDSC, namely by the StepScan technique, on a Pyris Diamond DSC instrument from PerkinElmer. Similarly to other MTDSC methods, this approach enables the separation of processes that occur simultaneously and overlap, according to Equation (2.8).

The difference in StepScan compared to other MTDSC techniques is that the sample is either linearly heated/cooled or held isothermally multiple times (Figure 3.3), instead of undergoing a constant sinusoidal temperature modulation such as that of Equation (2.7). During an isothermal step, for example, the heat flow information pertains only to kinetic transformations in the sample. One of the advantages that StepScan offers compared to sinusoidal modulations is the accuracy in temperature equilibration because the scan rate in sinusoidal MTDSC is constantly varying and, as a consequence, so do temperature gradients in the sample. Therefore, factors related to sample preparation or to the method itself such as sample size; amplitude and frequency of the modulation; and coupling of the sample to the pan contribute to thermal lag [117].

Baseline runs were completed for MTDSC tests with empty reference and sample pans that had been previously weighed. Then, around 7 mg to 9 mg of crude oils

A1 and A2 were weighed and sealed in the $10\,\mu L$ sample aluminum pans used for the baseline run. Subsequently, the sample was quickly brought to a temperature $T_i = 80\,^\circ C$ in the DSC equipment and kept at this temperature for 15 min, much like some of the analyses displayed in Table 3.1. The sample furnace was continuously purged with dry nitrogen ($20\,mL/\,min$) and, lastly, all MTDSC data were processed using the Pyris software.

The cooling process obeys the schematic representation in Figure 3.3, where ΔT_{SS}; Δt_{iso}; and the ratio $\frac{\Delta T_{SS}}{\Delta t_{SS}}$ are all adjustable parameters and correspond respectively to the temperature step; duration of the isothermal step; and applied cooling rate. For optimal data resolution; scanning equilibration; and given that

Figure 3.3: Schematic representation of the cooling process according to the StepScan method.
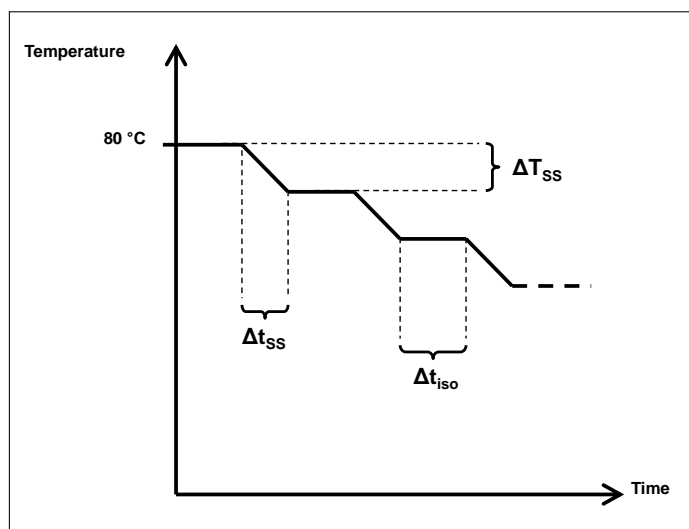
Reference: elaborated by the author (figure not drawn to scale).

the samples were complex fluids, values for these variables were chosen as follows: $\Delta T_{SS} = 1\,^\circ C$; $\Delta t_{iso} = 30\,s$; $\frac{\Delta T_{SS}}{\Delta t_{SS}} = 1\,^\circ C/\,min$. The final cooling temperature of $4\,^\circ C$ would, thus, amount to a temperature decrease of $80\,^\circ C - 4\,^\circ C = 76\,^\circ C$; and, along with the other conditions, total experiment time would be 126 min. This, in turn, would correspond to an equivalent, theoretical cooling rate of $\frac{76\,^\circ C}{126\,min} \approx 0.6\,^\circ C/\,min$. However, what actually determined total experiment time was the chosen criteria of $0.01\,mW$, which means t_{iso} may be shorter than 30 s if the heat flow information equilibrates within $0.01\,mW$.

μDSC

Microcalorimetric experiments were done on a SETARAM EVO VII model and sample masses of waxy crude oils A1 and A2 for this type of analysis were, respectively, 313.9 mg and 222.3 mg.

Before cooling began, samples were heated to a temperature of $80\,°C$ at $1\,°C/\min$ and kept at this temperature for $15\,\min$ in order for wax crystals to dissolve. Then, they were cooled to $-10\,°C$ at $1\,°C/\min$ and kept at $-10\,°C$ for $2\,\min$.

Microcalorimetry has been reported to be more sensitive for detecting wax crystallization [105, 107, 109]. Thus, by detecting crystallization peaks that would otherwise not be revealed, better, more accurate calculations of the total wax content in crude oils A1 and A2 can be made. This, in turn, and for Calorimetry in general, can be done using Equation (3.2):

$$w_{wax} = \frac{Q}{\Delta H \cdot m_s} \tag{3.2}$$

where w_{wax} is the total wax content in the sample in weight fraction; Q is the total heat released in the desired temperature range in Joule; m_s is the sample mass in gram; and ΔH is the heat of crystallization in $J\,g^{-1}$, for which an estimated value of $200\,J\,g^{-1}$ can be used [57, 97].

3.2.3 CPM

The microscope used was a Carl Zeiss AxioImager.A2m equipped with a AxioCam MRc5 digital camera and samples were viewed under reflected light with a 20x objective lens. Moreover, temperature control was managed by a Linkam T95-PE system.

Sample preparation for CPM consisted of placing a drop of oil onto a microscope slide and, afterwards, another identical glass slide was placed on top of the oil sample in order for it to spread out. The upper-slide was then pulled to the side so as to leave a thin film of crude oil open to the atmosphere on the lower glass slide. This was done because examination of waxy crude oil samples placed between two surfaces, and thus with a decreased oil film thickness, could bring about premature wax crystallization [9].

Investigation of wax crystal dimensions

Three runs on fresh samples were made for WAT determination and, additionally, micrographs were taken at $4\,°C$; at $28.9\,°C$ (crude oil A2); and also between $22.3\,°C$ to $23.6\,°C$ (crude oil A1) for studies of crystal dimensions. AxioVision version 4.8 image acquisition and processing software was used for processing of micrographs. More specifically, an Automatic Measurement Program was used to measure parameters of wax crystal dimensions. The parameters chosen for this study were:

i. Feret maximum (F_m): a measure based on the distance between two points on opposite sides of a region at 32 angle positions (Figure 3.4). The maximum

distance obtained in this fashion is computed as the Feret maximum;

ii. Feret ratio (F_r): ratio between the analogously determined values of Feret minimum and Feret maximum ($\frac{Feretminimum}{Feretmaximum}$);

iii. Area percent (A_p): Area percentage of all detected regions, with respect to the area of the measurement frame. The filled area of individual regions was computed (Figure 3.4);

Thus, these parameters serve, respectively, as estimations of wax crystal length; aspect ratio; and area.

Figure 3.4: Illustrative examples of measurement parameteres.
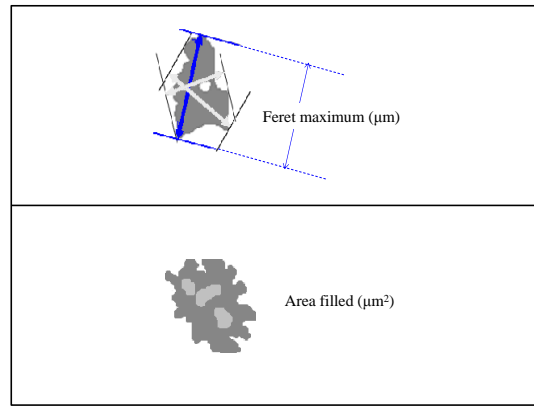
Reference: elaborated by the author.

Figure 3.5 illustrates how the automatic detection of wax crystal regions is carried out, where the green contours delineate individual regions for which calculations are made. According to this process, very small, gray regions, which cannot even be seen in the original frame, are included in the measurements. Therefore, in order for only the more relevant, whiter crystal structures to be counted, as a cut-off criterion for calculations, we did not consider detected regions with a F_m value smaller than 1 µm. This seems to be a reasonable assumption as far as the resolution of CPM is concerned [9, 11, 18, 23, 35, 109].

Figure 3.5: Illustrative example of automatic detection of wax crystals.
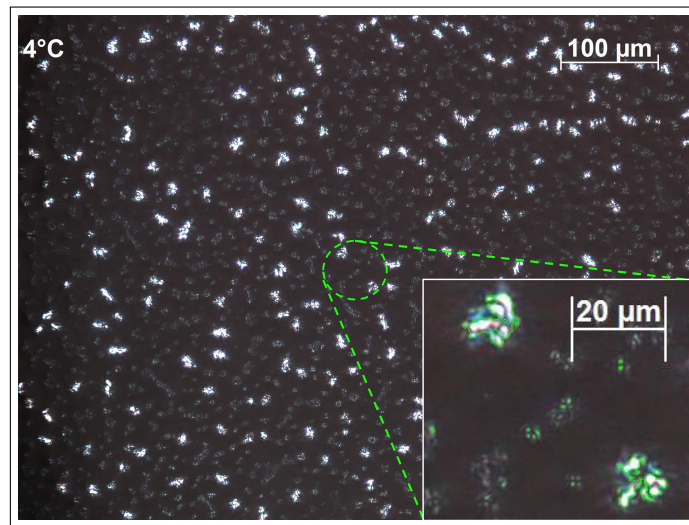
Reference: elaborated by the author.

Chapter 4

Results and Discussion

In this chapter, results from the chemical and physical characterization of crude oils A1 and A2 are first presented (Section 4.1). We then proceed to present and compare the precision/accuracy of measurement techniques in detecting the start of wax crystallization in oils A1 and A2 (Section 4.2).

All error bars in graphics from this chapter are based on standard error calculations. If they cannot be seen for certain data points, this is due to the error bar being too small.

4.1 Crude oil characterization

API gravity determination yielded values of 28.38°API for crude oil A1 and 23.25°API for crude oil A2. Therefore, in comparison with sample A1, A2 is a heavier crude oil.

4.1.1 GC

The chromatograms for both oil samples can be found in Figure 4.1. Alternately, Table 4.1 provides quantitative data on this analysis, in terms of the compounds that can be identified; their characteristic retention times; and respective peak area, which is directly proportional to their concentration in the samples.

We were only able to identify paraffins with an even number of carbons and, furthermore, we were unable to quantify them in absolute terms. However, given that equal concentrations of oil A1 and A2 were prepared and that the peak areas are directly proportional to the relative amount of each compound in the sample, valuable information can be obtained from the chromatograms.

Except for slightly higher contents of C_{20} and C_{32} n-paraffins in crude oil A2, A1 is the sample with the larger amount of straight-chain alkanes. Furthermore, both

Figure 4.1: GC chromatograms for the waxy crude oils under investigation.
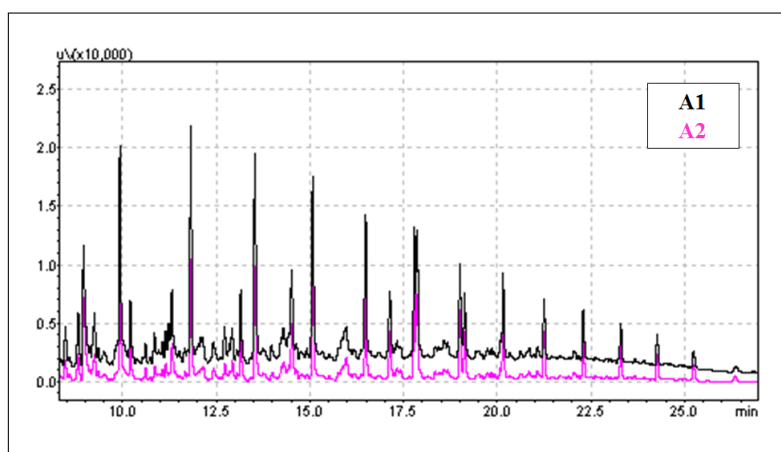
Table 4.1: Paraffin type and respective peak information detected by GC.

Type of compound	A1		A2	
	Retention time (min)	Peak area	Retention time (min)	Peak area
C_{12}	9.932	53181.6	9.935	28037.5
C_{14}	13.533	60834.1	13.541	30925.3
C_{16}	16.487	40466.6	16.489	24588.6
C_{18}	18.681	1575.8	18.683	1067.1
C_{20}	19.133	14193.6	19.008	16059.6
C_{22}	21.249	15733.7	21.248	12155.2
C_{24}	22.293	14415.4	22.293	11110.4
C_{26}	23.295	11530.3	23.297	9585.2
C_{28}	24.268	8768.1	24.273	7571.9
C_{30}	25.240	6332.2	25.242	5842.5
C_{32}	26.366	3447.9	26.347	3554.9

crude oils have similar n-paraffin distribution, and no n-alkanes with a chain length longer than 32 carbon atoms were detected.

It is important to mention that this kind of analysis does not provide information about microcrystalline wax (branched-chain and cyclic alkanes, for example) or other crystallizable components. Therefore, up to this point of the present work, no conclusions pertaining to the total wax content may be drawn yet.

4.1.2 FTIR

FTIR spectra are presented in Figure 4.2 and Table 4.2 indicates the absorption bands that can be identified in both spectra.

It is clear that the spectra from both crude oils are very similar and typical of compounds having long n-alkyl chains, given that all characteristic bending and stretching modes of normal alkanes are present [60, 109]. These absorb mainly at $2953\,cm^{-1}$; $2923\,cm^{-1}$; $2853\,cm^{-1}$; $1462\,cm^{-1}$; $1377\,cm^{-1}$; and $721\,cm^{-1}$, the latter one being specifically associated with long chain n-alkanes [60]. The other absorption

Figure 4.2: FTIR results for the two Brazilian crude oils: (a) FTIR spectrum for crude oil A1; (b) FTIR spectrum for crude oil A2.


(a)

(b)
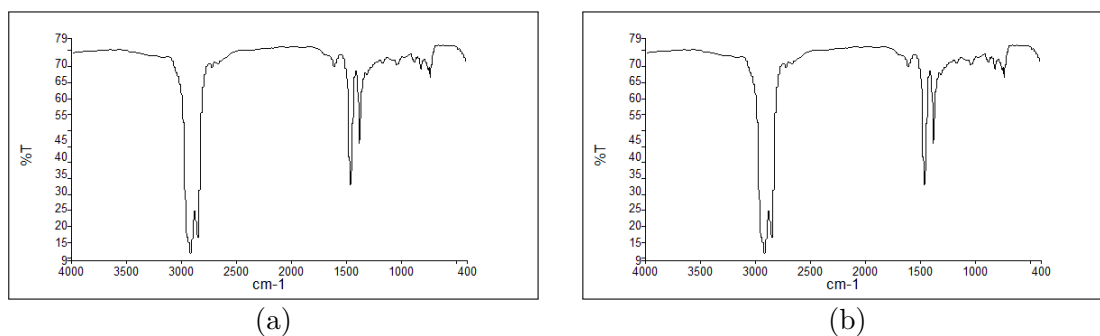
Table 4.2: Wavenumbers and associated molecular motion of absorption bands identified in FTIR spectra of crude oils A1 and A2.

Wavenumber (cm^{-1})	Type of vibrational motion	Type of chemical group
2953	asymmetrical stretching	CH_3
2923	asymmetrical stretching	CH_2
2853	symmetrical stretching	CH_2
1603	ring streching	C=C
1462	in-plane bending or scissoring	CH_2
1377	symmetrical bending	CH_3
1032	ring in-plane bending	CH
872	ring out-of-plane bending	CH
811	ring out-of-plane bending	CH
721	in-plane bending or rocking	CH_2

References: [60, 65].

bands may be related with a low content of aromatic compounds [60, 61, 63–66].

4.1.3 CHNS

Results for Elemental analysis are displayed in Table 4.3 and they consistently confirm the light, paraffinic character of the oil samples due to their low $\frac{C}{H}$ ratio. Furthermore, elemental weight percentages are individually in very close agreement between waxy crude oils A1 and A2. The very low nitrogen and sulphur contents resonate with the absence of carbonyl absorption bands at $\approx 1710\,\mathrm{cm}^{-1}$ in FTIR spectra [61, 62], and indicates a very low content of acidic substances in crude oils A1 and A2 [61, 62].

Table 4.3: Elemental analysis results.

Waxy crude oil	Elemental weight percentage (%)				$\frac{C}{H}$ (Molar ratio)
	C	H	N	S	
A1	86.1	12.3	0.5	<0.3	0.5833
A2	85.5	12.3	0.5	<0.3	0.5793

4.1.4 NMR and ASP Estimation

The relative proportions of ^{13}C and ^{1}H nuclei in each crude oil sample, along with calculated ASP, are presented in Table 4.4. Additionally, all NMR spectra can be found in Appendix A.

Table 4.4: ^{1}H-NMR and ^{13}C-NMR results (relative amount of different ^{13}C and ^{1}H nuclei) and ASP estimations.

Parameter	Waxy crude oil	
	A1	A2
C_{sat}	85.8%	82.9%
C_{ar}	14.2%	17.1%
C_{ar-H}	1.6%	1.8%
C_{ar-alk}	2.9%	3.7%
H_{α}	6.5%	7.6%
$H_{\beta 1}$	7.6%	7.3%
$H_{\beta 2}$	53.9%	55.2%
H_{β}	61.5%	62.5%
H_{γ}	28.9%	25.7%
H_{sat}	96.9%	95.8%
H_{mar}	0.9%	1.0%
H_{dar}	2.3%	3.2%
H_{ar}	3.1%	4.2%
f_a	0.142	0.171
C/H ratio	0.5383	0.5467
% SCA	33.6	33.3
ACL	17	17
% C_{Me-t}	3.9	3.9
% C_{Me-b}	6.6	5.5
(Total CH_3)/(paraffinic CH_2)	0.35	0.32
(Branched CH_3)/(paraffinic CH_2)	0.22	0.19

From NMR data, crude oils A1 and A2 are very similar in terms of ^{13}C and ^{1}H nuclei and ASP. Perhaps the most contrasting aspect is the slightly higher C_{ar}, H_{ar}, and H_{dar} proportions for oil A2. This might indicate a slightly higher content of asphaltenes and resins for this sample.

Another more dissimilar aspect is the slightly higher proportion of H_{γ} and C_{Me-b} for crude oil A1. Although this may indicate a greater degree of branching and, in a way, conflict with GC results, it is important to keep in mind that NMR analysis takes into account every chemical species in these crude oil samples. Therefore, these more branched compounds may not necessarily be related to the wax fraction. Consequently, the smaller proportion of H_{γ} in crude oil A2 likely pertains to extant cyclic compounds and/or alkyl chains attached to aromatic rings (C_{ar-alk}). These results may be an indication of a relatively larger amount of microcrystalline wax in oil A2 [118].

It is also interesting to note that the $\frac{C}{H}$ ratio by NMR analysis, calculated with Equation (3.1) and used for ASP estimation, correlates well with the $\frac{C}{H}$ value by CHNS. Moreover, although Gillet *et al.* [70] obtained an even better agreement between these techniques, their analyte was a far less complex mixture of alkylbenzenes.

4.1.5 TGA

TGA tests were performed in order to mimic as close as possible the conditions of rheological experiments. Therefore, crude oils A1 and A2 were submitted to both thermal history protocols described in Table 3.1. As for crude oil A3, it obeyed the "non-erased history" conditions described in Table 3.1 in order to resemble the experiments from Marchesini [115].

TGA curves for these crude oils are presented in Figure 4.3. While they do not exactly simulate the heating and cooling ramps from T_{gel} tests in view of our TGA instrument's cooling limitations, it is clear that the mass loss from samples A1 and A3 are comparable. Furthermore, crude oil A2 appears to be the one less prone to lose lighter components.

Figure 4.3: TGA curves for waxy crude oils A1, A2, and A3 according to their respective thermal history protocols.
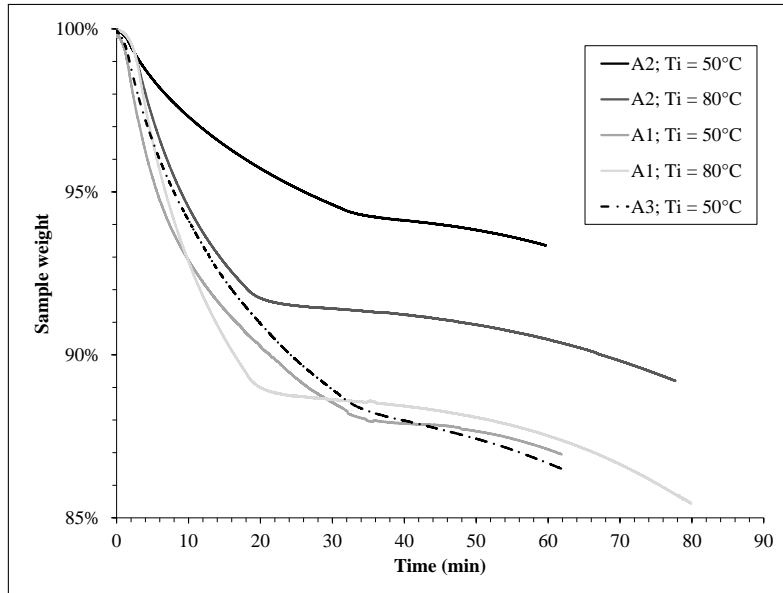
From the results shown in Figure 4.3, it is safe to say that the loss of light ends is not a significant source of error for crude oils A1 and A2, given that pretreated crude oil A3 loses a commensurate amount of mass with respect to our waxy crude oils.

4.2 WPT/T_{gel} measurements

In this section, we present the results from CPM, Rheometry, conventional DSC, MTDSC, and μDSC measurements, pertaining to their sensitivity in detecting the start of wax crystallization. We also evaluate, for Rheometry and conventional DSC, the effect of heating the waxy crude oils to an intermediate temperature ($T_i = 50\,^{\circ}\mathrm{C}$) on the detection of the start of wax crystallization. This temperature, in spite of not being high enough for complete wax dissolution, better reproduces oilfield conditions that crude oils A1 and A2 are submitted to.

4.2.1 Determination of T_{gel} by Rheometry

First, for the correct determination of T_{gel}, gap-independent results have to be obtained. Hence, we conducted thermal-cycle tests with several gap sizes, and these tests for sample A1 are shown in Figure 4.4. Moreover, Figure 4.5 summarizes η_{h0} and T_{gel} information that can be obtained from the thermal-cycle tests for crude oil A1.

Figure 4.4: Thermal-cycle tests for crude oil A1. Blue-colored curves pertain to the "non-erased history" case ($T_i = 50\,^{\circ}\mathrm{C}$), while red-colored curves pertain to $T_i = 80\,^{\circ}\mathrm{C}$.
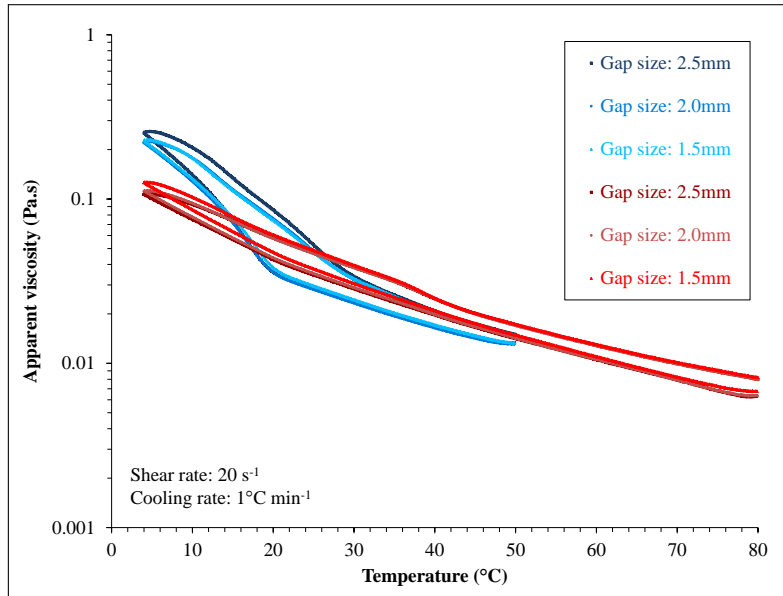
The analysis of gap-independent T_{gel} for the lower initial temperature is as follows. A slightly higher T_{gel} is obtained with a 1.5 mm and a 2.0 mm gap, even though these gaps do not seem to yield higher η_{h0}. The larger, 2.5 mm gap does seem to yield gap-independent results because of its slightly lower T_{gel} (Figure 4.5).

When cooling from 80 °C, a gap of 2.0 mm appears to be large enough for gap-independent results to be obtained because η_{h0} increases slightly when the gap is decreased to 1.5 mm and T_{gel} values statistically do not vary between these gaps

Figure 4.5: T_{gel} and η_{h0} as a function of gap size and thermal history protocol for crude oil A1.
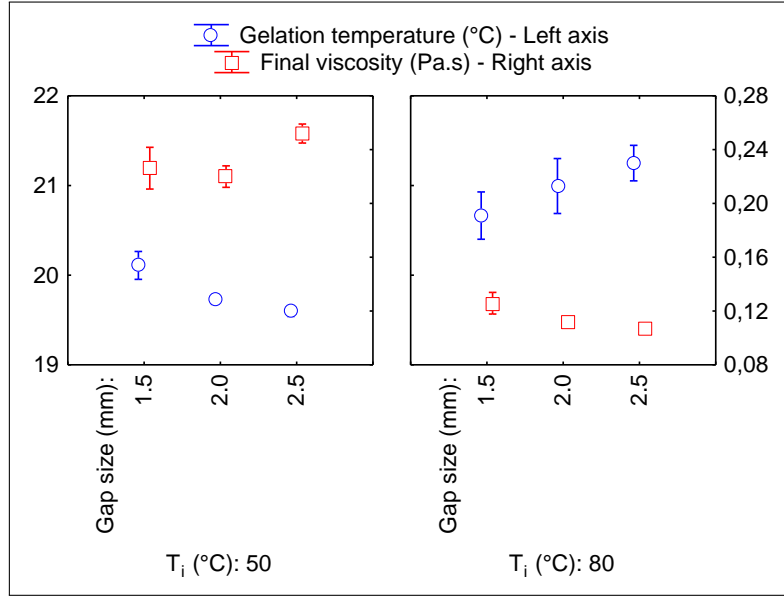
(Figure 4.5). The increase in viscosity at T_{gel} observed for $T_i = 80\,°C$ is also rather subtle (Figure 4.4) and it is possible that lower shear rates might enable a sharper viscosity increase to be distinguished [27, 41, 48].

For crude oil A1, it is also possible to note that the value of ξ slightly increases as the temperature is raised back up to $80\,°C$. Therefore, the Arrhenius heating and cooling portions of Figure 4.4 ($T_i = 80\,°C$) are not parallel, but rather slightly diverge. It is possible that this behavior derives from a greater extent of light end evaporation as the temperature reapproaches its initial value of $80\,°C$.

Another curious aspect of the thermal-cycle tests of crude oil A1 is the slightly higher η_{h0} for a $2.5\,mm$ gap (Figure 4.5). According to Fisher's LSD test, the difference for η_{h0} between gap sizes of $1.5\,mm$ and $2.5\,mm$ is marginally significant, with a p-level of 0.064128. Tests with a XPP geometry, illustrated in Figure 4.6, indicate that this behavior can still be observed with a XPP geometry type and, thus, this effect does not seem to pertain to wall slip. Furthermore, the lower viscosities observed at higher temperatures with the XPP geometry are probably explained by extant flow between its protrusions [27, 119]. As far as gap-independent results for this initial temperature are concerned, these findings seem to support our choice of a $2.5\,mm$ gap. The reason for this is that the thermal history protocol of $T_i = 50\,°C$ simulates an operational scenario for oil A1. Therefore, we consider a $2.5\,mm$ gap to be appropriate for rheological measurements of oil A1 in view of its more conservative η_{h0}. Moreover, although there is no rheological/rheometrical explanation for the slightly higher η_{h0} with a $2.5\,mm$ gap at this point, we believe this is probably related to an incomplete erasing of the fluid's thermal and shear histories.

Figure 4.6: Tests on crude oil A1 using a XPP geometry type with gaps of 1.5 mm and 2.5 mm ($T_i = 50\,°C$).
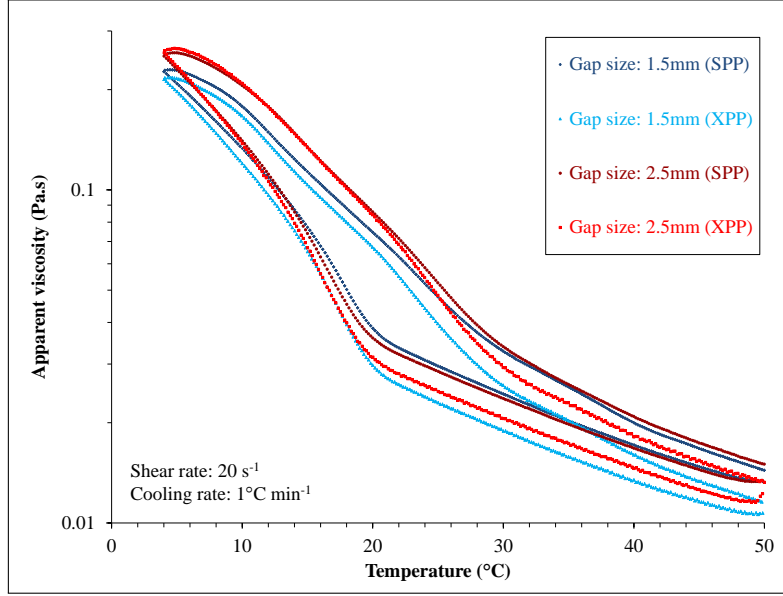
Rheological results for crude oil A2 are shown in Figure 4.7, and summarized in Figure 4.8. Similar trends can be observed for this waxy crude oil in terms of a lower η_{h0} and higher T_{gel} as the initial temperature is increased from $50\,°C$ to $80\,°C$. However, unlike crude oil A1, it appears that the effect of gap size on η_{h0} and on T_{gel} is the same independently of thermal history (Figure 4.8).

Furthermore, for crude oil A2, with a low enough 1.5 mm gap, there is a sudden change in viscosity during cooling in the Arrhenius portion of the curve at around $50\,°C$. Although this is likely correlated with wax crystallization, given that the slope of this Arrhenius portion of the curve does not change, and that this change in viscosity at $\approx 50\,°C$ is very subtle, we do not ascribe this event to T_{gel}.

It is also worth mentioning that the effect of an increase in T_{gel} as well as a decrease in η_{h0} with a higher initial temperature has also been observed in the past [41, 48, 115]. This is probably associated with a higher degree of dissolution of asphaltenes and resins in the waxy crude oil, that are in turn more "free" at higher temperatures to act as PPDs [115, 120].

Additionally, the Arrhenius cooling portion for $T_i = 80\,°C$ coincides with the Arrhenius heating portion for $T_i = 50\,°C$, in terms of viscosity values (Figures 4.4 and 4.7). This is similar to the results from the triple, consecutive thermal-cycle test carried out by Marchesini [115]. Because his waxy crude oil had been pretreated for suppressing evaporation of light ends, it is likely that these aforementioned effects derive from irreversible changes in microstructure within the sample, and not from the evaporation of light ends [115].

In fact, the rheological behavior of waxy crude oils A1 and A2 appears to be,

Figure 4.7: Thermal-cycle test for crude oil A2. Blue-colored curves pertain to the "non-erased history" case ($T_i = 50\,°\mathrm{C}$), while red-colored curves pertain to $T_i = 80\,°\mathrm{C}$.
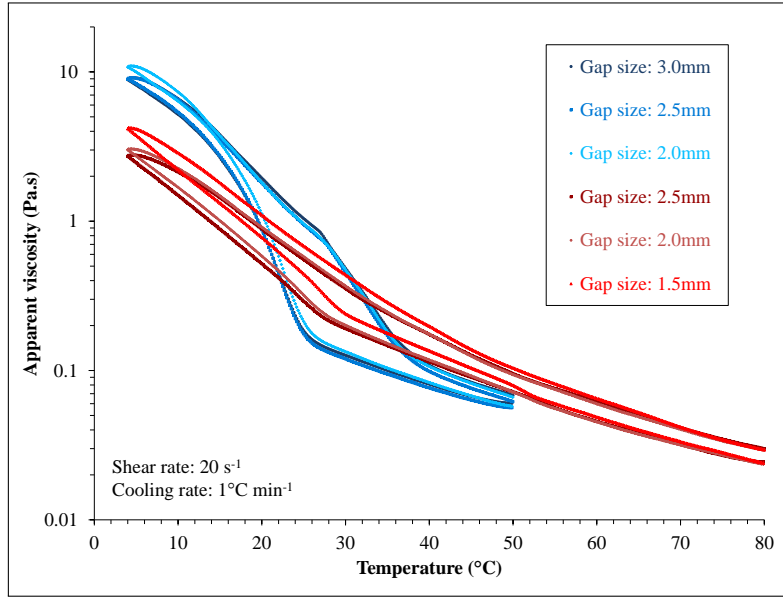
Figure 4.8: T_{gel} and η_{h0} as a function of gap size and thermal history protocol for crude oil A2.
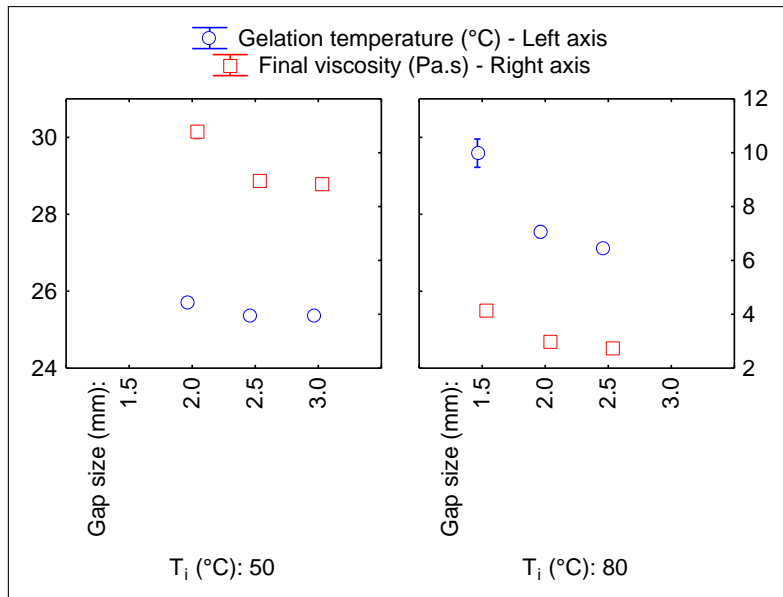
in terms of thermal history, a combination of the Arrhenius portions of Figure 4.9a and the lower temperature region of Figure 4.9b, both reproduced from the work of, and with permission from Marchesini [115].

Further evidence that the evaporation of light ends is not significant for crude oils A1 and A2 are the much lower η_{h0} values for $T_i = 80\,°\mathrm{C}$. The reason for this is that higher viscosities should be expected for a crude oil sample whose lighter components had evaporated [63].

Therefore, rheological results presented in this section suggest that choosing between operational resemblance or complete dissolution of wax crystals may impact

Figure 4.9: Thermal-cycle tests showing the effects of (a) irreversible changes in microstructure and (b) T_i on the rheological behavior of a waxy crude oil.

<table>
<tr><td>(a)</td><td>(b)</td></tr>
</table>
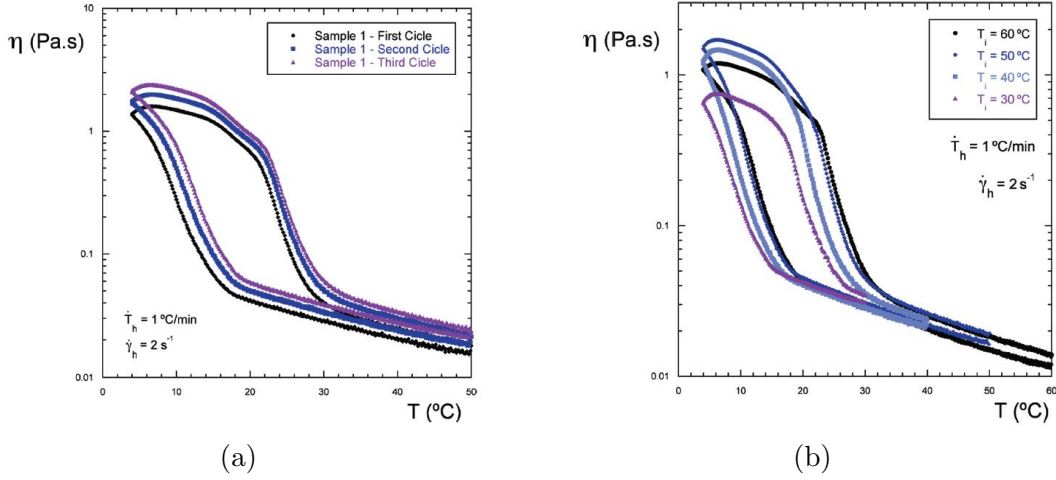
Reference: [115].

flow-restart operations drastically. As previously mentioned, the change in gap-dependency behavior with thermal history for sample A1 differs from that of oil A2. Finally, Table 4.5 summarizes T_{gel} and necessary gap size data obtained from the thermal-cycle tests and based on Fisher's LSD test analysis.

Table 4.5: T_{gel} measurements and necessary gap sizes for obtaining gap-independent results.

Waxy crude oil	$T_i = 50\,^{\circ}\text{C}$		$T_i = 80\,^{\circ}\text{C}$	
	T_{gel} (°C)	Gap size (mm)	T_{gel} (°C)	Gap size (mm)
A1	19.6	2.5	21.0	2.0
A2	25.4	2.5	27.1	2.5

4.2.2 Determination of WPT by DSC

All DSC thermograms from the present work can be found in Appendix B in Figures B.1, B.2, B.3, and B.4. Table 4.6 summarizes data obtained from these thermograms.

Table 4.6: WPT values of crude oils A1 and A2 by conventional DSC.

Waxy crude oil	T_i (°C)	WPT (°C)				
		Run 1	Run 2	Run 3	Average	Std. dev.
A1	50	23.39	23.07	22.13	22.86	0.53
	80	23.45	23.78	22.59	23.27	0.50
A2	50	28.76	29.04	28.69	28.83	0.15
	80	50.34	51.06	50.30	50.57	0.35

In general, these WPT values are 4 °C to 5 °C higher than T_{gel} when the initial temperature is 50 °C. However, perhaps the most interesting aspect of DSC ther-

mograms is the detection of the WPT at much higher temperatures for crude oil A2 when T_i is increased to $80\,°\text{C}$. This is due to the appearance of a second crystallization peak. More interestingly, it is in this temperature range ($\approx 50\,°\text{C}$) that sample A2 presents a sudden, slight increase in viscosity in its Arrhenius cooling portion with a low enough gap of $1.5\,\text{mm}$ and $T_i = 80\,°\text{C}$ (Figure 4.7).

Crude oil A1, in turn, does not display an additional crystallization peak for the higher T_i. Therefore, we are led to believe that, during the cooling process of waxy crude oil A2, by a temperature of $\approx 50\,°\text{C}$, there is already a sufficient amount of precipitated wax crystals, which is above the resolution of the DSC equipment, for an exothermic thermal effect to be recognized. This may indicate a larger overall amount of paraffins in this oil and/or, at least, a larger amount of specific paraffinic components that tend to crystallize in this temperature range. The former conclusion is also supported by the ubiquitously higher magnitude of the crystallizaton peaks for this crude oil, when approximately the same sample mass was used.

Moreover, there is an omnipresent, broad crystallization peak between $20\,°\text{C}$ to $30\,°\text{C}$ in the thermograms from both oil samples. Onset values for these peaks are statistically the same, independently of the thermal history protocol. This can be verified in Table 4.7, where average onset values for these events are presented along with their standard deviation. If different initial temperatures are in fact correlated with asphaltenes being more or less dispersed in the waxy crude oil, as observed from rheological results (Section 4.2.1), then this WPT tendency to not vary with T_i is expected, because the influence of asphaltenes on the crystallization onset by DSC (WPT) is only minor and does not depend on the origin of asphaltenic components [49, 51].

Table 4.7: Crystallization onset temperatures for the broad crystallization peaks in the $20\,°\text{C}$ to $30\,°\text{C}$ range.

Waxy crude oil	T_i (°C)	Onset (°C)	
		Average	Std. dev.
A1	50	22.86	0.53
	80	23.27	0.50
A2	50	28.83	0.15
	80	28.71	0.53

It is also interesting to note that these broad crystallization peaks from all DSC thermograms, occurring $\approx 5\,°\text{C}$ above their respective T_{gel}, look very similar to a glass transition phenomenon. More interestingly, as Larson [121] states, physical gels are conceptually not that different from glasses in a certain way, because they may be interpreted as two ends of a continuum. At one end, a network of irreversible chemical bonds is regarded as a strong gel; while, at the other extreme, a material experiencing reversing molecular motion, that gradually slows down during cooling,

could be called a fragile glass [121].

Consequently, based solely on conventional DSC results with a $T_i = 50\,°\mathrm{C}$, one could even argue that the event in question is directly related with waxy crude oil gelation phenomena, and that no other transformation, such as crystallization itself, is taking place. This discussion is an example of the importance of utilizing several techniques for studying the complex process of wax crystallization in crude oils. It also constitutes yet another reason for the further MTDSC analysis of oils A1 and A2, which follows in the next section.

MTDSC

From MTDSC thermograms (Appendix B, Figures B.5 and B.6), two exothermic events can be distinguished in each sample, which appear on the non-reversing component of the heat flow data (Iso-K curve). While these peaks are better defined for crude oil A2, peaks in the Iso-K curve of crude oil A1 are accompanied by peaks of lower magnitude on the reversing component of the thermogram, herein referred to as simply "Heat Flow". Although there is no work on the use of the StepScan technique for studying wax crystallization in crude oils, these results resonate with previous studies of crystallization processes using the StepScan method [122, 123]. The appearance of exothermic events on the Iso-K curve make it very clear that transformations occurring in the waxy crude oils pertain to wax crystallization, and not to glass transition.

Table 4.8 summarizes information with respect to the sensitivity of this specific type of MTDSC in detecting the start of paraffin crystallization. MTDSC appears to be more sensitive than conventional DSC, especially because of a second crystallization peak for crude oil A1. Onset values for the crystallization peaks in the $20\,°\mathrm{C}$ to $30\,°\mathrm{C}$ range agree fairly well with those by regular DSC analysis in the corresponding temperature range.

Table 4.8: Detection of the WPT by MTDSC.

Waxy crude oil	Crystallization onset (°C)	
	1st peak (WPT)	2nd peak
A1	49.86	24.89
A2	50.24	28.92

Moreover, the fact that petroleum is chemically very complex explains the higher degree of noise present in the thermograms. Nevertheless, this technique still needs to be optimized by testing other values for the experimental parameters ΔT_{SS}, Δt_{iso}, and $\frac{\Delta T_{SS}}{\Delta t_{SS}}$. Their influence on the detection of wax crystallization and on noise reduction can thus be analyzed and this technique may ultimately be improved.

μDSC

Figures 4.10 and 4.11 illustrate that two crystallization peaks for each sample were disclosed by μDSC analysis. This is in accordance with the results from Duncke [109], Palermo *et al.* [107], and De Oliveira *et al.* [95].

Figure 4.10: Microcalorimetric results for crude oil A1.
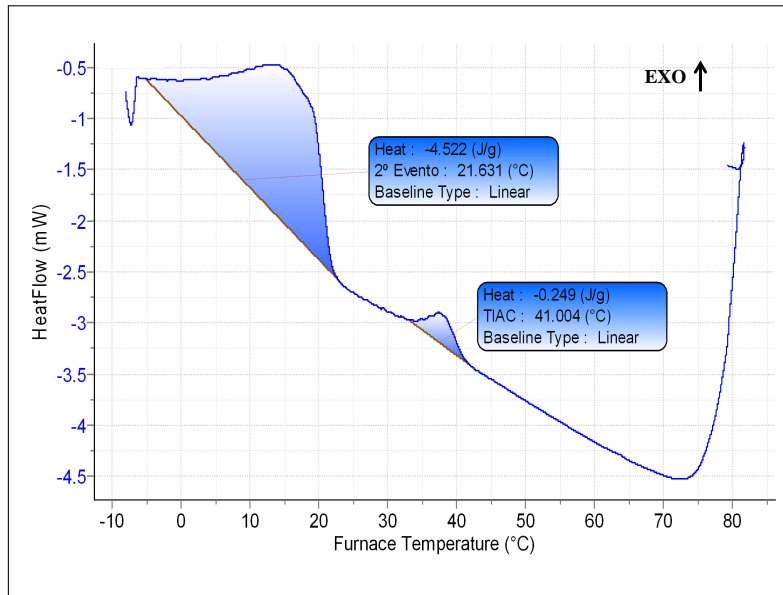
Figure 4.11: Microcalorimetric results for crude oil A2.
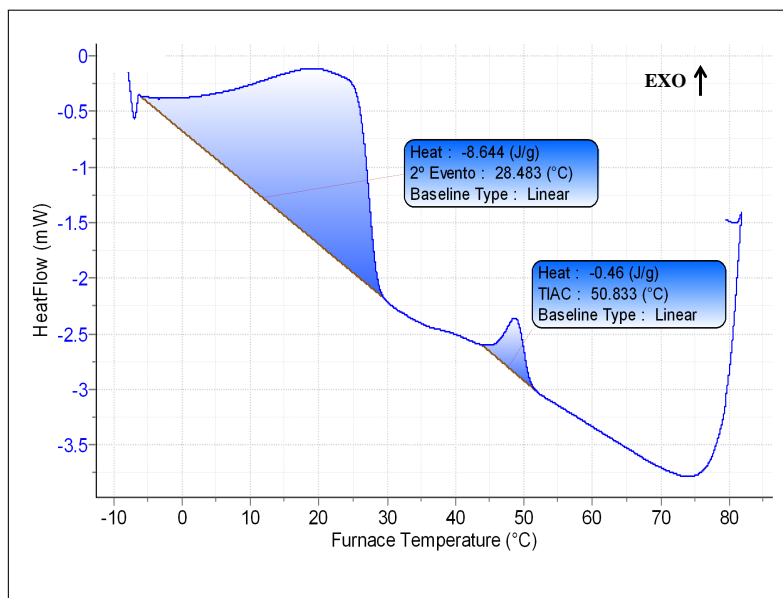
Perhaps more interestingly, the higher resolution of μDSC enabled the detection of WPT at much higher temperatures for crude oil A1. This other crystallization peak at $\approx 40\,°\mathrm{C}$ was disregarded by the DSC technique. Table 4.9 summarizes all relevant μDSC data, including the computation of the total wax content of both crude oils according to Equation (3.2).

Table 4.9: WPT by μDSC and computation of wax content.

| Waxy crude oil | Sample mass (mg) | Crystallization onset (°C) | | Q (J) | w_{wax} (%) |
		1st peak (WPT)	2nd peak		
A1	313.9	41.004	21.631	1.498	2.39
A2	222.3	50.833	28.483	2.024	4.55

According to Table 4.9, crude oil A2 has around twice as much waxy, crystallizable components as crude oil A1. A larger exothermic effect can be observed for crude oil A2 for the first crystallization peak (WPT), even when a smaller sample mass was used. This indicates that A2 contains a larger amount of paraffins that precipitate at that point of the cooling process. This, in turn, makes them detectable by conventional DSC and is in accordance with the results and conclusions from conventional DSC experiments.

4.2.3   Determination of WAT by CPM

Results for WAT measurements by CPM are displayed in Table 4.10. Much like several other works in the literature, these results imply that CPM is the most sensitive technique in detecting the start of wax crystallization among the techniques employed in the present work. Furthermore, it is the only one among these techniques that allows detection of the actual WAT, making it clear that Rheometry and Calorimetry, for example, rely on precipitated crystals for physical effects to be distinguished.

Table 4.10: WAT of crude oils A1 and A2.

| Waxy crude oil | WAT (°C) | | | | |
	Run 1	Run 2	Run 3	Average	Std. dev.
A1	53.2	51.1	51.1	51.8	1.0
A2	60.4	64.0	58.1	60.8	2.4

Investigation of wax crystal dimensions

For all the runs in Table 4.10, micrographs were taken at 4 °C and at specific temperatures corresponding to the broad crystallization peaks detected by conventional DSC experiments (Section 4.2.2). These temperatures (T_{DSC}) were chosen due to the ubiquitous character of these peaks in DSC thermograms, and because the resulting temperature range (T_{DSC} to 4 °C) would also encompass T_{gel} values for both crude oils. This was done with the aim of comparing the evolution of wax crystal growth between these temperatures.

Therefore, as previously mentioned in Section 3.2.3, for crude oil A1, micrographs pertaining to the broad crystallization region were taken between 22.3 °C

and 23.6 °C; while, for crude oil A2, these were taken at 28.9 °C.

All micrographs are presented in Appendix C. Figures 4.12 and 4.13 serve as comparative examples of wax crystal number and size in both crude oils when they undergo the same thermal history. It is possible to learn from these Figures that, in our case, deciding whether to reproduce oilfield conditions (50 °C) or to completely erase the oil's thermal and shear histories has a profound effect on wax crystal size and their number.

Figure 4.12: CPM images of wax crystals ($T_i = 80$ °C) from (a) crude oil A1 and (b) crude oil A2.

(a)   (b)
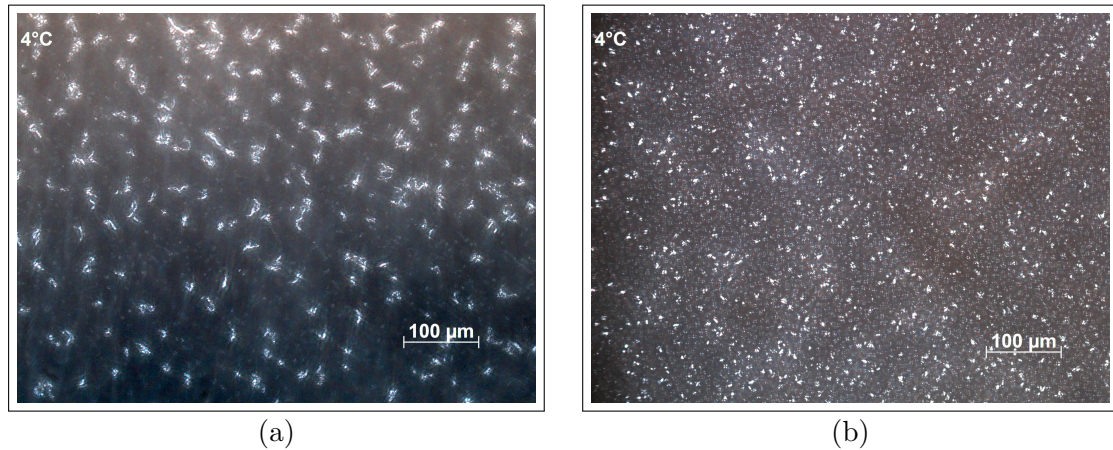
Figure 4.13: CPM images of wax crystals ($T_i = 50$ °C) from (a) crude oil A1 and (b) crude oil A2.

(a)   (b)
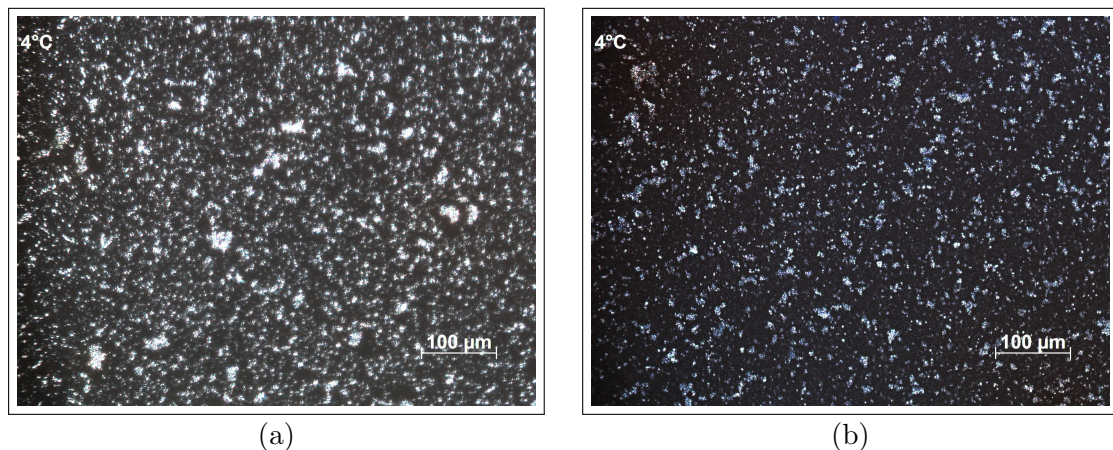
When cooled from 50 °C, wax crystals seem to grow less "orderly"/homogeneously in comparison with $T_i = 80$ °C. This is due to the fact that, when cooling from an intermediate temperature, with a lower degree of asphaltene dissolution, these components and non-dissolved wax tend to work as nucleating sites for wax crystals [20, 21, 30, 120, 124, 125]. They would then contribute to a more heterogeneous nucleation and, also, intergrowing of crystals would allow for a decrease in the effectiveness of asphaltenes as natural PPDs [56].

50

This is in accordance with results from the literature and seems to explain the rheological behavior of crude oils A1 and A2 appropriately.

Table 4.11 summarizes information about wax crystal dimensions that can be obtained from CPM micrographs at $4\,^{\circ}\mathrm{C}$ and at T_{DSC}. Average values of Area percent and F_r are presented and, additionally, maximum values of F_m among the three runs are also provided.

Table 4.11: Average and maximum values for the parameters obtained from CPM micrographs by running an Automatic Measurement Program.

Waxy crude oil	T_i (°C)	4 °C			T_{DSC}		
		Area (%)	Max. F_m (µm)	F_r	Area (%)	Max. F_m (µm)	F_r
A1	50	5.52	33.68	0.65	1.84	32.34	0.64
	80	3.23	43.53	0.60	1.03	23.70	0.59
A2	50	7.67	41.52	0.65	1.88	22.33	0.63
	80	2.85	14.62	0.60	1.47	11.60	0.64

As one might expect from observation of Figure 4.12, crude oil A1 presents significantly larger crystals than crude oil A2 for $T_i = 80\,^{\circ}\mathrm{C}$. Nevertheless, other trends are not as easy to be seen or are not reflected by maximum values alone. Hence, distribution of wax crystal size in terms of F_m measurements are also provided. Figure 4.14, for example, illustrates that there is a significant larger proportion of detected regions at higher F_m values for crude oil A1 when its "memory" is completely erased, although Table 4.11 indicates that they are only slightly ($\approx 10\,\mu\mathrm{m}$) larger.

Figure 4.14: F_m distribution of crude oil A1.
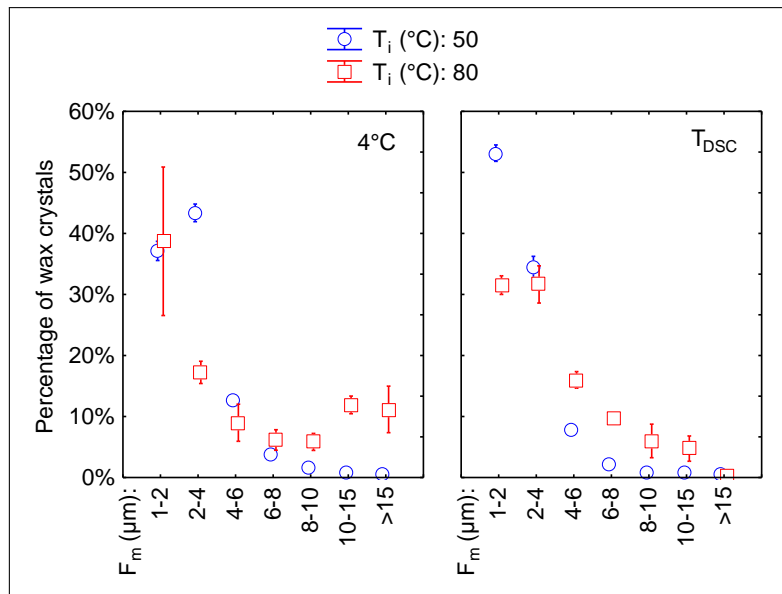
On the other hand, for crude oil A2, Figure 4.15 indicates similar F_m distributions between thermal history protocols at $4\,^{\circ}\mathrm{C}$ and slightly larger crystals for a initial

temperature of 80 °C. However, additional information from Table 4.11 discloses definitively that, in all three runs, either at 4 °C or at T_{DSC}, no region with a F_m greater than 14.62 μm can be observed when a initial temperature of 80 °C is used. These results may indicate that, from T_{DSC} to 4 °C, wax crystals from crude oil A2 do not grow as significantly for $T_i = 80$ °C as they do for $T_i = 50$ °C. For crude oil A1, the opposite trend is observed: maximum F_m values vary, from T_{DSC} to 4 °C, to much a greater extent for an initial temperature of 80 °C than for 50 °C (Table 4.11).

Figure 4.15: F_m distribution of crude oil A2.
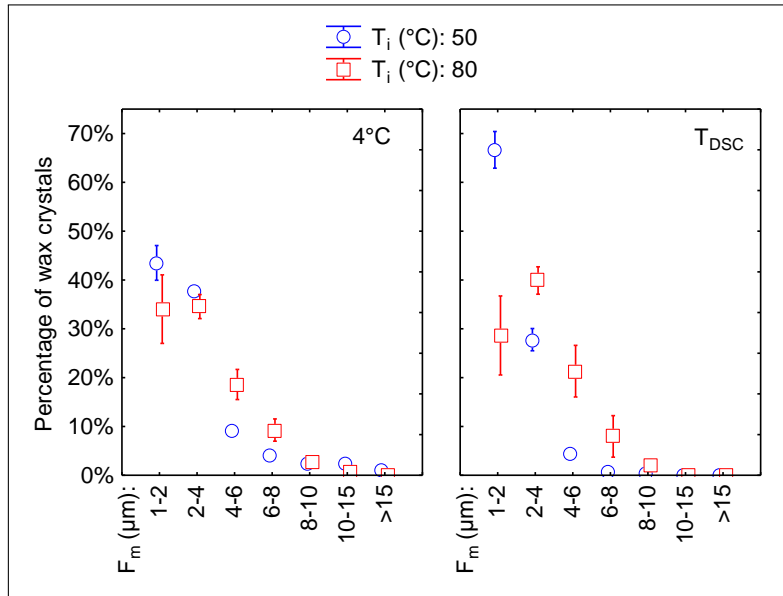
Although we are presently not able to evaluate the effect of shearing on wax crystal size, Table 4.12 combines minimum gap size information with maximum F_m values for both oils. Therefore, much like Japper-Jaafar *et al.* [4] concluded for their crude oil samples, the wax crystallization and gelation processes need to be studied further for, ultimately, some kind of relationship between gap-dependence and wax crystal size to be delineated.

Table 4.12: F_m maxima and necessary gap sizes for obtaining gap-independent results.

| Waxy crude oil	$T_i = 50$ °C		$T_i = 80$ °C	
	F_m (μm)	Gap size (mm)	T_m (μm)	Gap size (mm)
A1	33.68	2.5	43.53	2.0
A2	41.52	2.5	14.62	2.5

The error bars for the 1 μm to 2 μm F_m range are very large because of a greater or lesser extent of detection of the very small regions distinguished in Figure 3.5. It is also possible that the previously mentioned "extinction" effect (Section 2.5.3), that is, crystals that are not as white, plays a role in increasing this uncertainty. Never-

theless, F_m distributions and data from Table 4.11 seem to suit well our purposes of studying wax crystal dimensions.

Furthermore, it is also worth mentioning that wax crystals tend to become slightly more elongated when they are dissolved completely prior to cooling. This can be observed by the average F_r values displayed in Table 4.11 or by the F_r distribution at 4 °C, displayed in Figure 4.16. Data points in this Figure shift to lower F_r values for a T_i of 80 °C. This would indicate an orthorhombic character of wax crystals because needle-like, elongated crystals are in accordance with an orthorhombic lattice [35, 109, 126–128]. This configuration has been typically observed in the literature many times, along with plate-like wax crystals deriving from a hexagonal lattice [10, 109, 126, 129, 130].

On the other hand, also supported by visual observation of micrographs, wax crystal lattice is a little more difficult to be interpreted for an initial temperature of 50 °C in view of (i) incomplete erasing of the fluid's "memory"; (ii) heterogeneous nucleation; (iii) formation of irregular-shaped malcrystalline forms [44, 109].

Figure 4.16: F_r distribution at 4 °C.
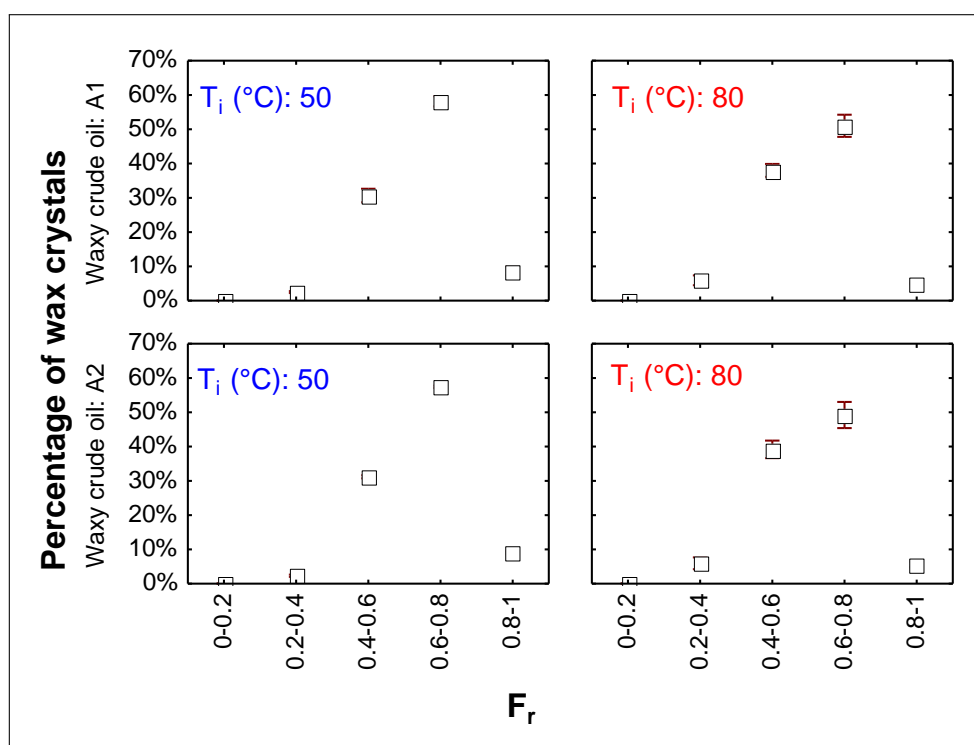
Wax crystal dimension observations are in accordance with results presented in this chapter and an explanation for this is as follows. In crude oil A1, the higher concentration of macrocrystalline wax, indicated by GC, favors the formation of larger, more elongated crystals from a higher initial temperature. The reason for this is that, while crystals composed of n-paraffins are much larger, branched paraffins interefere with regular crystal growth [99, 130, 131].

It may also be possible that the lower proportion of aromatic carbons in this sample, as indicated by NMR, contributes to less steric hindrance in the wax crystal growth process, because crystalline polymers and wax crystals in crude oils are less likely to form when they present bulky substituents [120, 131, 132]. These factors would then facilitate the formation of larger crystals for crude oil A1.

On the other hand, crude oil A2 presents significantly smaller crystals when cooled from the same initial temperature of 80 °C. This, in turn, is in accordance with a higher concentration of microcrystalline waxes, as inferred from NMR and calorimetric results [130]. For example, a higher proportion of microcrystalline domains in the alkyl chains, where the amorphous parts protrude away from the crystal lattice, would inhibit wax crystal growth by steric hindrance [99, 120, 131, 132].

Furthermore, through the same reasoning, a higher proportion of C_{ar}, H_{ar}, and H_{dar} by NMR may also indicate a higher content of asphaltenes/resins. These fractions have bulky aromatic rings in their chemical structure and are able to participate more actively in wax crystal formation with $T_i = 80$ °C. Hence, they would in turn be more prone to restrain wax crystal growth for oil A2 [120, 132].

Chapter 5

Conclusion

In the present work, the complexity of wax crystallization detection was addressed to show that different techniques possess differing degrees of sensitivty. Hence, most of them are not able to detect the very start of wax crystallization, or the WAT, except for CPM. In view of this, conventional PP and CP standard techniques are rather imprecise/inaccurate, given that they do not rely on well-controlled thermal and shear history conditions.

Figures 5.1 and 5.2 summarize gathered data from the present work pertaining to the wax crystallization process. It is worth mentioning that, in these figures, WPT measurements by MTDSC do not follow exactly the same thermal protocol of the other analyses under investigation, that is, cooling at $1\,°C/\min$, in view of the specific temperature program inherent to the StepScan technique.

In a way, Rheometry is the less sensitive technique because it detects a sharp increase in viscosity that pertains to oil gelation. Furthermore, it has been shown by CPM that wax crystals are already present at T_{gel} and at the WPT, measured by Calorimetry.

Conventional DSC, in turn, appears to provide dubious WPT results, because it was not able to detect wax crystallization at higher temperatures for crude oil A1, the way MTDSC and μDSC did. In fact, the higher microcrystalline wax content or overall wax content in crude oil A2 are likely responsible for the appearance of a second exothermic peak $\approx 10\,°C$ below the WAT.

While MTDSC is the most sensitive calorimetric technique because of its higher WPT for crude oils A1 and A2, it should still be improved by testing the influence of each individual parameter on noise reduction and on WPT measurement accuracy.

Results also indicate that a higher proportion of microcrystalline wax or a higher proportion of aromatic components, such as resins and asphaltenes, favor the formation of smaller crystals by steric hindrance. The latter components are also associated with a more heterogeneous crystallization for the lower initial temperature, providing nucleating sites for wax crystals.

Figure 5.1: Summary for crude oil A1 with "erased-history" conditions and gap-independent behavior.
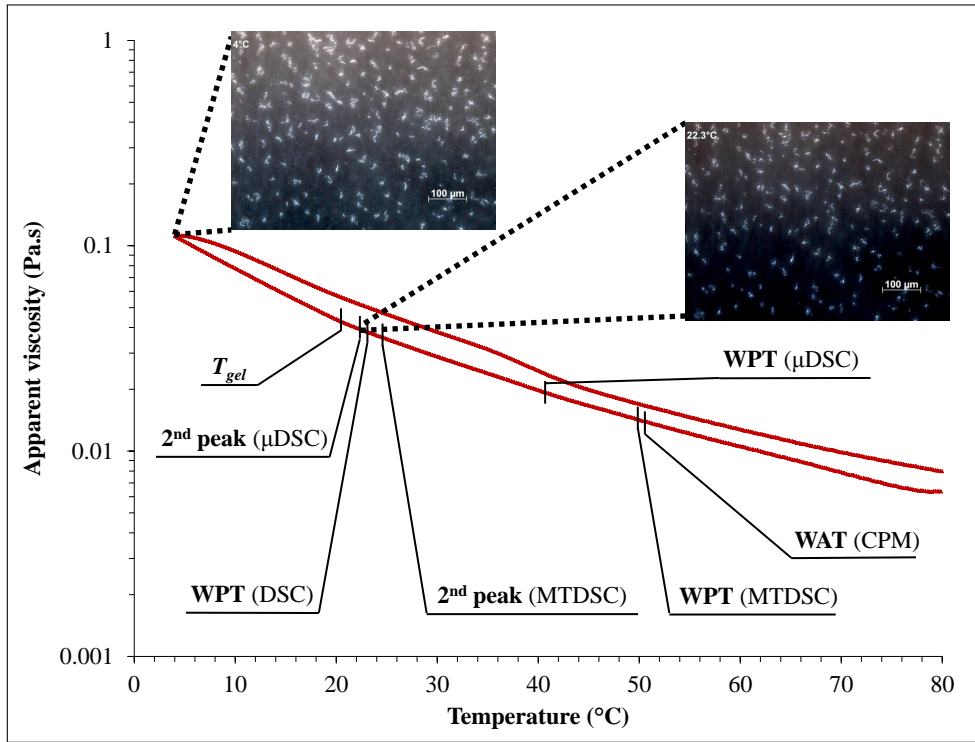

Figure 5.2: Summary for crude oil A2 with "erased-history" conditions and gap-independent behavior.
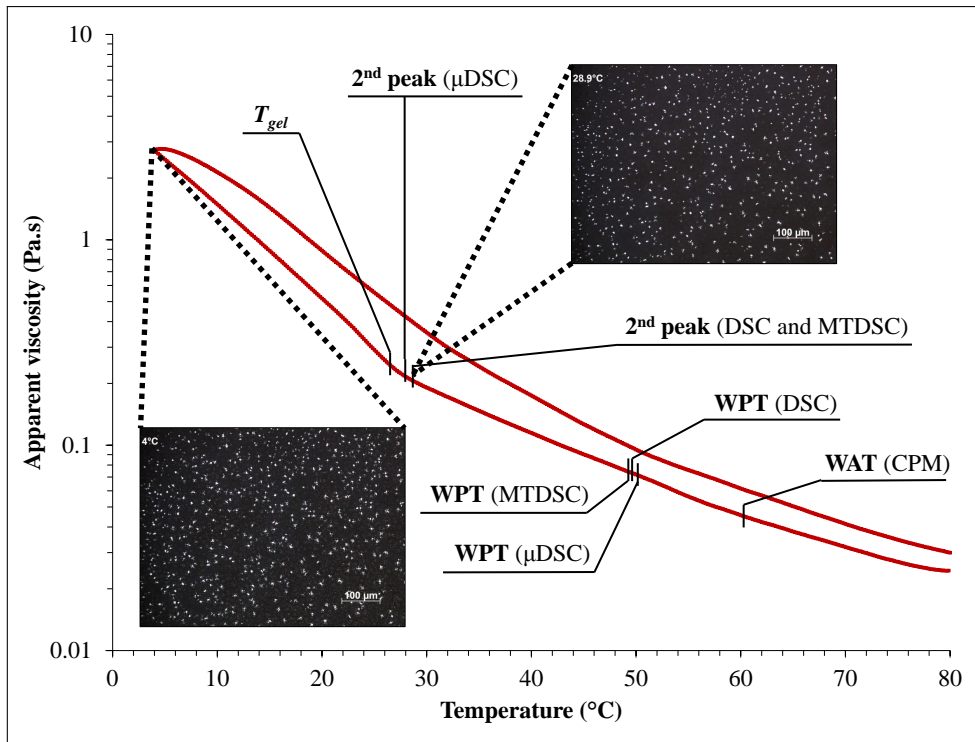
The increased number of nucleating sites also contributes to a larger area of the CPM frame being occupied by wax crystals, and, according to rheological results,

much higher η_{h0} are then recorded. However, when asphaltenes and resins (natural PPDs) are dissolved in the waxy crude oils to a greater extent, they are able to actively participate in the wax crystal growth process and, consequently, they improve the oil's flow properties.

In the context of Rheometry, it appears that smaller gap sizes yield higher viscosities and higher T_{gel} values. However, our results do not indicate a direct relationship between wax crystal size and minimum rheometer gap size necessary for gap-independent results.

It is very clear that the choice of the initial cooling temperature has a decisive influence on wax crystal size, number, and aspect ratio, ultimately defining the rheological behavior of both waxy crude oils. Not only the entire rheological behavior of crude oil A1 changes with T_i, but also the gap trend of T_{gel} and η_{h0} changes with the choice of the initial temperature. This suggests that measuring the true flow properties and obtaining reproducible rheological results for oil A1 in the laboratory may be even trickier. Moreover, another evidence of this behavior is the slightly higher η_{h0} from the rheological curve with a gap of 2.5 mm, which does not seem to be related with wall slip effects. Therefore, by this reasoning, this oil appears to be more affected by the choice of T_i.

As suggestions for future work, we recommend that the role of microcrystalline wax in the wax crystallization process be assessed. Given that these components may not be entirely made up by straight-chain alkanes, we believe that they might not align with flow as easily as would other paraffin types. Therefore, it is possible that they are related with observed effects of premature wax crystallization and higher η_{h0} values under shear.

A lot more work still has to be done on the type of gap-dependency that waxy crude oils possess. For instance, the influence of several parameters – such as microcrystalline and overall wax content, cooling rate, and initial cooling temperature – on the rheological behavior of model and waxy crude oil samples with respect to gap size and geometry is in order.

Furthermore, estimation of average structural parameters of extracted wax and asphaltene fractions from different crude oils may be useful in understanding the mechanism by which paraffins and asphaltenes interact, ultimately determining the oil's rheological behavior.

Bibliography

[1] BROWN, L. D. "Flow Assurance: A $\pi 3$ Discipline". In: *Offshore Technology Conference*, Houston, TX, USA, 2002. Offshore Technology Conference. ISBN: 978-1-55563-249-6. doi: 10.4043/14010-MS. Available at: <`http://www.onepetro.org/doi/10.4043/14010-MS`>.

[2] GUPTA, A., ANIRBID, S. "Need of Flow Assurance for Crude Oil Pipelines: A Review", *International Journal of Multidisciplinary Sciences and Engineering*, v. 6, n. 2, pp. 43–49, 2015. Available at: <`www.ijmse.org/Volume6/Issue2/paper6.pdf`>.

[3] PADGETT, F. W., HEFLEY, D. G., HENRIKSEN, A. "Wax Crystallization - A Preliminary Report", *Industrial and Engineering Chemistry*, v. 18, n. 8, pp. 832–835, 1926. ISSN: 0019-7866. doi: 10.1021/ie50200a022. Available at: <`http://pubs.acs.org/doi/abs/10.1021/ie50200a022`>.

[4] JAPPER-JAAFAR, A., BHASKORO, P., SEAN, L., et al. "Yield stress measurement of gelled waxy crude oil: Gap size requirement", *Journal of Non-Newtonian Fluid Mechanics*, v. 218, pp. 71–82, 2015. ISSN: 03770257. doi: 10.1016/j.jnnfm.2015.02.001. Available at: <`http://linkinghub.elsevier.com/retrieve/pii/S0377025715000257`>.

[5] WOOD, F. E., YOUNG, H. W., BUELL, A. W. "Handling Congealing Oils and Paraffin in Salt Creek Field, Wyoming", *Transactions of the AIME*, v. 77, n. 01, pp. 262–268, 1927. doi: 10.2118/927262-G.

[6] BREWSTER, F. M. "Handling Congealing Oil and Paraffin Problems in the Appalachian Fields", *Transactions of the AIME*, v. 77, n. 01, pp. 253–261, 1927. doi: 10.2118/927253-G. Available at: <`http://dx.doi.org/10.2118/927253-G`>.

[7] REISTLE JR., C. E. "Summary of Existing Information on Handling Congealing Oils and Paraffin", *Transactions of the AIME*, v. 77, n. 01, pp. 227–252, 1927. doi: 10.2118/927227-G.

[8] WARDHAUGH, L. T., BOGER, D. V. "Measurement of the Unique Flow Properties of Waxy Crude Oils", *Chemical Engineering Research and Design*, v. 65, pp. 74–83, 1987.

[9] ROENNINGSEN, H. P., BJOERNDAL, B., BALTZER HANSEN, A., et al. "Wax precipitation from North Sea crude oils: 1. Crystallization and dissolution temperatures, and Newtonian and non-Newtonian flow properties", *Energy & Fuels*, v. 5, n. 6, pp. 895–908, 1991. ISSN: 0887-0624. doi: 10.1021/ef00030a019.

[10] SRIVASTAVA, S., HANDOO, J., AGRAWAL, K., et al. "Phase-transition studies in n-alkanes and petroleum-related waxes—A review", *Journal of Physics and Chemistry of Solids*, v. 54, n. 6, pp. 639–670, 1993. ISSN: 00223697. doi: 10.1016/0022-3697(93)90126-C.

[11] BACON, M. M., ROMERO-ZERON, L. B., CHONG, K. "Using Cross-Polarized Microscopy To Optimize Wax-Treatment Methods". In: *SPE Annual Technical Conference and Exhibition*, pp. 1–8, New Orleans, Louisiana, 2009. Society of Petroleum Engineers. doi: 10.2118/124799-MS. Available at: <http://www.onepetro.org/doi/10.2118/124799-MS>.

[12] DIMITRIOU, C. J., MCKINLEY, G. H., VENKATESAN, R. "Rheo-PIV analysis of the yielding and flow of model waxy crude oils", *Energy and Fuels*, v. 25, n. 7, pp. 3040–3052, 2011. ISSN: 08870624. doi: 10.1021/ef2002348.

[13] GOLCZYNSKI, T. S., KEMPTON, E. C. "Understanding wax problems leads to deepwater flow assurance solutions", *World Oil*, pp. D–7 – D–10, 2006. ISSN: 00438790. Available at: <http://www.woodgroup.com/SiteCollectionDocuments/news-tech-articles/2006-03_UnderstandWaxProbsWorldOil_MSiKenny.pdf>.

[14] DIMITRIOU, C. J. *The rheological complexity of waxy crude oils: Yielding, thixotropy and shear heterogeneities*. Phd thesis, Massachusetts Institute of Technology, 2013. Available at: <http://web.mit.edu/chrisd/Public/chevron/main.pdf>.

[15] KRUKA, V., CADENA, E., LONG, T. "Cloud-Point Determination for Crude Oils", *Journal of Petroleum Technology*, v. 47, n. 8, pp. 681–687, 1995. ISSN: 01492136. doi: 10.2118/31032-PA. Available at: <https://www.onepetro.org/download/journal-paper/SPE-31032-PA?id=journal-paper/SPE-31032-PA>.

[16] MONGER-MCCLURE, T., TACKETT, J., MERRILL, L. "Comparisons of Cloud Point Measurement and Paraffin Prediction Methods", *SPE Production & Facilities*, v. 14, n. 1, pp. 4–16, 1999. ISSN: 1064-668X. doi: 10.2118/54519-PA. Available at: <https://www.onepetro.org/download/journal-paper/SPE-54519-PA?id=journal-paper/SPE-54519-PA>.

[17] LEONTARITIS, K. J., LEONTARITIS, J. D. "Cloud Point and Wax Deposition Measurement Techniques". In: *SPE International Symposium on Oilfield Chemistry*, v. 80267, Houston, TX, USA, 2003. Society of Petroleum Engineers. doi: 10.2118/80267-ms. Available at: <https://www.onepetro.org/download/journal-paper/SPE-54519-PA?id=journal-paper/SPE-54519-PA>.

[18] ERICKSON, D. D., NIESEN, V. G., BROWN, T. S. "Thermodynamic Measurement and Prediction of Paraffin Precipitation in Crude Oil". In: *SPE Annual Technical Conference and Exhibition*, pp. 353–368, Houston, TX, USA, 1993. Society of Petroleum Engineers. doi: 10.2523/26548-MS. Available at: <http://www.spe.org/elibrary/servlet/spepreview?id=00026548>.

[19] SASTRY, M. I. S., RAMAN, N. S., JAIN, N., et al. "Determination of Wax Appearance Temperature and Wax Dissolution Temperature of Waxy Crude Oils by Temperature Programmed IR Spectroscopy". In: *Petrotech*, pp. 1–7, New Delhi, India, 2010. Petrotech Society. Available at: <http://www.petrotechsociety.org/wp-content/themes/continuum/pdf/20100930-FP.pdf>.

[20] GARCÍA, M. D. C., OREA, M., CARBOGNANI, L., et al. "The effect of paraffinic fractions on crude oil wax crystallization", *Petroleum science ...*, v. 19, pp. 37–41, 2001. ISSN: 1091-6466. doi: 10.1081/LFT-100001233. Available at: <http://www.tandfonline.com/doi/abs/10.1081/LFT-100001233>.

[21] ZHU, T., WALKER, J. A., LIANG, J. *Evaluation of Wax Deposition and Its Control During Production of Alaska North Slope Oils*. Technical report, University of Alaska, Fairbanks, Alaska, USA, 2008. Available at: <http://www.osti.gov/scitech/servlets/purl/963363>.

[22] DARIDON, J.-L., COUTINHO, J. "The Limitations of the Cloud Point Measurement Techniques and the Influence of the Oil Composition on Its Detection", *Petroleum Science and Technology*, v. 23, pp. 1113–1128, 2005. doi: 10.1081/LFT-200035541. Available at: <http:

//www.researchgate.net/profile/Joao_Coutinho/publication/
224893105_The_limitations_of_the_cloud_point_measurement_
techniques_and_the_influence_of_the_oil_composition_on_its_
detection/links/09e415100665454aa5000000.pdf>.

[23] HAMMAMI, A., RAINES, M. "Paraffin Deposition From Crude Oils: Comparison of Laboratory Results With Field Data", *SPE Journal*, v. 4, n. 1, pp. 9–18, 1999. doi: 10.2118/54021-PA. Available at: <https://www.onepetro.org/download/journal-paper/SPE-54021-PA?id=journal-paper/SPE-54021-PA>.

[24] ALCAZAR-VARA, L. A., BUENROSTRO-GONZALEZ, E. "Characterization of the wax precipitation in Mexican crude oils", *Fuel Processing Technology*, v. 92, n. 12, pp. 2366–2374, 2011. ISSN: 0378-3820. doi: 10.1016/j.fuproc.2011.08.012. Available at: <http://dx.doi.org/10.1016/j.fuproc.2011.08.012>.

[25] ELSHARKAWY, A. M., AL-SAHHAF, T. A., FAHIM, M. A. "Wax deposition from Middle East crudes", *Fuel*, v. 79, pp. 1047–1055, 2000.

[26] KÖK, M. V., LÉTOFFÉ, J. M., CLAUDY, P., et al. "Comparison of wax appearance temperatures of crude oils by differential scanning calorimetry, thermomicroscopy and viscometry", *Fuel*, v. 75, n. 7, pp. 787–790, 1996.

[27] MARCHESINI, F. H., ALICKE, A. A., DE SOUZA MENDES, P. R., et al. "Rheological characterization of waxy crude oils: Sample preparation", *Energy and Fuels*, v. 26, n. 5, pp. 2566–2577, 2012. ISSN: 08870624. doi: 10.1021/ef201335c.

[28] MERAY, V. R., VOLLE, J.-L., SCHRANZ, C., et al. "Influence of Light Ends on the Onset Crystallization Temperature of Waxy Crudes Within the Frame of Multiphase Transport". In: *SPE Annual Technical Conference and Exhibition*, pp. 369–378, Houston, TX, USA, 1993. Society of Petroleum Engineers.

[29] PASO, K., KOMPALLA, T., OSCHMANN, H. J., et al. "Rheological Degradation of Model Wax-Oil Gels", *Journal of Dispersion Science and Technology*, v. 30, n. 4, pp. 472–480, 2009. ISSN: 0193-2691. doi: 10.1080/01932690802548924.

[30] ZHAO, Y., PASO, K., NORRMAN, J., et al. "Utilization of DSC, NIR, and NMR for wax appearance temperature and chemical additive performance characterization", *Journal of Thermal Analysis and Calorime-*

try, v. 120, pp. 1427–1433, 2015. ISSN: 1388-6150. doi: 10.1007/ s10973-015-4451-1. Available at: <http://link.springer.com/10. 1007/s10973-015-4451-1>.

[31] CLAUDY, P., LÉTOFFÉ, J.-M., NEFF, B., et al. "Diesel fuels: determination of onset crystallization temperature, pour point and filter plugging point by differential scanning calorimetry. Correlation with standard test methods", *Fuel*, v. 65, n. 6, pp. 861–864, 1986. ISSN: 00162361. doi: 10.1016/0016-2361(86)90082-7. Available at: <http://ac.els-cdn. com/0016236186900827/1-s2.0-0016236186900827-main.pdf?_tid= 69f574fe-0546-11e5-adf1-00000aab0f6c&acdnat=1432823748_ dd6acccca48454c72189d3524cea7a29>.

[32] NOEL, F. "Thermal analysis of lubricating oils", *Thermochimica Acta*, v. 4, n. 3-5, pp. 377–392, 1972. ISSN: 00406031. doi: 10.1016/0040-6031(72)87019-9. Available at: <http://ac.els-cdn. com/0040603172870199/1-s2.0-0040603172870199-main.pdf?_tid= a3818780-055a-11e5-afd7-00000aacb35d&acdnat=1432832435_ b90cd8e2252275b2ef8ec1eea2573ec7>.

[33] TIWARY, D., MEHROTRA, A. K. "Phase Transformation and Rheological Behaviour of Highly Paraffinic " Waxy " Mixtures", *The Canadian Journal of Chemical Engineering*, v. 82, pp. 162–174, 2004.

[34] KARAN, K., RATULOWSKI, J., GERMAN, P. "Measurement of Waxy Crude Properties Using Novel Laboratory Techniques". In: *SPE Annual Technical Conference and Exhibition*, pp. 1–12, Dallas, Texas, 2000. Society of Petroleum Engineers. doi: 10.2523/62945-MS. Available at: <https://www.onepetro.org/conference-paper/SPE-62945-MS>.

[35] CAZAUX, G., BARRE, L., BRUCY, F. "Waxy Crude Cold Start: Assessment Through Gel Structural Properties". In: *SPE Annual Technical Conference and Exhibition*, pp. 729–739, New Orleans, Louisiana, 1998. Society of Petroleum Engineers. doi: 10.2118/49213-MS.

[36] VENKATESAN, R., SINGH, P., FOGLER, H. "Delineating the Pour Point and Gelation Temperature of Waxy Crude Oils", *SPE Journal*, v. 7, n. 4, pp. 349–352, 2002. ISSN: 1086-055X. doi: 10. 2118/72237-PA. Available at: <https://www.onepetro.org/download/ journal-paper/SPE-72237-PA?id=journal-paper/SPE-72237-PA>.

[37] JIANG, Z., HUTCHINSON, J. M., IMRIE, C. T. "Measurement of the wax appearance temperatures of crude oils by temperature modulated differential scanning calorimetry", *Fuel*, v. 80, pp. 367–371, 2001.

[38] HAMMAMI, A., RATULOWSKI, J., COUTINHO, J. A. A. P. "Cloud Points: Can We Measure or Model Them?" *Petroleum Science and Technology*, v. 21, n. 3-4, pp. 345–358, 2003. ISSN: 1091-6466. doi: 10.1081/LFT-120018524. Available at: <http://www.tandfonline.com/doi/abs/10.1081/LFT-120018524>.

[39] WARDHAUGH, L. T., BOGER, D. V. "Flow Characteristics of Waxy Crude Oils: Application to Pipeline Design", *AIChE Journal*, v. 37, n. 6, pp. 871–885, 1991a.

[40] PERKINS, T., TURNER, J. "Starting Behavior of Gathering Lines and Pipelines Filled with Gelled Prudhoe Bay Oil", *Journal of Petroleum Technology*, v. 23, n. 3, pp. 301–308, 1971. ISSN: 01492136. doi: 10.2118/2997-PA. Available at: <https://www.onepetro.org/journal-paper/SPE-2997-PA>.

[41] SMITH, P. B., RAMSDEN, R. M. "The Prediction Of Oil Gelation In Submarine Pipelines And The Pressure Required For Restarting Flow". In: *SPE European Petroleum Conference*, pp. 283–290, London, United Kingdom, 1978. Society of Petroleum Engineers. doi: 10.2118/8071-MS. Available at: <http://www.onepetro.org/doi/10.2118/8071-MS>.

[42] VENKATESAN, R., NAGARAJAN, N. R., PASO, K., et al. "The strength of paraffin gels formed under static and flow conditions", *Chemical Engineering Science*, v. 60, n. 13, pp. 3587–3598, 2005. ISSN: 00092509. doi: 10.1016/j.ces.2005.02.045.

[43] KANÉ, M., DJABOUROV, M., VOLLE, J. L. "Rheology and structure of waxy crude oils in quiescent and under shearing conditions", *Fuel*, v. 83, n. 11-12, pp. 1591–1605, 2004. ISSN: 00162361. doi: 10.1016/j.fuel.2004.01.017.

[44] CHANG, C., BOGER, D. V., NGUYEN, Q. D. "Influence of Thermal History on the Waxy Structure of Statically Cooled Waxy Crude Oil", *SPE Journal*, v. 5, n. 2, pp. 148–157, 2000. ISSN: 1086055X. doi: 10.2118/57959-PA.

[45] VISINTIN, R. F. G., LAPASIN, R., VIGNATI, E., et al. "Rheological behavior and structural interpretation of waxy crude oil gels", *Langmuir*, v. 21,

n. 14, pp. 6240–6249, 2005. ISSN: 0743-7463. doi: 10.1021/la050705k. Available at: <http://www.ncbi.nlm.nih.gov/pubmed/15982026>.

[46] GUO, X., PETHICA, B. A., HUANG, J. S., et al. "Effect of cooling rate on crystallization of model waxy oils with microcrystalline poly(ethylene butene)", *Energy and Fuels*, v. 20, n. 1, pp. 250–256, 2006. ISSN: 08870624. doi: 10.1021/ef050163e.

[47] GUO, X., PETHICA, B. A., HUANG, J. S., et al. "Crystallization of Mixed Paraffin from Model Waxy Oils and the Influence of Micro-crystalline Poly(ethylene-butene) Random Copolymers", *Energy & Fuels*, v. 18, n. 4, pp. 930–937, 2004. ISSN: 0887-0624. doi: 10.1021/ef034098p. Available at: <http://pubs.acs.org/doi/abs/10.1021/ef034098p>.

[48] ANDRADE, D. E. V., CRISTINE, A., CRUZ, B., et al. "The Influence of Cooling and Shear on the Gel Strength of Waxy Crude Oil". In: *22nd International Congress of Mechanical Engineering*, pp. 6162–6168, Ribeirão Preto, SP, Brazil, 2013. Associaçao Brasileira de Engenharia e Ciências Mecânicas. Available at: <http://www.abcm.org.br/anais/cobem/2013/PDF/1419.pdf>.

[49] COTO, B., MARTOS, C., ESPADA, J. J., et al. "Experimental study of the effect of inhibitors in wax precipitation by different techniques", *Energy Science & Engineering*, v. 2, n. 4, pp. 196–203, 2014. ISSN: 20500505. doi: 10.1002/ese3.42. Available at: <http://doi.wiley.com/10.1002/ese3.42>.

[50] ANDRADE, D. E. V., CRUZ, A. C. B., FRANCO, A. T., et al. "Influence of the initial cooling temperature on the gelation and yield stress of waxy crude oils", *Rheologica Acta*, v. 54, n. 2, pp. 149–157, 2015. doi: 10.1007/s00397-014-0812-0.

[51] ALCAZAR-VARA, L. A., GARCIA-MARTINEZ, J. A., BUENROSTRO-GONZALEZ, E. "Effect of asphaltenes on equilibrium and rheological properties of waxy model systems", *Fuel*, v. 93, pp. 200–212, 2012. ISSN: 00162361. doi: 10.1016/j.fuel.2011.10.038. Available at: <http://dx.doi.org/10.1016/j.fuel.2011.10.038>.

[52] BROWN, T., NIESEN, V., ERICKSON, D. "The Effects of Light Ends and High Pressure on Paraffin Formation". In: *SPE Annual Technical Conference and Exhibition*, pp. 415–429, New Orleans, Louisiana, 1994. Society of Petroleum Engineers. doi: 10.2118/28505-MS. Available at: <http://www.onepetro.org/doi/10.2118/28505-MS>.

[53] WARDHAUGH, L. T., BOGER, D. V. "The measurement and description of the yielding behavior of waxy crude oil", *Journal of Rheology*, v. 35, n. 6, pp. 1121–1156, 1991b. ISSN: 01486055. doi: 10.1122/1.550168.

[54] SKOOG, D. A., HOLLER, F. J., CROUCH, S. R. *Principles of Instrumental Analysis*. 6th ed. Belmont, CA, USA, Thomson Brooks/Cole, 2007.

[55] SILVA, S. L., SILVA, A. M. S., RIBEIRO, J. C., et al. "Chromatographic and spectroscopic analysis of heavy crude oil mixtures with emphasis in nuclear magnetic resonance spectroscopy: A review", *Analytica Chimica Acta*, v. 707, n. 1-2, pp. 18–37, 2011. ISSN: 00032670. doi: 10.1016/j.aca.2011.09.010. Available at: <http://dx.doi.org/10.1016/j.aca.2011.09.010>.

[56] YI, S., ZHANG, J. "Shear-induced change in morphology of wax crystals and flow properties of waxy crudes modified with the pour-point depressant", *Energy and Fuels*, v. 25, n. 12, pp. 5660–5671, 2011. ISSN: 08870624. doi: 10.1021/ef201187n.

[57] FOGLER, H. S., ZHENG, S., HUANG, Z. *Wax Deposition - Experimental Characterizations, Theoretical Modeling, and Field Practices*. CRC Press, 2015. ISBN: 978-1-4665-6766-5.

[58] LEE, H. S., SINGH, P., THOMASON, W. H., et al. "Waxy oil gel breaking mechanisms: Adhesive versus cohesive failure", *Energy and Fuels*, v. 22, n. 1, pp. 480–487, 2008. ISSN: 08870624. doi: 10.1021/ef700212v.

[59] VENKATESAN, R., ÖSTLUND, J. A., CHAWLA, H., et al. "The effect of Asphaltenes on the Gelation of Waxy Oils", *Energy and Fuels*, v. 17, n. 6, pp. 1630–1640, 2003. ISSN: 08870624. doi: 10.1021/ef034013k.

[60] SILVERSTEIN, R. M., WEBSTER, F. X., KIEMLE, D. J. *Spectrometric Identification of Organic Compounds*. John Wiley & Sons, Inc, 2005. ISBN: 0-471-39362-2.

[61] ASKE, N., KALLEVIK, H., SJÖBLOM, J. "Determination of Saturate, Aromatic, Resin, and Asphaltenic (SARA) Components in Crude Oils by Means of Infrared and Near-Infrared Spectroscopy", *Energy & Fuels*, v. 15, n. 5, pp. 1304–1312, sep 2001. ISSN: 0887-0624. doi: 10.1021/ef010088h. Available at: <http://pubs.acs.org/doi/abs/10.1021/ef010088h>.

[62] WANG, Y. Z., ZHONG, D. L., DUAN, H. L., et al. "Removal of naphthenic acids from crude oils by catalytic decomposition using Mg-Al

hydrotalcite/γ-Al2O3 as a catalyst", *Fuel*, v. 134, pp. 499–504, 2014. ISSN: 00162361. doi: 10.1016/j.fuel.2014.06.026. Available at: <`http://dx.doi.org/10.1016/j.fuel.2014.06.026`>.

[63] SETH, S., TOWLER, B. "Diachronic viscosity increase in waxy crude oils", *Journal of Petroleum Science and Engineering*, v. 43, n. 1-2, pp. 13–23, 2004. ISSN: 09204105. doi: 10.1016/j.petrol.2003.11.004. Available at: <`http://linkinghub.elsevier.com/retrieve/pii/S0920410503002067`>.

[64] ADEBIYI, F., AKHIGBE, G. "Characterization of paraffinic hydrocarbon fraction of Nigerian bitumen using multivariate analytical techniques", *Journal of Unconventional Oil and Gas Resources*, v. 12, pp. 34–44, 2015. ISSN: 22133976. doi: 10.1016/j.juogr.2015.09.003. Available at: <`http://www.sciencedirect.com/science/article/pii/S2213397615000415`>.

[65] DEHKISSIA, S., LARACHI, F., RODRIGUE, D., et al. "Characterization of Doba–Chad heavy crude oil in relation with the feasibility of pipeline transportation", *Fuel*, v. 83, n. 16, pp. 2157–2168, 2004. ISSN: 00162361. doi: 10.1016/j.fuel.2004.06.014. Available at: <`http://linkinghub.elsevier.com/retrieve/pii/S0016236104001772`>.

[66] MELÉNDEZ, L. V., LACHE, A., ORREGO-RUIZ, J. A., et al. "Prediction of the SARA analysis of Colombian crude oils using ATR–FTIR spectroscopy and chemometric methods", *Journal of Petroleum Science and Engineering*, v. 90-91, pp. 56–60, 2012. ISSN: 09204105. doi: 10.1016/j.petrol.2012.04.016. Available at: <`http://linkinghub.elsevier.com/retrieve/pii/S0920410512001076`>.

[67] THOMPSON, M. *CHNS Elemental Analysers*. In: Analytical Methods Committee AMCTB Nr. 29, Royal Society of Chemistry, 2008.

[68] EDWARDS, J. "Applications of NMR Spectroscopy in Petroleum Chemistry". In: Kishore Nadkarni, R. (Ed.), *Spectroscopic Analysis of Petroleum Products and Lubricants*, cap. 16, Bridgeport, NJ, USA, ASTM International, 2011. Available at: <`http://www.researchgate.net/publication/200802375_Applications_of_NMR_Spectroscopy_in_Petroleum_Chemistry`>.

[69] HASAN, M., ALI, M., BUKHARI, A. "Structural characterization of Saudi Arabian heavy crude oil by NMR spectroscopy", *Fuel*, v. 62, n. 5, pp. 518–523, 1983. ISSN: 00162361. doi: 10.1016/0016-2361(83)90219-3.

[70] GILLET, S., RUBINI, P., DELPUECH, J.-J., et al. "Quantitative carbon-13 and proton nuclear magnetic resonance spectroscopy of crude oil and petroleum products. 2. Average structure parameters of representative samples", *Fuel*, v. 60, n. 3, pp. 226–230, mar. 1981a. ISSN: 00162361. doi: 10.1016/0016-2361(81)90184-8. Available at: <http://linkinghub.elsevier.com/retrieve/pii/0016236181901848>.

[71] GILLET, S., RUBINI, P., DELPUECH, J.-J., et al. "Quantitative carbon-13 and proton nuclear magnetic resonance spectroscopy of crude oil and petroleum products. 1. Some rules for obtaining a set of reliable structural parameters", *Fuel*, v. 60, n. 3, pp. 221–225, 1981b. ISSN: 00162361. doi: 10.1016/0016-2361(81)90183-6. Available at: <http://linkinghub.elsevier.com/retrieve/pii/0016236181901836>.

[72] LEE, S., GLAVINCEVSKI, B. "NMR method for determination of aromatics in middle distillate oils", *Fuel Processing Technology*, v. 60, n. 1, pp. 81–86, 1999. ISSN: 03783820. doi: 10.1016/S0378-3820(99)00013-2. Available at: <http://www.sciencedirect.com/science/article/pii/S0378382099000132>.

[73] HASAN, M., BUKHARI, A., ALI, M. "Structural characterization of Saudi Arabian medium crude oil by NMR spectroscopy", *Fuel*, v. 64, n. 6, pp. 839–841, 1985. ISSN: 00162361. doi: 10.1016/0016-2361(85)90020-1.

[74] HASAN, M., ALI, M., ARAB, M. "Structural characterization of Saudi Arabian extra light and light crudes by 1H and 13C NMR spectroscopy", *Fuel*, v. 68, n. 6, pp. 801–803, 1989. ISSN: 00162361. doi: 10.1016/0016-2361(89)90224-X.

[75] POVEDA, J. C., MOLINA, D. R. "Average molecular parameters of heavy crude oils and their fractions using NMR spectroscopy", *Journal of Petroleum Science and Engineering*, v. 84-85, pp. 1–7, 2012. ISSN: 09204105. doi: 10.1016/j.petrol.2012.01.005. Available at: <http://dx.doi.org/10.1016/j.petrol.2012.01.005>.

[76] KUSHNAREV, D., AFONINA, T., KALABIN, G., et al. "Investigation of the composition of crude oils and condensates from the south of the Siberian platform using H and C NMR spectroscopy", *Petroleum Chemistry U.S.S.R.*, v. 29, n. 3, pp. 149–159, 1989. ISSN: 00316458. doi: 10.1016/0031-6458(89)90048-8. Available at: <http://linkinghub.elsevier.com/retrieve/pii/0031645889900488>.

[77] SANCHEZ-MINERO, F., ANCHEYTA, J., SILVA-OLIVER, G., et al. "Predicting SARA composition of crude oil by means of NMR", *Fuel*, v. 110, pp. 318–321, 2013. ISSN: 00162361. doi: 10.1016/j.fuel.2012.10.027. Available at: <http://dx.doi.org/10.1016/j.fuel.2012.10.027>.

[78] SUZUKI, T., ITOH, M., TAKEGAMI, Y., et al. "Chemical structure of tarsand bitumens by 13C and 1H n.m.r. spectroscopic methods", *Fuel*, v. 61, n. 5, pp. 402–410, 1982. ISSN: 00162361. doi: 10.1016/0016-2361(82) 90062-X. Available at: <http://linkinghub.elsevier.com/retrieve/pii/001623618290062X>.

[79] WOODS, J., KUNG, J., KINGSTON, D., et al. "Canadian Crudes: A Comparative Study of SARA Fractions from a Modified HPLC Separation Technique", *Oil & Gas Science and Technology - Revue de l'IFP*, v. 63, n. 1, pp. 151–163, 2008. ISSN: 1294-4475. doi: 10.2516/ogst:2007080.

[80] TAKEGAMI, Y., WATANABE, Y., SUZUKI, T., et al. "Structural investigation on column-chromatographed vacuum residues of various petroleum crudes by 13C nuclear magnetic resonance spectroscopy", *Fuel*, v. 59, n. 4, pp. 253–259, 1980. ISSN: 00162361. doi: 10.1016/0016-2361(80)90144-1. Available at: <http://www.sciencedirect.com/science/article/pii/0016236180901441$\delimiter"026E30F$nhttp://linkinghub.elsevier.com/retrieve/pii/0016236180901441>.

[81] YOKOYAMA, S., BODILY, D. M., WISER, W. H. "Structural characterization of coal-hydrogenation products by proton and carbon-13 nuclear magnetic resonance", *Fuel*, v. 58, n. 3, pp. 162–170, 1979. ISSN: 00162361. doi: 10.1016/0016-2361(79)90113-3. Available at: <http://www.sciencedirect.com/science/article/pii/0016236179901133>.

[82] MENCZEL, J., PRIME, R. *Thermal Analysis of Polymers: Fundamentals and Applications*. Hoboken, New Jersey, Wiley, 2009. ISBN: 9780470423776.

[83] PASO, K., KALLEVIK, H., SJÖBLOM, J. "Measurement of wax appearance temperature using near-infrared (NIR) scattering", *Energy and Fuels*, v. 23, n. 10, pp. 4988–4994, 2009. ISSN: 08870624. doi: 10.1021/ef900173b. Available at: <http://pubs.acs.org/doi/pdf/10.1021/ef900173b>.

[84] GOMES, E. A. D. S. *Estudo da cristalização de parafinas em sistemas solventes/tensoativos/água*. Doutorado thesis, Universidade Federal do Rio Grande do Norte, 2009. Available at: <http://www.nupeg.ufrn.br/documentos_finais/teses_de_doutorado/erika.pdf>.

[85] SANTANA, E. A. *Avaliação da Temperatura de Cristalização da Parafina em Sistemas: Parafina, Solvente e Tensoativo.* Doutorado thesis, Universidade Federal do Rio Grande do Norte, 2005. Available at: <ftp://dns.ufrn.br/pub/biblioteca/ext/bdtd/ErikaaAS.pdf>.

[86] BARNES, H. A., HUTTON, J. F., WALTERS, K. *An Introduction to Rheology.* First ed. Amsterdam, The Netherlands, Elsevier, 1989. ISBN: 0444871403.

[87] BARNES, H. A. *A Handbook Of Elementary Rheology.* Aberystwyth, University of Wales, 2000. ISBN: 0-9538032-0-1.

[88] PASO, K., SILSET, A., SOØ RLAND, G., et al. "Characterization of the formation, flowability, and resolution of brazilian crude oil emulsions", *Energy and Fuels*, v. 23, n. 1, pp. 471–480, 2009. ISSN: 08870624. doi: 10.1021/ef800585s.

[89] BARNES, H. "A review of the slip (wall depletion) of polymer solutions, emulsions and particle suspensions in viscometers: its cause, character, and cure", *Journal of Non-Newtonian Fluid Mechanics*, v. 56, pp. 221–251, 1995. ISSN: 03019322. doi: 10.1016/S0301-9322(97)88450-9.

[90] BARBATO, C., NOGUEIRA, B., KHALIL, M., et al. "Contribution to a more reproductible method for measuring yield stress of waxy crude oil emulsions", *Energy and Fuels*, v. 28, n. 3, pp. 1717–1725, 2014. ISSN: 08870624. doi: 10.1021/ef401976r. Available at: <http://pubs.acs.org/doi/pdf/10.1021/ef401976r>.

[91] CHANG, C., BOGER, D. V., NGUYEN, Q. D. "The yielding of waxy crude oils", *Industrial & engineering chemistry research*, v. 37, n. 4, pp. 1551–1559, 1998. ISSN: 08885885. doi: 10.1021/ie970588r. Available at: <http://pubs.acs.org/doi/abs/10.1021/ie970588r$\delimiter"026E30F$npapers3://publication/uuid/F9899E4D-A7BA-4432-83E8-F543B0D9B965>.

[92] SINGH, P., FOGLER, H. S., NAGARAJAN, N. "Prediction of the wax content of the incipient wax-oil gel in a pipeline: An application of the controlled-stress rheometer", *Journal of Rheology*, v. 43, n. 6, pp. 1437, 1999. ISSN: 01486055. doi: 10.1122/1.551054.

[93] WEBBER, R. M. "Low temperature rheology of lubricating mineral oils: Effects of cooling rate and wax crystallization on flow properties of base oils", *Journal of Rheology*, v. 43, n. 4, pp. 911, 1999. ISSN: 01486055. doi:

10.1122/1.551045. Available at: <http://link.aip.org/link/JORHD2/v43/i4/p911/s1{&}Agg=doi>.

[94] BARNES, H. A. "Measuring the viscosity of large-particle (and flocculated) suspensions - a note on the necessary gap size of rotational viscometers", *Journal of Non-Newtonian Fluid Mechanics*, v. 94, n. 2-3, pp. 213–217, 2000. ISSN: 03770257. doi: 10.1016/S0377-0257(00)00162-2.

[95] DE OLIVEIRA, M. C. K., TEIXEIRA, A., VIEIRA, L. C., et al. "Flow assurance study for waxy crude oils", *Energy and Fuels*, v. 26, n. 5, pp. 2688–2695, 2012. ISSN: 08870624. doi: 10.1021/ef201407j.

[96] HANSEN, A. B., LARSEN, E., BATSBERG PEDERSEN, W., et al. "Wax precipitation from North Sea crude oils. 3. Precipitation and dissolution of wax studied by differential scanning calorimetry", *Energy & Fuels*, v. 5, n. 6, pp. 914–923, 1991. doi: 10.1021/ef00030a021. Available at: <http://dx.doi.org/10.1021/ef00030a021>.

[97] CLAUDY, P., LÉTOFFÉ, J. M., CHAGUÉ, B., et al. "Crude oils and their distillates: characterization by differential scanning calorimetry", *Fuel*, v. 67, pp. 58–61, 2000.

[98] ZHAO, Y., PASO, K., SJÖBLOM, J. "Thermal behavior and solid fraction dependent gel strength model of waxy oils", *Journal of Thermal Analysis and Calorimetry*, v. 117, n. 1, pp. 403–411, 2014. ISSN: 1388-6150. doi: 10.1007/s10973-014-3660-3. Available at: <http://link.springer.com/10.1007/s10973-014-3660-3>.

[99] VIGNATI, E., PIAZZA, R., VISINTIN, R. F. G., et al. "Wax crystallization and aggregation in a model crude oil", *Journal of Physics: Condensed Matter*, v. 17, n. 45, pp. S3651–S3660, 2005. ISSN: 0953-8984. doi: 10.1088/0953-8984/17/45/061.

[100] CHEN, J., ZHANG, J., LI, H. "Determining the wax content of crude oils by using differential scanning calorimetry", *Thermochimica Acta*, v. 410, pp. 23–26, 2004. doi: 10.1016/S0040-6031(03)00367-8.

[101] KÖK, M., LETOFFE, J. M., CLAUDY, P., et al. "Thermal characteristics of crude oils treated with rheology modifiers", *Journal of Thermal Analysis*, v. 49, n. 2, pp. 727–736, 1997. ISSN: 0022-5215. doi: 10.1007/BF01996756.

[102] KÖK, M. V., LETOFFE, J. M., CLAUDY, P. "DSC and Rheometry Investigations of Crude Oils", *Journal of Thermal Analysis and Calorimetry*, v. 56, pp. 959–965, 1999. ISSN: 13886150.

[103] LÉTOFFÉ, J. M., CLAUDY, P., KÖK, M., et al. "Crude oils: characterization of waxes precipitated on cooling by DSC and thermomicroscopy", *Fuel*, v. 74, n. 6, pp. 810–817, 1995.

[104] HEINO, E.-L. "Determination of cloud point for petroleum middle distillates by differential scanning calorimetry", *Thermochimica Acta*, v. 114, pp. 125–130, 1987. Available at: <http://www.sciencedirect.com/science/article/pii/0040603187802502>.

[105] GIMZEWSKI, E., AUDLEY, G. "Monitoring wax crystallisation in diesel using differential scanning calorimetry (DSC) and microcalorimetry", *Thermochimica Acta*, v. 214, n. 1, pp. 149–155, jan. 1993. ISSN: 00406031. doi: 10.1016/0040-6031(93)80050-K. Available at: <http://linkinghub.elsevier.com/retrieve/pii/004060319380050K>.

[106] VIEIRA, L. C., BUCHUID, M. B., LUCAS, E. F. "Effect of Pressure on the Crystallization of Crude Oil Waxes. I. Selection of Test Conditions by Microcalorimetry", *Energy & Fuels*, v. 24, n. 4, pp. 2208–2212, 2010. ISSN: 0887-0624. doi: 10.1021/ef900711d. Available at: <http://pubs.acs.org/doi/abs/10.1021/ef900711d>.

[107] PALERMO, L. C. M., SOUZA JR, N. F., LOUZADA, H. F., et al. "Development of Multifunctional Formulations for Inhibition of Waxes and Asphaltenes Deposition", *Brazilian Journal of Petroleum and Gas*, v. 7, n. 4, pp. 181–192, 2014. ISSN: 19820593. doi: 10.5419/bjpg2013-0015. Available at: <http://www.portalabpg.org.br/bjpg/index.php/bjpg/article/view/340>.

[108] FLYNN, B., PARRY-HILL, M., DAVIDSON, M. "Nikon MicroscopyU - Birefringent Crystals in Polarized Light". Available at: <http://www.microscopyu.com/tutorials/java/polarized/crystal/>. Access: January 15th, 2016.

[109] DUNCKE, A. C. P. *Morfologia de Parafinas em Petróleo, Sistemas Modelo e Emulsões Água/Óleo por meio de Microscopia Óptica.* Master's thesis, Universidade Federal do Rio de Janeiro, 2015.

[110] PASO, K., SENRA, M., YI, Y., et al. "Paraffin polydispersity facilitates mechanical gelation", *Industrial and Engineering Chemistry Research*, v. 44, n. 18, pp. 7242–7254, 2005. ISSN: 08885885. doi: 10.1021/ie050325u.

[111] YI, S., ZHANG, J. "Relationship between waxy crude oil composition and change in the morphology and structure of wax crystals induced by pour-

point-depressant beneficiation", *Energy and Fuels*, v. 25, pp. 1686–1696, 2011. ISSN: 08870624. doi: 10.1021/ef200059p.

[112] GAO, P., ZHANG, J., MA, G. "Direct image-based fractal characterization of morphologies and structures of wax crystals in waxy crude oils", *Journal of Physics: Condensed Matter*, v. 18, n. 50, pp. 11487–11506, dec 2006. ISSN: 0953-8984. doi: 10.1088/0953-8984/18/50/006. Available at: <http://stacks.iop.org/0953-8984/18/i=50/a=006?key=crossref.ec69d978f7d73518b2ec6b5be3217f8a>.

[113] ZHANG, J., YU, B., LI, H., et al. "Advances in rheology and flow assurance studies of waxy crude", *Petroleum Science*, v. 10, n. 4, pp. 538–547, 2013. ISSN: 1672-5107. doi: 10.1007/s12182-013-0305-2. Available at: <http://link.springer.com/10.1007/s12182-013-0305-2>.

[114] LU, X., LANGTON, M., OLOFSSON, P., et al. "Microstructure of wax crystals in bitumen". In: *The 3rd Eurasphalt & Eurobitume Congress*, pp. 1–11, Vienna, Austria, 2004.

[115] MARCHESINI, F. H. *Rheology of waxy crude oils*. Doctor's thesis, Pontifícia Universidade Católica-RJ, 2012.

[116] COUTINHO, J. A. P., DARIDON, J.-L. "Low-Pressure Modeling of Wax Formation in Crude Oils", *Energy & Fuels*, v. 15, n. 6, pp. 1454–1460, nov 2001. ISSN: 0887-0624. doi: 10.1021/ef010072r. Available at: <http://dx.doi.org/10.1021/ef010072rhttp://pubs.acs.org/doi/abs/10.1021/ef010072r>.

[117] CASSEL, B., PACKER, R. *Modulated Temperature DSC and the DSC 8500: A Step Up in Performance*. Technical report, Perkin Elmer, Inc., Shelton, CT, USA, 2010.

[118] SHOCK, D., SUDBURY, J., CROCKETT, J. "Studies of the Mechanism of Paraffin Deposition and Its Control", *Journal of Petroleum Technology*, v. 7, n. 09, pp. 23–28, 1955. ISSN: 0149-2136. doi: 10.2118/384-G. Available at: <https://www.onepetro.org/journal-paper/SPE-384-G?sort={&}start=0{&}q=Studies+of+the+Mechanism+of+Paraffin+Deposition+and+Its+Control{&}from{_}year={&}peer{_}reviewed={&}published{_}between={&}fromSearchResults=true{&}to{_}year={&}rows=10{#}>.

[119] MARCHESINI, F. H., ALICKE, A. A., MENDES, P. R. D. S. "Thixotropic behavior of drilling muds". In: *13th Brazilian Congress of Thermal*

Sciences and Engineering, Uberlandia, MG, Brazil, 2010. Associaçao Brasileira de Engenharia e Ciências Mecânicas. Available at: <`http://www.abcm.org.br/anais/encit/2010/PDF/ENC10-0381.pdf`>.

[120] VOZKA, P., STRAKA, P., MAXA, D. "Effect of Asphaltenes on structure of paraffin particles in crude oil", *Fuels (Paliva)*, v. 7, n. 2, pp. 42–47, 2015.

[121] LARSON, R. *The Structure and Rheology of Complex Fluids*. Oxford University Press, 1999.

[122] PIELICHOWSKI, K., FLEJTUCH, K. "Thermal properties of poly(ethylene oxide)/lauric acid blends: A SSA-DSC study", *Thermochimica Acta*, v. 442, n. 1-2, pp. 18–24, 2006. ISSN: 00406031. doi: 10.1016/j.tca.2005.11.013.

[123] PIELICHOWSKI, K., FLEJTUCH, K., PIELICHOWSKI, J. "Step-scan alternating DSC study of melting and crystallisation in poly(ethylene oxide)", *Polymer*, v. 45, n. 4, pp. 1235–1242, 2004. ISSN: 00323861. doi: 10.1016/j.polymer.2003.12.045.

[124] GARCIA, M. C. "Crude Oil Wax Crystallization . The Effect of Heavy n-Paraffins and Flocculated Asphaltenes", *Energy & Fuels*, v. 14, n. 16, pp. 1043–1048, 2000.

[125] KRIZ, P., ANDERSEN, S. I. "Effect of asphaltenes on crude oil wax crystallization", *Energy and Fuels*, v. 19, n. 3, pp. 948–953, 2005. ISSN: 08870624. doi: 10.1021/ef049819e.

[126] SANJAY, M., SIMANTA, B., KULWANT, S. "Paraffin Problems in Crude Oil Production And Transportation: A Review", *SPE Production & Facilities*, v. 10, n. 1, pp. 50–54, 1995. ISSN: 1064668X. doi: 10.2118/28181-PA.

[127] DIRAND, M., CHEVALLIER, V., PROVOST, E., et al. "Multicomponent paraffin waxes and petroleum solid deposits: structural and thermodynamic state", *Fuel*, v. 77, n. 12, pp. 1253–1260, 1998. ISSN: 00162361. doi: 10.1016/S0016-2361(98)00032-5.

[128] HUTTER, J. L., HUDSON, S., SMITH, C., et al. "Banded crystallization of tricosane in the presence of kinetic inhibitors during directional solidification", *Journal of Crystal Growth*, v. 273, n. 1-2, pp. 292–302, 2004. ISSN: 00220248. doi: 10.1016/j.jcrysgro.2004.08.017.

[129] KANÉ, M., DJABOUROV, M., VOLLE, J. L., et al. "Morphology of paraffin crystals in waxy crude oils cooled in quiescent conditions and under flow",

Fuel, v. 82, n. 2, pp. 127–135, 2003. ISSN: 00162361. doi: 10.1016/
S0016-2361(02)00222-3.

[130] HANDOO, J., SRIVASTAVA, S. P., AGRAWAL, K. M., et al. "Thermal
properties of some petroleum waxes in relation to their composition",
Fuel, v. 68, n. 10, pp. 1346–1348, oct 1989. ISSN: 00162361. doi: 10.1016/
0016-2361(89)90254-8. Available at: <http://linkinghub.elsevier.
com/retrieve/pii/0016236189902548>.

[131] WITTCOFF, H., REUBEN, B., PLOTKIN, J. S. *Industrial organic chem-
icals*. John Wiley & Sons, Inc, 2004. ISBN: 0-471-44385-9. doi:
10.1016/S0304-3894(96)01845-6.

[132] AL-SABAGH, A., EL-HAMOULY, S., KHIDR, T., et al. "Synthesis of ph-
thalimide and succinimide copolymers and their evaluation as flow im-
provers for an Egyptian waxy crude oil", *Egyptian Journal of Petroleum*,
v. 22, n. 3, pp. 381–393, 2013. ISSN: 11100621. doi: 10.1016/j.ejpe.2013.
10.008. Available at: <http://linkinghub.elsevier.com/retrieve/
pii/S1110062113000779>.

# Appendix A

NMR spectra

Figure A.1: ^{1}H-NMR spectrum for crude oil A1.
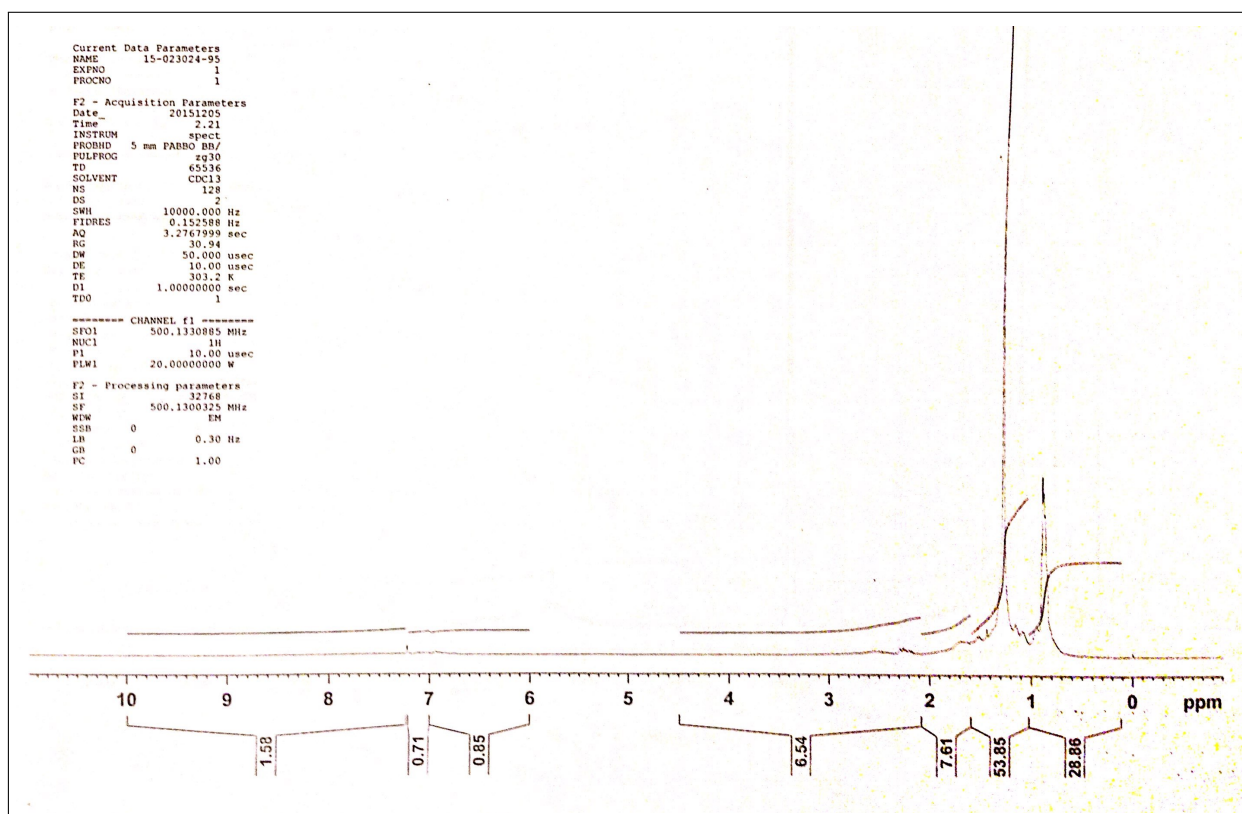
Figure A.2: ^{13}C-NMR spectrum for crude oil A1.

Sample Name:

Data Collected on:
  inova1-inova300
Archive directory:

Sample directory:

FidFile: 15-023024-95_C13

Pulse Sequence: CARBON (s2pul)
Solvent: cdcl3
Data collected on: Dec 4 2015

 Temp. 29.0 C / 302.1 K
Operator: vnmr1

 Relax. delay 6.000 sec
 Pulse 90.0 degrees
 Acq. time 0.869 sec
 Width 18859.0 Hz
 5000 repetitions
OBSERVE C13, 75.4300798 MHz
DECOUPLE H1, 299.9815748 MHz
 Power 30 dB
 on during acquisition
 off during delay
 WALTZ-16 modulated
DATA PROCESSING
 Line broadening 5.0 Hz
FT size 65536
Total time 0 min 0 sec

Figure A.3: ^{1}H-NMR spectrum for crude oil A2.

Current Data Parameters
NAME   15-023026-57
EXPNO   1
PROCNO   1

F2 - Acquisition Parameters
Date_   20151205
Time   2.35
INSTRUM   spect
PROBHD   5 mm PABBO BB/
PULPROG   zg30
TD   65536
SOLVENT   CDCl3
NS   128
DS   2
SWH   10000.000 Hz
FIDRES   0.152588 Hz
AQ   3.2767999 sec
RG   30.94
DW   50.000 usec
DE   10.00 usec
TE   303.2 K
D1   1.00000000 sec
TD0   1

======== CHANNEL f1 ========
SFO1   500.1330885 MHz
NUC1   1H
P1   10.00 usec
PLW1   20.00000000 W

F2 - Processing parameters
SI   32768
SF   500.1300322 MHz
WDW   EM
SSB   0
LB   0.30 Hz
GB   0
PC   1.00

Figure A.4: ^{13}C-NMR spectrum for crude oil A2.
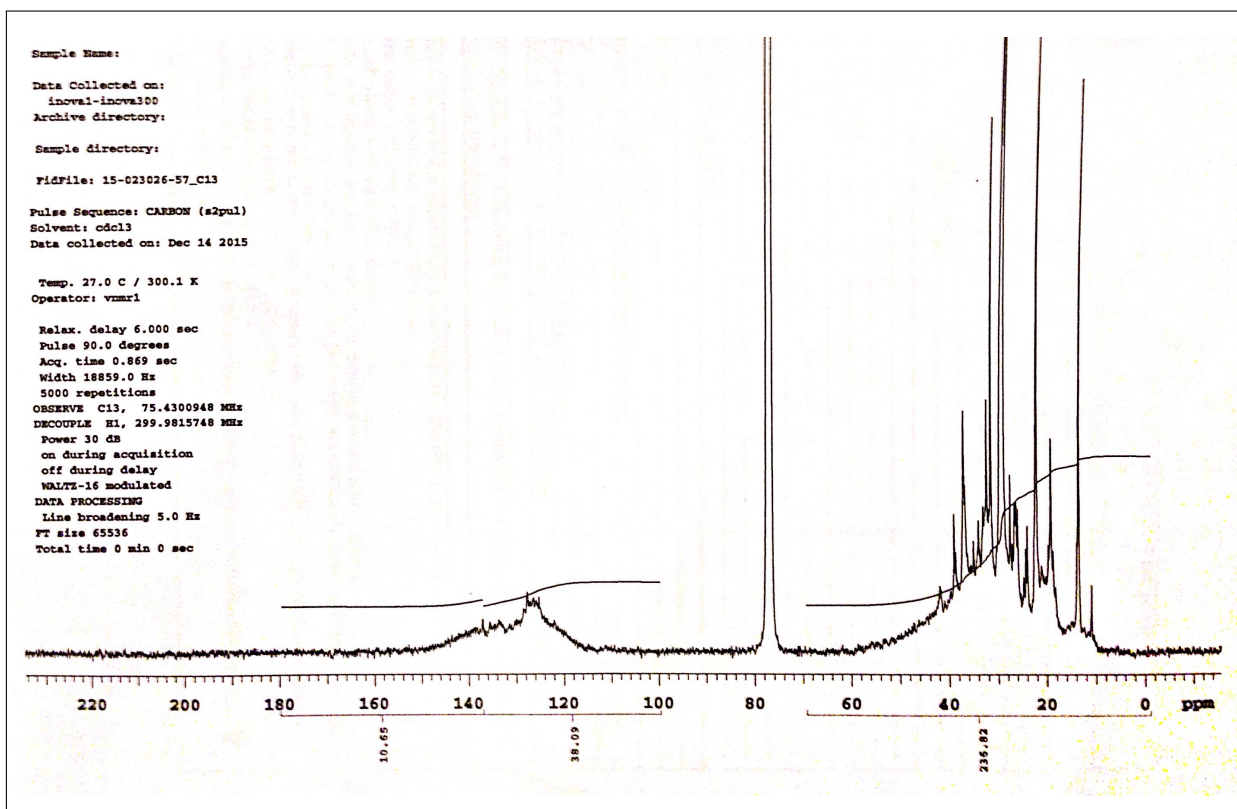
Appendix B

DSC thermograms

Figure B.1: WPT measurement for crude oil A1 ($T_i = 80\,°\mathrm{C}$).
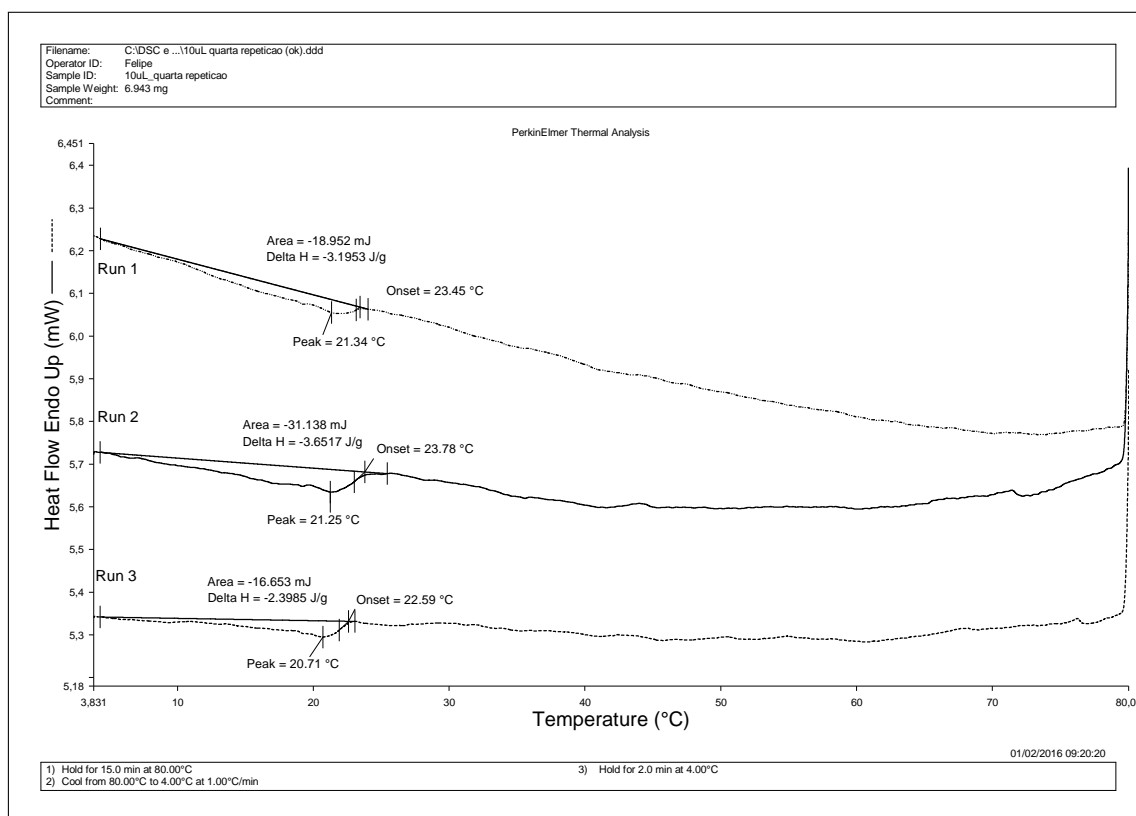
Figure B.2: WPT measurement for crude oil A2 ($T_i = 80\,°C$).
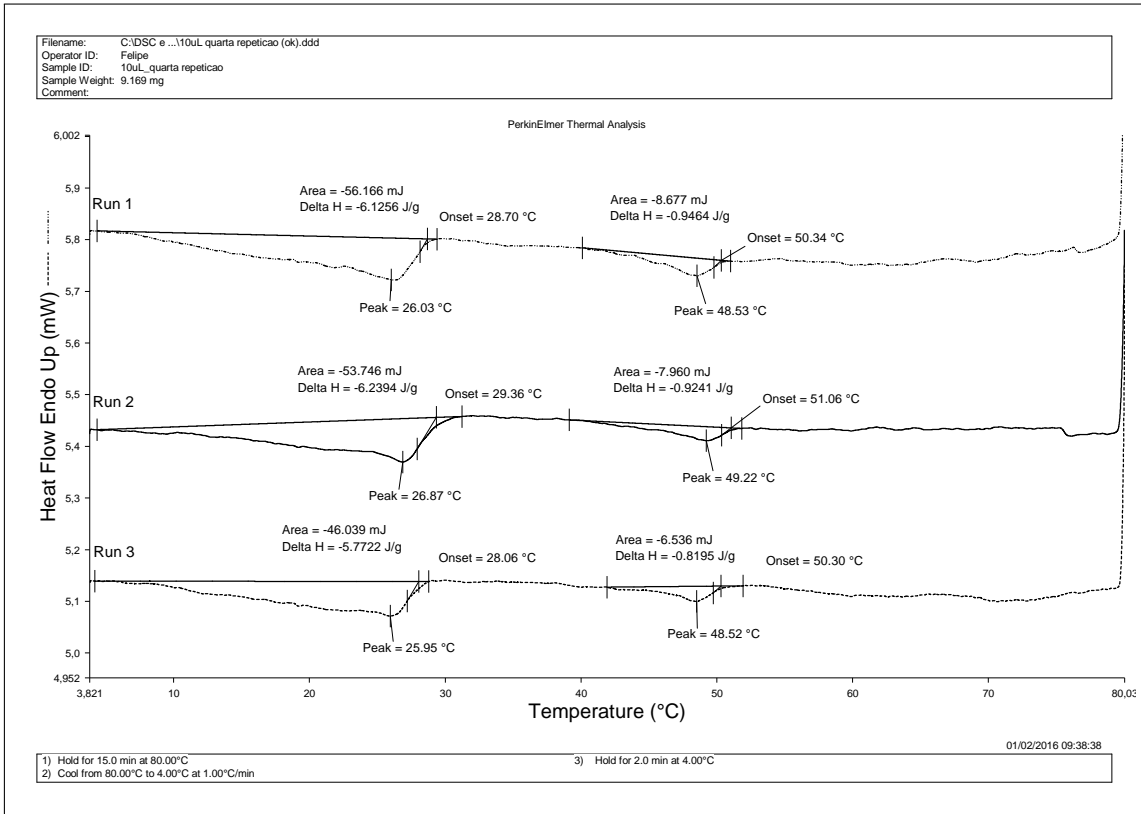

Figure B.3: WPT measurement for crude oil A1 ($T_i = 50\,°C$).

79
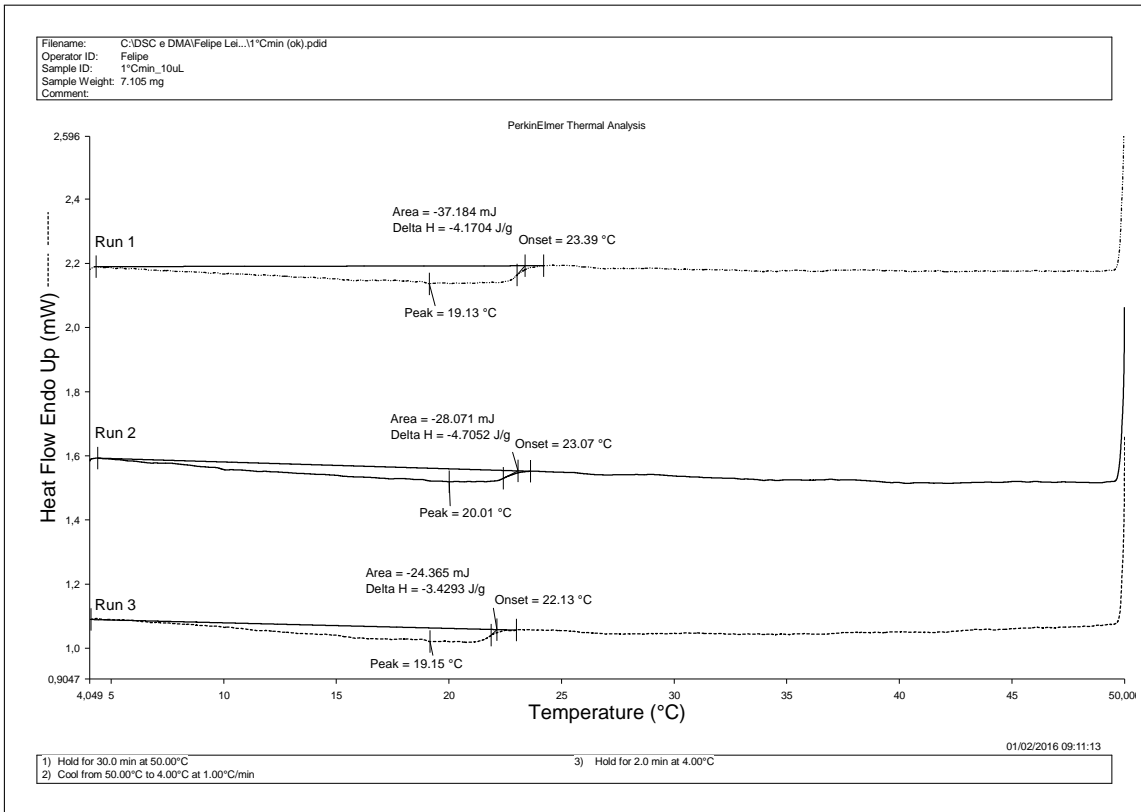
Figure B.4: WPT measurement for crude oil A2 ($T_i = 50\,°C$).
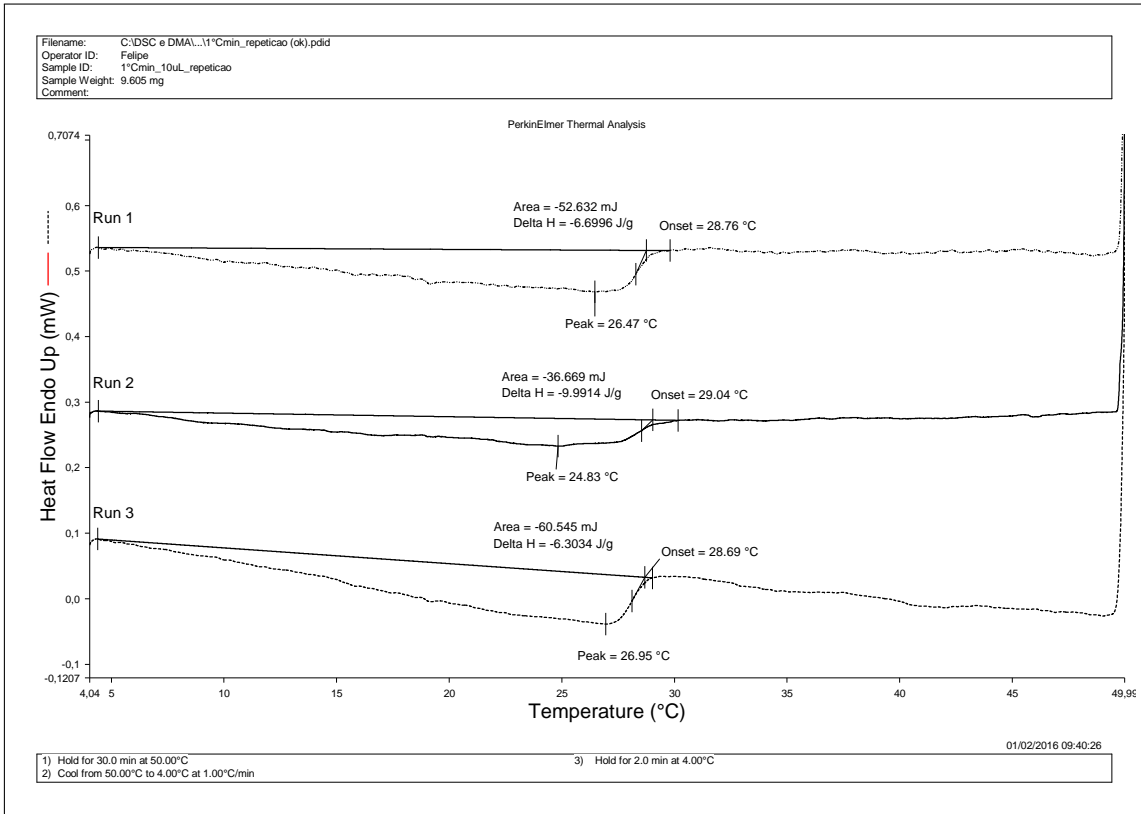
Figure B.5: MTDSC test with the StepScan technique for crude oil A1.
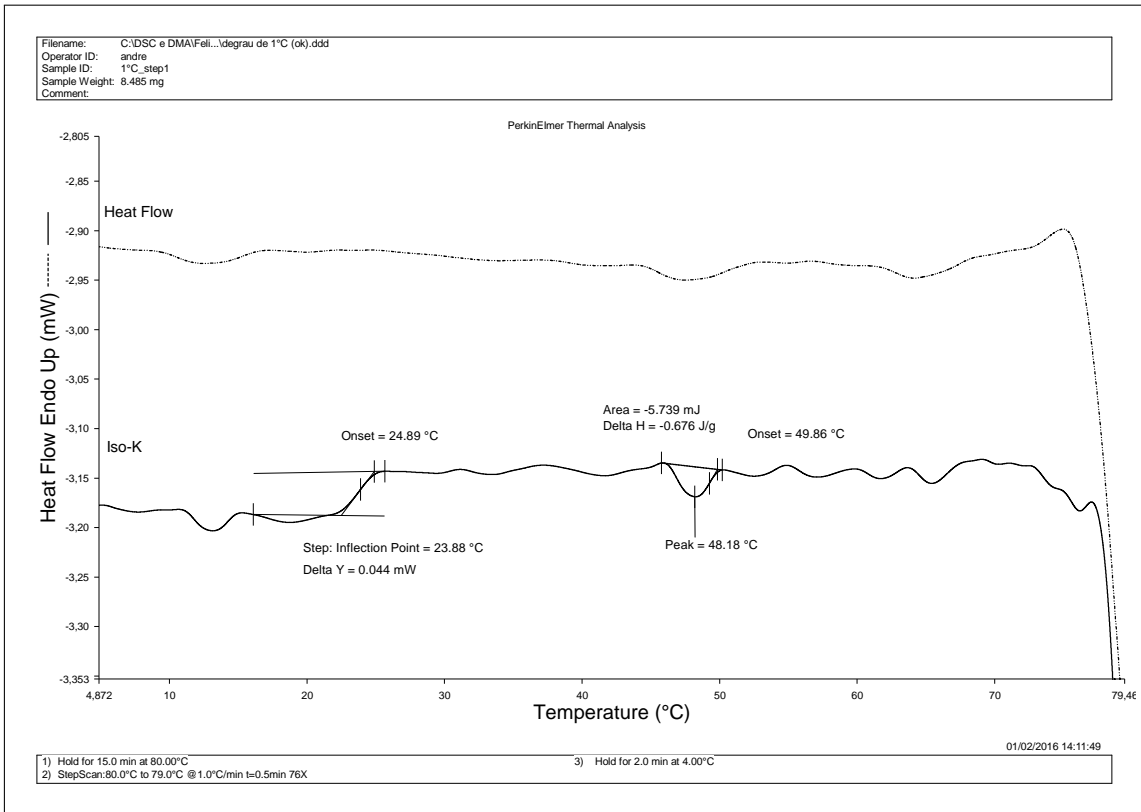
Figure B.6: MTDSC test with the StepScan technique for crude oil A2.
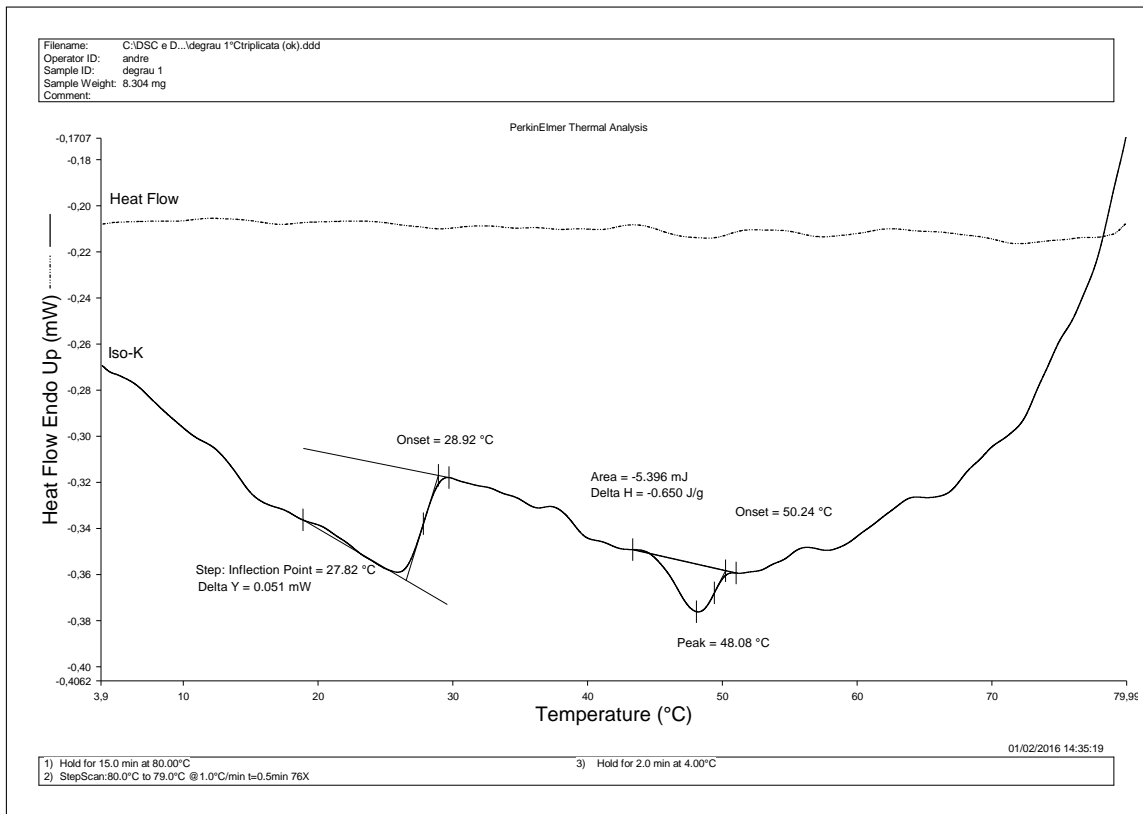
Appendix C

CPM micrographs

Figure C.1: Micrographs from crude oil A1 with an initial temperature of 80 °C. Run 1: (a) and (b); run 2: (c) and (d); run 3: (e) and (f).


(a)

(b)

(c)

(d)

(e)

(f)
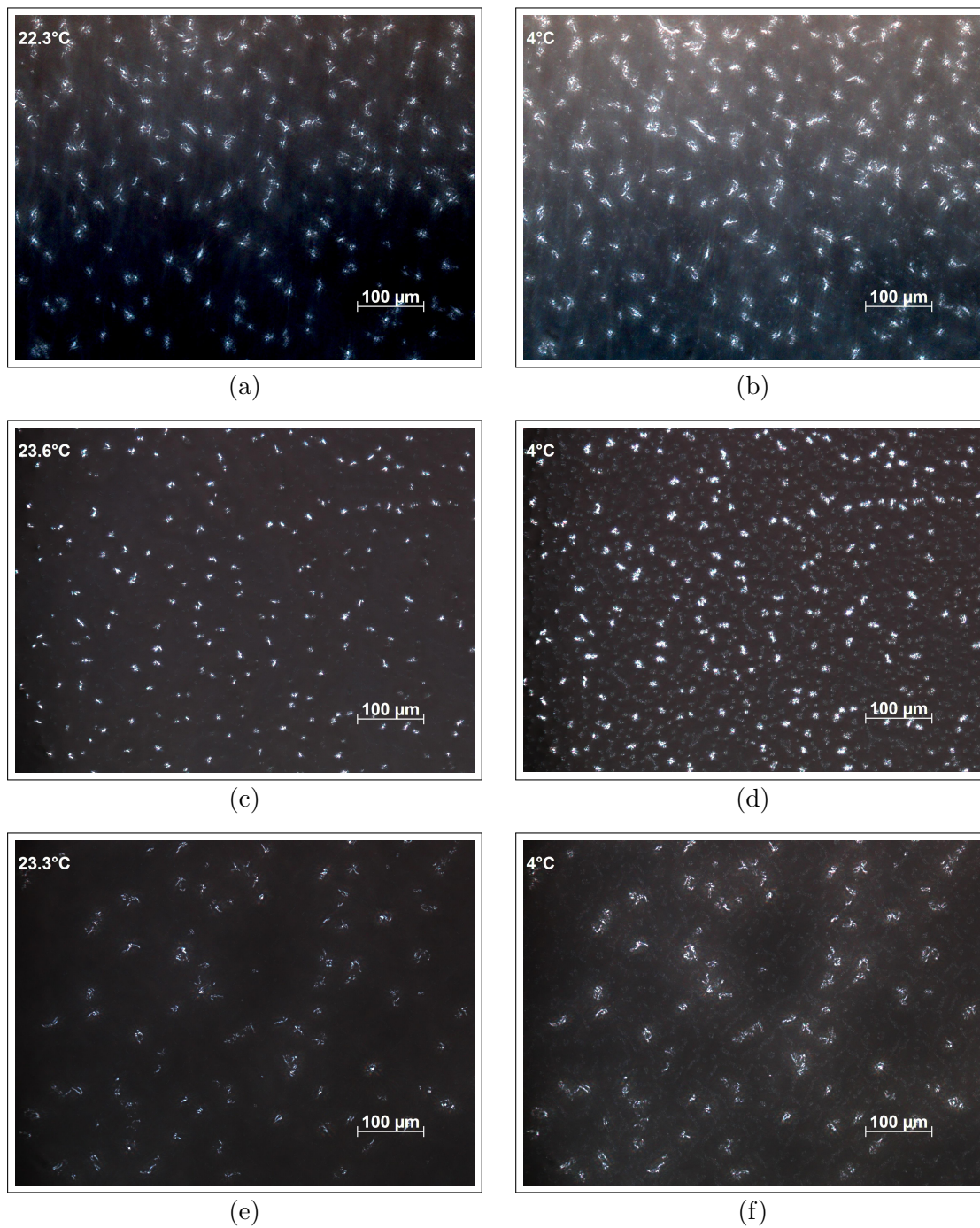
Figure C.2: Micrographs from crude oil A1 with an initial temperature of 50 °C. Run 1: (a) and (b); run 2: (c) and (d); run 3: (e) and (f).


(a)

(b)

(c)

(d)

(e)

(f)
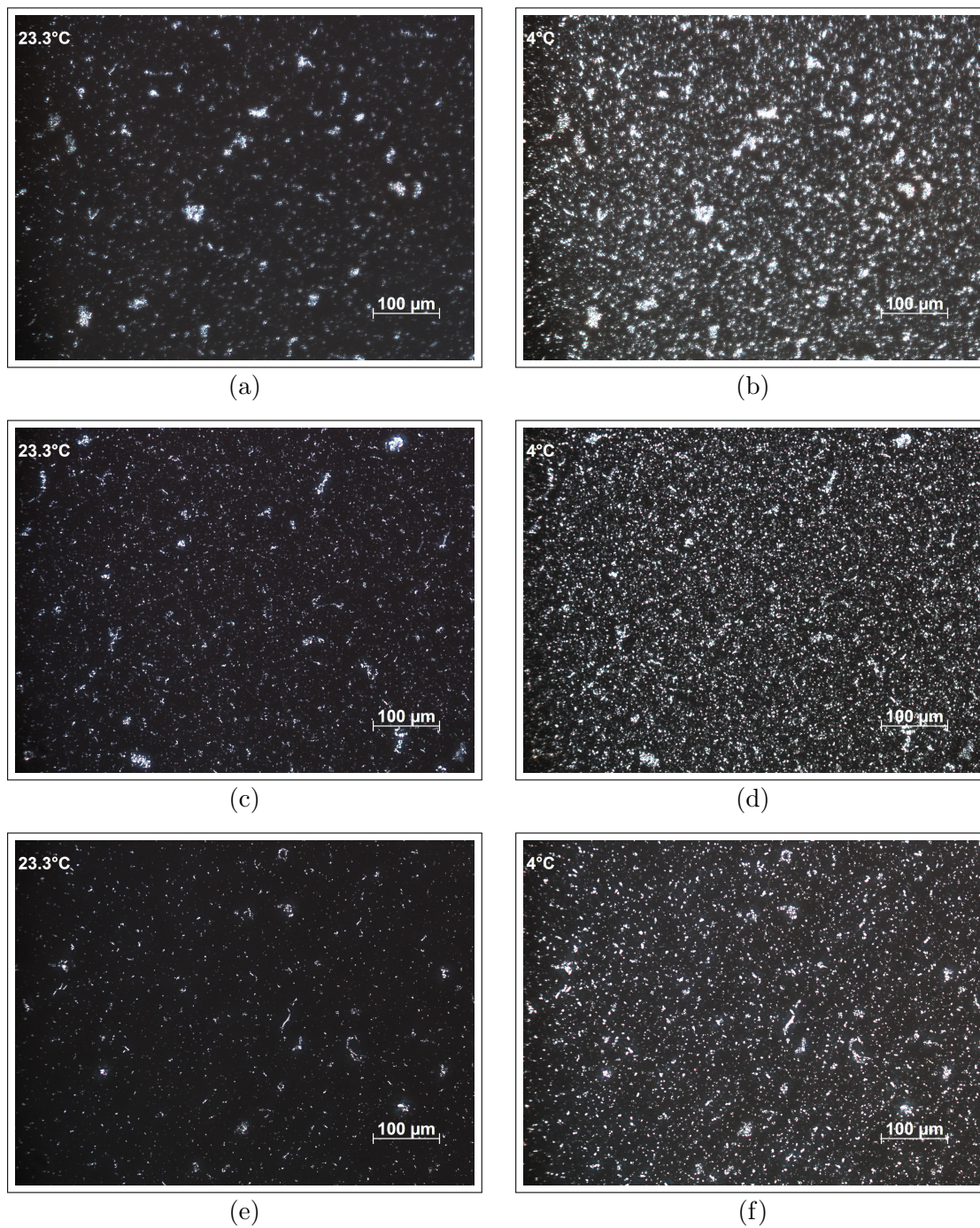
Figure C.3: Micrographs from crude oil A2 with an initial temperature of 80 °C. Run 1: (a) and (b); run 2: (c) and (d); run 3: (e) and (f).



(a)

(b)

(c)

(d)

(e)

(f)
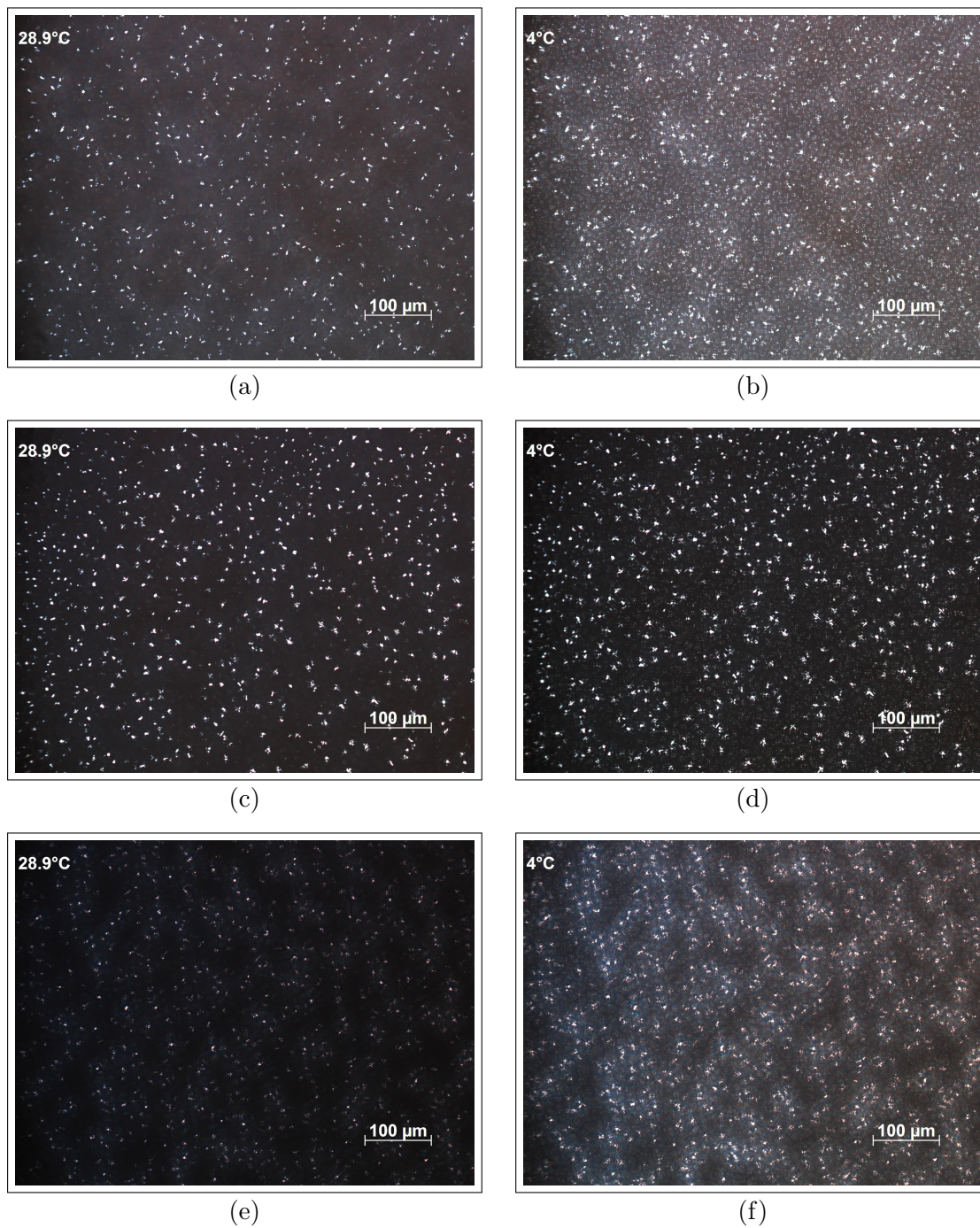
Figure C.4: Micrographs from crude oil A2 with an initial temperature of 50 °C. Run 1: (a) and (b); run 2: (c) and (d); run 3: (e) and (f).

(a)

(b)

(c)

(d)

(e)

(f)